

Digital Design of Photoplethysmogram (PPG) based Cardiovascular Disease Classifiers



By

Aditta Chowdhury

19MEE007P

A thesis submitted in partial fulfillment of the requirements for the
degree of MASTER of SCIENCE in Electrical and Electronic
Engineering

Department of Electrical and Electronic Engineering
CHITTAGONG UNIVERSITY OF ENGINEERING AND
TECHNOLOGY

September 2023

Copyright Declaration

I hereby declare that I am the sole author of the thesis titled “Digital Design of Photoplethysmogram (PPG) based Cardiovascular Disease Classifiers”. Along with this, submitted a softcopy is true copy of my final hardcopy thesis including any required final revisions, as accepted by the board of examination.

I hereby release my copyright to Chittagong University of Engineering and Technology (CUET) for uploading the electronic version of the same to the ‘Digital Repository (Institutional Repository)’ of CUET after one year from the day of submission. Apart from this, the existing or to be approved Open Education Resources (OER) policies and procedures of Chittagong University of Engineering and Technology (CUET) shall be applicable to this research work.

I also acknowledge my sincere delivering of copyright to Chittagong University of engineering and Technology (CUET) to reproduce this thesis by reprography or by other means, in total or by part at the necessity of individuals for the purpose of scholarly research.

Aditta Chowdhury

Declaration

I hereby declare that the work contained in this thesis has not been previously submitted to meet requirements for an award at this or any other higher education institution. To the best of my knowledge and belief, the thesis contains no material previously published or written by another person except where due reference is cited.

Aditta Chowdhury

19MEE007P

Department of Electrical and Electronic Engineering
Chittagong University of Engineering & Technology (CUET)

Copyrights in relation to this thesis.

Copyright ©Aditta Chowdhury, 2023

This work may not be copied without permission of the author or Chittagong University of Engineering & Technology

Dedication

To my parents, wife, and other family members for their continuous support

List of Publications

Journal Article

- Publication 1: **Aditta Chowdhury**, Diba Das, Sampad Ghosh, Ray C. C. Cheung, Mehdi Hasan Chowdhury, “FPGA Implementation of PPG-based Cardiovascular Diseases and Diabetes Classification Algorithm”, *SN Computer Science*. (Under review)
- Publication 2: **Aditta Chowdhury**, Diba Das, Kamrul Hasan, Ray C. C. Cheung, Mehdi Hasan Chowdhury, “An FPGA Implementation of Multiclass Disease Detection from PPG”, *IEEE Sensors Letters*. (Under review)
- Publication 3: **Aditta Chowdhury**, Diba Das, Abdelrahman B. M. Eldaly, Ray C. C. Cheung, Mehdi Hasan Chowdhury, “FPGA Based Design for Heart Rate and Blood Pressure Estimation with Hypertension Classification from Photoplethysmogram”, *IPEM Translation*. (Under review)
- Publication 4: **Aditta Chowdhury**, Diba Das, Sampad Ghosh, Ray C. C. Cheung, Mehdi Hasan Chowdhury, “Hardware and Software Co-Design for Detecting Hypertension from Photoplethysmogram”, *IEEE Embedded Systems Letters*. (Under review)

Conference

- Publication 1: **Aditta Chowdhury**, Diba Das, Ray C. C. Cheung, Mehdi Hasan Chowdhury, “Hardware/Software Co-design of an ECG- PPG Preprocessor: A Qualitative & Quantitative Analysis”, *2023 International Conference on Electrical, Computer and Communication Engineering (ECCE), Chittagong, Bangladesh, 2023*, pp. 1-6. (Published)

Approval by the Supervisor

This is to certify that Aditta Chowdhury has carried out this work under my supervision, and that he has fulfilled relevant Academic Ordinance of the Chittagong University of Engineering and Technology, so that he is qualified to submit the following thesis in application for the degree of MASTER of SCIENCE in Electrical and Electronic Engineering

Dr. Mehdi Hasan Chowdhury

Associate Professor

Department of Electrical and Electronic Engineering
Chittagong University of Engineering & Technology (CUET)

Acknowledgement

I would like to thank Dr. Ray C. C. Cheung, Dr. Sampad Ghosh, Abdurrashid Ibrahim Sanka, Abdelrahman B. M. Eldaly, and Diba Das for their significant support and insights that helped me to complete my research work and write my thesis. My heartfelt gratitude goes to the examination committee members for their time and patience.

Also, I am grateful to my supervisor Dr. Mehdi Hasan Chowdhury for his continuous mentorship and endless support in every step of my thesis. His insights and knowledge with a humble research approach helped to complete my thesis.

I would like to acknowledge the Department of Electrical Engineering, City University of Hong Kong, Kowloon, Hong Kong for helping me with the implementation of this study.

I am forever grateful to all the members of the Department of Electrical and Electronic Engineering for their continuous support. Also, I would like to thank my parents and other family members.

সারাংশ

ফটোস্থিসমোগ্রাম হল একটি আলোকপ্রাপ্ত সংকেত যা রক্তের আয়তনগত পরিবর্তনের উপর ভিত্তি করে কাজ করে। যেহেতু হৃদরোগ রক্ত পাম্প করার সাথে সম্পর্কিত, তাই হৃদরোগ সনাক্ত করার জন্য পিপিজি অধ্যয়ন করা যেতে পারে। গবেষকরা ইতিমধ্যে উচ্চ রক্তচাপ, করোনারি ধমনী রোগ, ডায়াবেটিস সহ বিভিন্ন রোগ সনাক্তকরণের জন্য পিপিজি সংকেত বিশ্লেষণ করেছেন। এছাড়াও, দুটি গুরুত্বপূর্ণ স্বাস্থ্য নির্দেশক : হৃদস্পন্দন এবং রক্তচাপ বিভিন্ন গবেষণায় পিপিজি সংকেত থেকে নির্ণয় করা হয়। তবে পূর্বের বেশিরভাগ কাজই সফটওয়্যার পর্যায়ে করা হয়েছে কোনো হার্ডওয়্যার বাস্তবায়ন ছাড়াই। এছাড়াও, মস্তিষ্কে রক্ত প্রবাহ সম্পর্কিত দুটি গুরুত্বপূর্ণ হৃদরোগ: সেরিব্রাল ইনফার্কশন এবং সেরিব্রোভাসকুলার রোগ এখনও পিপিজি সংকেতের উপর ভিত্তি করে বের করা হয়নি। তাই, এই গবেষণার লক্ষ্য হল একটি হার্ডওয়্যার-ভিত্তিক সিস্টেম তৈরি করা যা বিভিন্ন কার্ডিওভাসকুলার রোগ - উচ্চ রক্তচাপ, সেরিব্রাল ইনফার্কশন, সেরিব্রোভাসকুলার রোগ সহ ডায়াবেটিস সনাক্ত করতে পারে। গবেষণাটি একটি বাইনারি শ্রেণিবিন্যাস পদ্ধতিতে এবং একটি বহুশ্রেণীর শ্রেণিবিন্যাস পদ্ধতিতে পৃথকভাবে এই রোগগুলি সনাক্ত করার সম্ভাব্যতা পরীক্ষা করে। এছাড়াও, এই রোগগুলির সংমিশ্রণ সনাক্তকরণের সম্ভাব্যতা একটি বহুমুখী শ্রেণীর শ্রেণীবিভাগ সিস্টেম ডিজাইন করে বিশ্লেষণ করা হয়। পিপিজি সংকেত থেকে হৃদস্পন্দন এবং রক্তচাপের পূর্বাভাসের জন্য একটি সিস্টেমও প্রয়োগ করা হয়। Zedboard zynq 7000 এবং zynq ultrascale+ FPGA বোর্ডকে লক্ষ্য করে Xilinx সিস্টেম জেনারেটরে সিস্টেমগুলি তৈরি করা হয়েছে। উচ্চ রক্তচাপ, সেরিব্রাল ইনফার্কশন, সেরিব্রোভাসকুলার ডিজিজ এবং ডায়াবেটিস সনাক্ত করার ক্ষেত্রে যথাক্রমে ৯৬.৩৭%, ৯৩.৪৮%, ৯৬.৪৩% এবং ৮৮.৪৬% সঠিকতা পাওয়া যায়। বাইনারি শ্রেণিবিন্যাস পদ্ধতিতে ১১টি বৈশিষ্ট্য ও SVM শ্রেণীবিভাগ প্রয়োগের ফলে ০.৬৯৩ ওয়াট শক্তি ব্যবহৃত হয়। বহুমুখী শ্রেণীর শ্রেণীবিভাগ সিস্টেম মোট ১.৪০৩ ওয়াট শক্তি ব্যবহার করে, যা ৭ শ্রেণীর রোগ সনাক্ত করার জন্য ৭৯.৮৩% নির্ভুলতা প্রদান করে। এছাড়াও, হৃদস্পন্দন এবং রক্তচাপ অনুমান সিস্টেম ০.৩৫৩ ওয়াট শক্তি ব্যবহৃত হয়। হার্টের হার ৪.০৪% ত্রুটির সাথে পূর্বাভাস করা হয় যেখানে সর্বোচ্চ সংকোচন চাপ এবং সর্বনিম্ন প্রসারণ চাপ যথাক্রমে ৩.৭৭% এবং ৪.৮% ত্রুটির সাথে অনুমান করা হয়। পরিধানযোগ্য যন্ত্র, স্মার্টওয়াচ তৈরির জন্য পরিকল্পিত প্রোটোটাইপকে আরও উন্নত করা যেতে পারে এবং চিকিৎসা ও বিশ্লেষণের জন্য উপযোগী হতে পারে।

Abstract

Photoplethysmogram is an optically obtained signal working based on the volumetric change of blood. As heart diseases are correlated with the pumping of blood, PPG can be studied for detecting cardiovascular diseases. Researchers have already analyzed PPG signals for various disease detection, including hypertension, coronary artery disease, diabetes, and others. Also, two important health parameters: heart rate and blood pressure have been predicted from PPG signals in several studies. However, most of the work has been done at the software level without any hardware implementation. In addition, two important cardiovascular diseases related to blood flow in the brain: cerebral infarction and cerebrovascular disease are yet to be explored based on PPG signal. Hence, this study aims to develop a hardware-based system that can detect several cardiovascular diseases - hypertension, cerebral infarction, cerebrovascular disease, diabetes, and a few combinations of them. The study checks the feasibility of detecting these diseases individually in a binary classification system and also in a multiclass classification system. A system is also implemented for predicting heart rate and blood pressure from PPG signals. The systems are developed in Xilinx system generator targeting Zedboard zynq 7000 and zynq ultrascale+ FPGA board. The binary classification system uses 11 features and applied SVM classifier to get the accuracy of 96.37%, 93.48%, 96.43%, and 88.46% for detecting hypertension, cerebral infarction, cerebrovascular disease, and diabetes, respectively, consuming a total of 0.693 W power. The multi-class classification system utilizes a total of 1.403 W of power, providing an accuracy of 79.83% for detecting 7 classes of diseases. Also, the heart rate and blood pressure estimation system utilizes 0.353 W of power. The heart rate is predicted with 4.04% error while systolic and diastolic blood pressure are estimated with 3.77% and 4.8% error, respectively. The designed prototype can be further extended to develop wearable devices, and smartwatches and can be useful for medical treatment and analysis.

Contents

Copyright Declaration	i
Declaration	ii
Dedication	iii
List of publication	iv
Approval by the Supervisor	v
Acknowledgement	vi
Abstract	viii
List of Figures	xii
List of Tables	xiv
Nomenclature	xv
1 Introduction	1
1.1 Background	1
1.2 Present State of the Problem	4
1.3 Specific Objectives	4
1.4 Significance of the Work	5
1.5 Thesis Outline	6
2 Literature Review	8
2.1 Photoplethysmogram Application	8
2.2 Cardiovascular Disease Classification	13
2.2.1 Hypertension	14

2.2.2	Cerebral Infarction	16
2.2.3	Cerebrovascular Disease	17
2.2.4	Diabetes Detection	17
2.3	Health Parameter Estimation	18
2.3.1	Blood Pressure Estimation	19
2.3.2	Heart Rate Measurement	20
2.4	Hardware-based Implementation	21
2.5	Summary and Implications	22
3	Software Framework	24
3.1	Complete Methodology	24
3.2	Dataset Selection	25
3.3	Segment Selection	26
3.4	Preprocessing	28
3.5	Feature Extraction	29
3.6	Classifier	32
4	Hardware Architecture	39
4.1	Methodology for Hardware Design	39
4.2	Device selection	40
4.2.1	Zedboard zynq-7000	40
4.2.2	Zynq Ultrascale+	42
4.3	Design Tool Selection	43
4.4	Normalization	44
4.5	Preprocessor Subsystem	44
4.6	Feature Extractor	45
4.7	Classification Subsystem	49
4.7.1	Classifier for Binary Classification	50
4.7.2	Classifier Design for Multiclass Classification	52
4.7.3	Classifier Design for BP and Heart Rate Estimation	54
5	Performance Analysis	56
5.1	Results of Preprocessing Subsystem	56
5.2	Performance of Feature Extractor	58

5.3	Performance of the classifier	60
5.3.1	Hypertension Detection	63
5.3.2	Cerebral Infarction Detection	64
5.3.3	Cerebrovascular Disease Detection	64
5.3.4	Diabetes Detection	65
5.3.5	Multiclass Classification	66
5.3.6	Heart Rate and Blood Pressure Estimation Classifier	67
5.4	Resource and Power Utilization Analysis	68
5.4.1	Binary Classification Architecture	68
5.4.2	Multiclass Classification Architecture	69
5.4.3	Heart Rate and Blood Pressure Estimation Architecture	70
5.5	Comparative Study	72
5.6	Key Findings	80
6	Conclusions	81
6.1	Conclusions	81
6.2	Limitations	82
6.3	Future Scopes	82
7	Bibliography	85
8	Appendices	101

List of Figures

Fig. 1.1	AC and DC component of a PPG signal	2
Fig. 1.2	PPG acquisition process	3
Fig. 1.3	Structure of the thesis	6
Fig. 2.1	Applications of PPG signal	9
Fig. 3.1	Overall methodology of the study	24
Fig. 3.2	PPG data acquisition process in the PPG BP dataset	25
Fig. 3.3	Preprocessing stage of proposed the system	28
Fig. 3.4	Boundary between two categories defined by a hyperplane . .	34
Fig. 3.5	One-to-one approach in multiclass SVM	36
Fig. 3.6	One-to-rest approach in multiclass SVM	36
Fig. 3.7	A simple linear regression process	37
Fig. 4.1	Overall methodology of hardware design	39
Fig. 4.2	Zynq-7000 FPGA board structure	41
Fig. 4.3	Zynq-ultrascale+ FPGA board structure	42
Fig. 4.4	Normalization of the raw PPG signal	44
Fig. 4.5	Preprocessing stage of proposed the system	45
Fig. 4.6	Memory and control subsystem for feature extraction	46
Fig. 4.7	Mean feature extraction in hardware level	47
Fig. 4.8	MAD extraction in Xilinx system genrator	47
Fig. 4.9	SUM extraction in the hardware design	47
Fig. 4.10	AE extraction for the FPGA design	48
Fig. 4.11	RMS extraction in Xilinx system generator	48
Fig. 4.12	Standard deviation extraction for FPGA design	48
Fig. 4.13	Variance extraction for classifier design	49
Fig. 4.14	Skewness extraction at the hardware level	49

Fig. 4.15 Kurtosis extraction for hardware design	49
Fig. 4.16 Complete feature extraction process in Xilinx system generator	50
Fig. 4.17 SVM Classifier for binary classification	51
Fig. 4.18 Individual SVM classifier architecture for multi-class classification	52
Fig. 4.19 Comparator in multiclass classification	53
Fig. 4.20 Linear regression classifier for heart rate and BP estimation . .	55
Fig. 5.1 Pearson Correlation coefficient for extracted software and hardware features	59
Fig. 5.2 Boxplot of RSE for different features	60
Fig. 5.3 Confusion matrix for binary classification using 9 and 11 features	63
Fig. 5.4 Confusion matrix for multiclass classification	66
Fig. 5.5 Power Utilization for the binary classifier in Zedboard	69
Fig. 5.6 Power Utilization for the multiclass classifier in zynq Ultrascale+	71
Fig. 5.7 Zedboard power Utilization for heart rate and blood pressure estimation	72

List of Tables

Table 2.1	Hypertension Categories	15
Table 3.1	Sample selection from the database for the study	27
Table 5.1	Resource utilization for different filtering approaches	56
Table 5.2	Preprocessing stage performance	57
Table 5.3	Pearson correlation coefficient for extracted features for 331 PPG recordings	59
Table 5.4	Confusion matrix and classifier performance for hypertension detection	64
Table 5.5	Confusion matrix and classifier performance for cerebral infarction detection	64
Table 5.6	Confusion matrix and classifier performance for cerebrovascular disease detection	65
Table 5.7	Confusion matrix and classifier performance for type-2 diabetes mellitus detection	65
Table 5.8	System performance analysis for binary classification	66
Table 5.9	Performance analysis for different features	68
Table 5.10	Zedboard Resource utilization for binary classifier	68
Table 5.11	Zynq Ultrascale+ Resource utilization analysis for multiclass classification	70
Table 5.12	Resource utilization analysis of the developed prototypes in zedboard	71
Table 5.13	Comparative study on CVD detection from PPG	74
Table 5.14	Comparative study for diabetes classification from PPG	75
Table 5.15	Comparison study of heart rate estimation from PPG	77
Table 5.16	Comparison study of blood pressure estimation from PPG	79

Nomenclature

AE = Absolute Energy

BMI = Body Mass Index

BP = Blood Pressure

BRAM = Block Random Access Memory

CPLD = Complex Programmable Logic Device

CVD = Cardiovascular Disease

DVP = Digital Volume Pulse

FA = False Alarm

FF = Flipflop

FFT = Fast Fourier Transform

FN = False Negative

FP = False Positive

FPGA = Field Programmable Gate Array

HR = Heart Rate

LUT = Lookup Table

LUTRAM = Lookup Table Random Access Memory

MAD = Mean Absolute Deviation

MAE = Mean Absolute Error

RSE = Root Squared Error SPLD= Simple Programmable Logic Device

POC = Point of Care PPG = Photoplethysmogram

SD = Standard Deviation

TN = True Negative

TP = True Positive

XSG = Xilinx System Generator

Chapter 1: Introduction

Point-of-care (POC) systems are becoming essential in this modern era. It helps to detect abnormalities and alarm people about their hidden health conditions at the initial level when a patient consults a physician. Specially for monitoring cardiovascular fitness, digital systems are becoming more prevalent. This is because people may be affected by many cardiovascular diseases without showing symptoms. Photoplethysmogram (PPG) is a non-invasive biosignal that can be analyzed to detect these CVDs. This chapter gives a brief review of photoplethysmogram. After that the applications of PPG signal are depicted. Also, the problem statement of this thesis is shared. This chapter outlines the background in Section 1.1, the present state of the problem in Section 1.2 and specific objectives in Section 1.3. Section 1.4 describes the significance and scope of this research. Finally, Section 1.5 includes an outline of the remaining chapters of the thesis.

1.1 Background

A biosignal obtained from the body, the photoplethysmogram shows changes in blood volume [1], [2]. Being a simple optical method, PPG is used to find changes in blood volume in peripheral circulation. It is an inexpensive, non-invasive technique that measures skin surface parameters. It measures how much light is reflected or absorbed by human tissues. This optical waveform is sometimes referred to as a digital volume pulse (DVP) [3]. PPG is linked to changes in blood volume in the microvascular bed of tissue, which contains important details about the neurological, respiratory, and cardiovascular systems [4]. The toe and fingertip are usually selected for measuring the PPG signal along with the earlobe, wrist, forearm, and forehead [5] as these areas are suitable for measuring light absorption by blood. The PPG signal is an electrical signal produced based on the volume of blood or in another way total absorption of light.

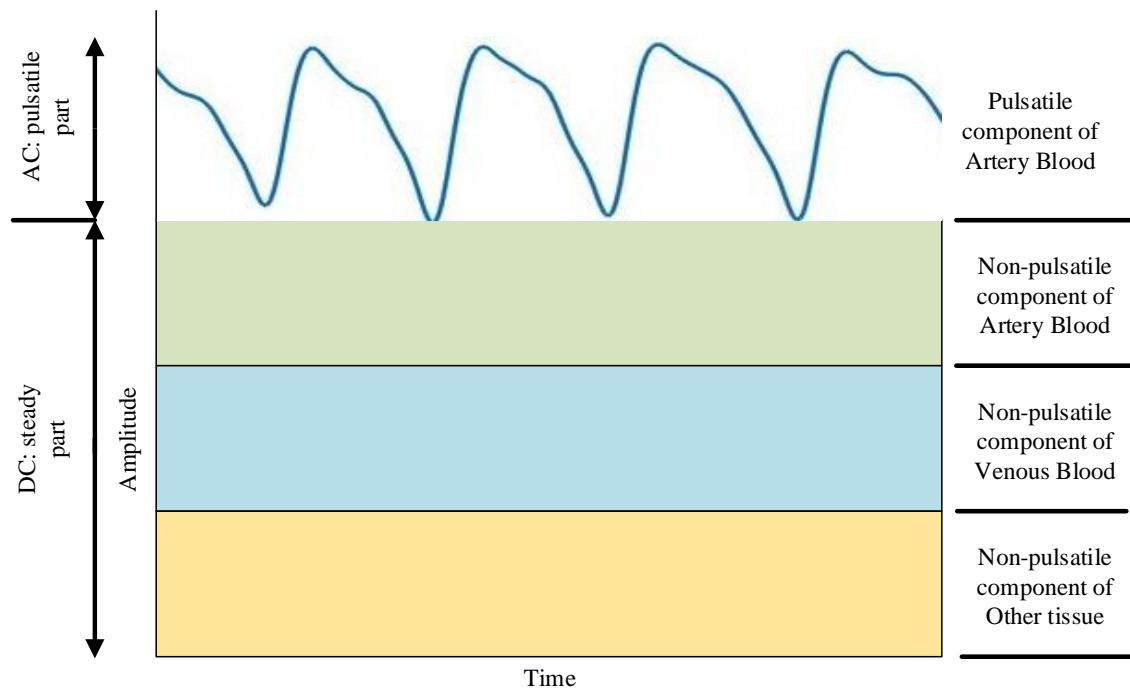


Fig. 1.1 AC and DC component of a PPG signal

Pulsatile (AC) and superimposed (DC) components make up the PPG signal which is shown in Fig. 1.1. The fluctuations in blood volume caused by heartbeats give the AC component, whereas the sympathetic nervous system activity, breathing, and temperature control shape the DC component [4]. The systolic and diastolic phases of phasic cardiac activity, represented by the AC's systolic and diastolic components, cause changes in blood volume. The pulse wave's systolic peak occurs at the end of the systolic phase (also known as the "rise time"), which starts with a valley. Another dip at the diastolic period's conclusion indicates the pulse wave's termination. Using features like rising time, amplitude, and shape, the ensuing waveform graphed from this data can forecast vascular changes in the bloodstream.

The primary light source for PPG sensors is typically an infrared light emitting diode (IR-LED) or a green LED. While green light is typically used to calculate the absorption of oxygen in oxyhemoglobin (oxygenated blood) and deoxyhemoglobin (blood without oxygen present), IR-LEDs are more sensitive for measuring the flow of blood that is more deeply concentrated in certain parts of the body, such as the muscles [6]. For exact measurement of changes in blood volume in the microvascular tissue bed, the light source, specifically the

wavelength, should absorb blood more thoroughly than other tissue constituents. Shorter wavelengths of light are strongly absorbed by melanin, whereas longer and ultraviolet wavelengths of light are absorbed by water [7]. As a result, PPG sensors often use red and near-IR light as their light sources. However, as green light is better absorbed by haemoglobin and oxyhemoglobin than red light [8], more and more devices began to employ this wavelength. A better signal with less noise was the consequence of this. As a result, green LED light is chosen and most frequently employed despite alternatives since it can measure things more precisely because it can penetrate tissue more deeply. The general PPG operating principle is shown in Fig. 1.2.

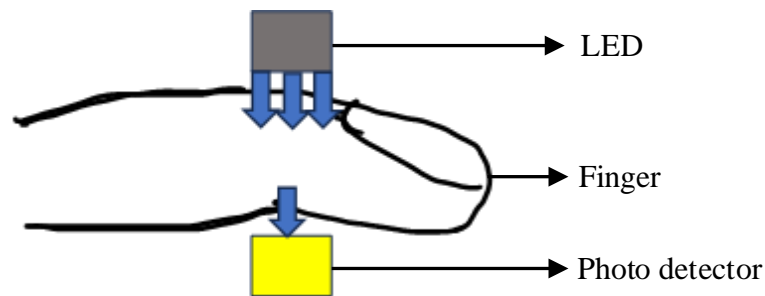


Fig. 1.2 PPG acquisition process

In its simplest form, it needs a light source to illuminate the tissue and a photodetector to track minute changes in light intensity caused by changes in perfusion in the catchment volume. PPG uses low-intensity infrared green (IR) light from the LED source. When light passes through biological tissues, it is absorbed by venous and arterial blood, skin pigments, and bones. PPG sensors can detect variations in blood flow as changes in light intensity because blood more strongly absorbs light than the surrounding tissues. The amount of blood flowing through the blood vessels is inversely correlated with the voltage signal from PPG. Using this technique, even minute variations in blood volume can be identified with higher precision.

The recorded PPG signal can be examined for blood-based health monitoring systems due to its link with blood. The volumetric change of blood can indicate a number of heart-related characteristics since the heart regulates blood pumping. Therefore, PPG can be utilized for heart checks and health

monitoring, significantly improving the healthcare system [9].

1.2 Present State of the Problem

As the medical field is developing with the development of new technologies, PPG is also utilized more for health monitoring. New wearable devices are being designed which provides multiple functionality. The wearable device basically works on the principle of PPG signal. Hence, study on more health parameters and disease detection from PPG signals will benefit medical technology. Utilizing the PPG signal for various disease detection processes will help to identify severe diseases at an early stage and thus will help to start treatment early. Much of the disease detection has been done at the software level. However, digital systems may help to reach a patient's information to doctors and relatives so that precautions and steps can be taken upon serious action. Digital systems may also help to develop Point-of-care (POC) systems. POC systems are hospital or outpatient information systems with bedside terminals or other devices for data collection and entry at the location where patients receive care. It will help to monitor the patient continuously. In an emergency, the system can alert the doctors or other persons engaged for the patients. This will help to save a lot of lives.

Cardiovascular diseases are increasing at an alarming rate in the whole world [10]. Due to people's modern and busy lifestyle, diseases are increasing rapidly. With the spread of coronavirus, cardiovascular diseases have increased among people more rapidly [11]. In most cases, the symptoms cannot be detected until they reach a severe stage. So, early detection is needed for prevention of this disease. Software-based work lacks in instantaneous disease detection or health parameter determination. The need for a digital hardware-based system arises to tackle this issue, which this thesis addresses.

1.3 Specific Objectives

The study's main aim is to develop a digital system that can detect several cardiovascular diseases and predict heart rate and blood pressure from recorded

PPG signals. As software-based disease detection is commonly done, the feasibility of a hardware-based system needs to be checked. Hypertension is one of the most common cardiovascular diseases, which is in focus. Also, two cardiovascular diseases related to blood flow are yet to be explored from the PPG signal. Diabetes is another growing disease in the world that has a connection with cardiovascular diseases. The designed system will try to detect this disease from PPG signal. Also, a system can be designed for heart rate and blood pressure estimation. This will help to check the health condition of subjects during any activity or of a patient for monitoring. So the specific objectives of this thesis are as follows:

- 1) To classify different cardiovascular diseases based on PPG signals & implement the classification model on FPGA.
- 2) To estimate heart rate and blood pressure from FPGA implementation.

1.4 Significance of the Work

PPG signals are already used in wearable devices for oxygen saturation monitoring. Also, some PPG-based devices measure heart rate and blood pressure. If a digital system is developed for classifying cardiovascular diseases from PPG signals, it can be readily integrated with modern e-health systems. Smartwatches and other wearable devices can be used to implement the proposed system for greater convenience. Diabetes measuring from PPG will also help to control the disease in the world in a non-invasive manner. Furthermore, the development of this system will open the door for other diseases to be detected from the PPG signal. It will also help to monitor the heart rate and blood pressure continuously. As the acquisition of PPG signal is very simple through a PPG sensor, there will be scope to detect other health parameters, which can be implemented at the hardware level.

In short, this research will pave the way for the study of many other cardiac conditions and disease analyses along with different health parameters in the future.

1.5 Thesis Outline

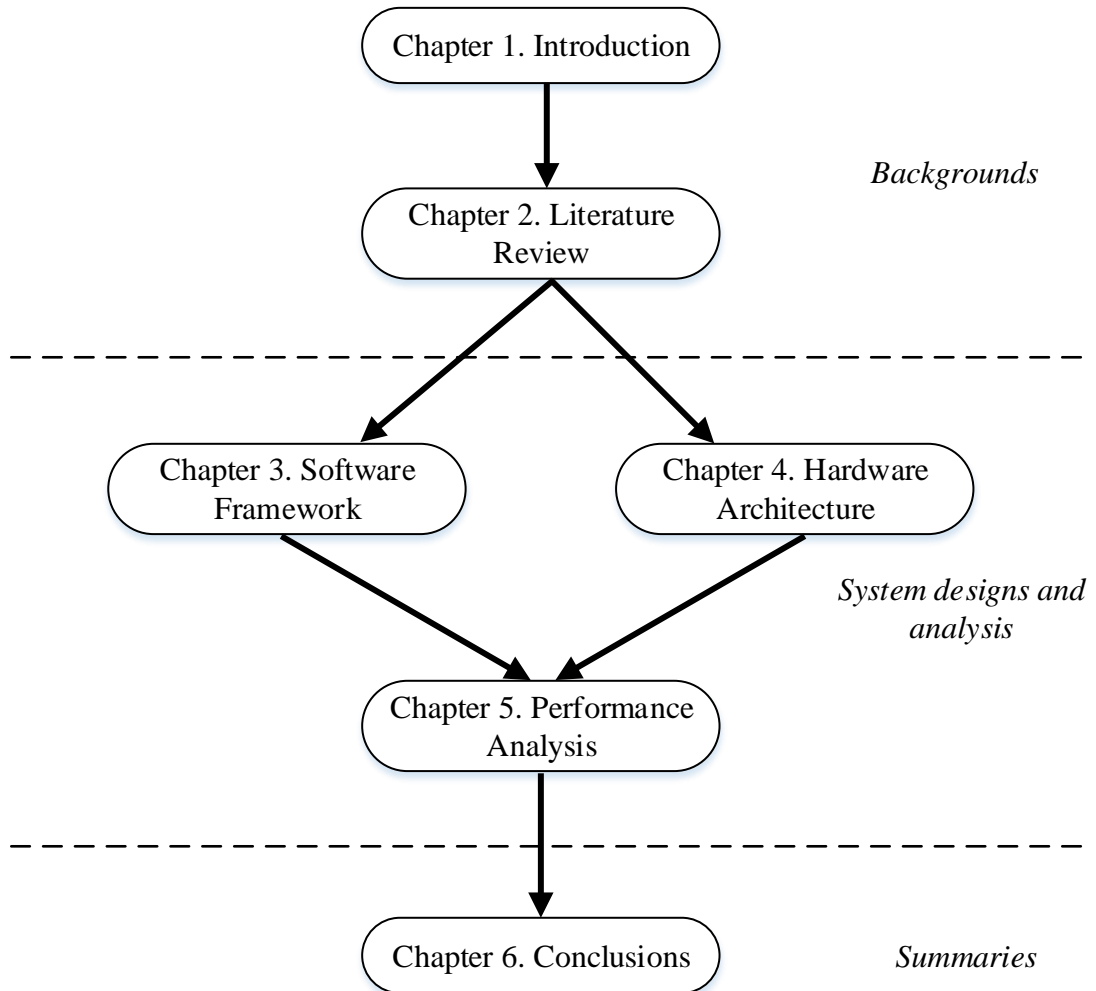


Fig. 1.3 Structure of the thesis

The thesis presents the design of the software framework and the hardware architecture of some systems for detecting cardiovascular disease, diabetes, and heart rate, and blood pressure estimation. The software framework and hardware design are explained in separate chapters. The overall thesis organization is depicted in Fig. 1.3.

The first chapter describes the background of photoplethysmogram signal. The working principle of PPG signal acquisition and its basic characteristics are explained. The problem statement and significance of the study are also

discussed.

Chapter 2 reviews the application of photoplethysmogram signals in various sectors. The previous works on PPG signals are discussed. The main focus has been given to the previous works for classifying cardiovascular diseases, diabetes, heart rate, and blood pressure estimation from PPG signals. PPG-based Hardware system development studies are also analyzed in this chapter.

Chapter 3 shows the software framework of the study. The design procedure on Matlab for developing the preprocessing stage, feature extraction, and classifier is explained in this chapter.

Chapter 4 illustrates the system architecture of hardware design of various subsystems in Xilinx system generator.

Chapter 5 shows the overall results of the software-based system and hardware-based system. It gives an overview of the performances of the designed systems. Also, a comparison between the software systems and hardware systems is depicted. Resource utilization and power consumption analysis are done in this chapter. Finally, the performances of the systems are compared with previous works.

Chapter 6 summarizes the research work and shows the key findings of this work. Limitations of the study are illustrated and some recommendations for future study are mentioned.

Chapter 2: Literature Review

There are many research works on detecting cardiovascular diseases from PPG signals. Also, diabetes detection and heart rate, and blood pressure estimation from PPG signals have been done by many researchers. However, not much work has been done at the hardware level so far. This section shows the application of photoplethysmograms in various health parameter analyses and disease detection. The study is focused on cardiovascular disease along with diabetes detection. Hence in this section, previous works on cardiovascular disease and diabetes are mentioned. Also, the other objective of this study is to determine heart rate and blood pressure from PPG signals. Hence, publications on this topic are also analyzed in this chapter. Recent works focused on hardware implementation are also highlighted at the end.

2.1 Photoplethysmogram Application

Photoplethysmogram has a relation with the change in the volume of blood flow. So, it can be analyzed for blood-related health complications. Heart conditions are correlated with blood problems. Therefore, it can be studied for cardiac system monitoring and heart complication analysis. Also, various diseases are connected with blood and heart, so PPG has the potential to detect these diseases also. Beyond its use in a clinical environment, photoplethysmogram (PPG) is increasingly used for measuring the physiological state of an individual in daily life [12]. PPG is typically used for measuring blood oxygen saturation (pulse oximetry), peripheral vascular tone, and changes in peripheral blood flow according to the respiratory cycle [13]. The general application of PPG is shown in Fig. 2.1.

many wearable devices for measuring oxygen saturation utilize PPG signals. However, nowadays, it is also used in various cardiovascular disease detection, diabetes detection, heart rate variability checking, blood glucose measurement, heart rate, blood pressure measurement, and others. Recent research indicates

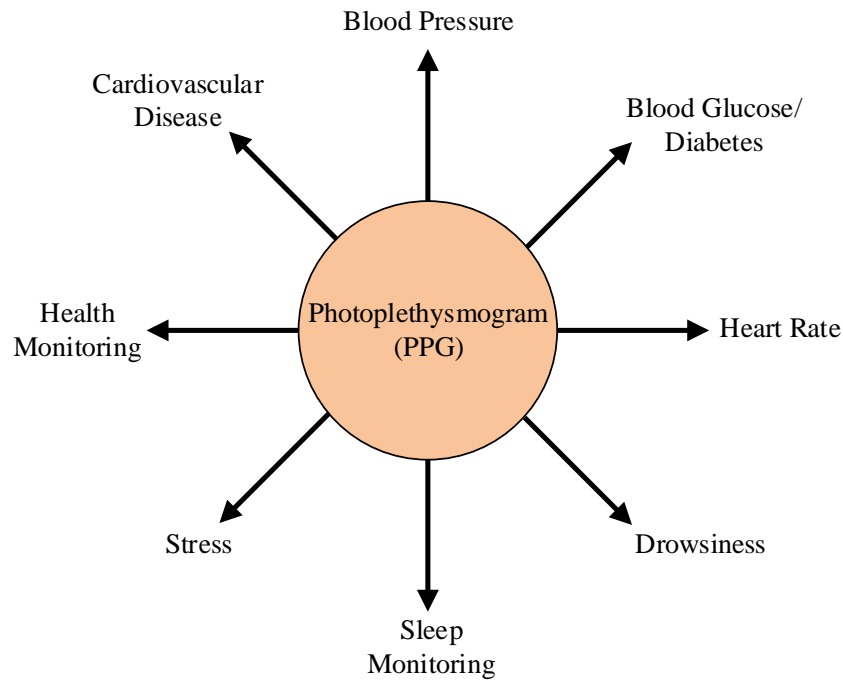


Fig. 2.1 Applications of PPG signal

that Photoplethysmography (PPG) signals carry more information than oxygen saturation level (SpO_2) and can be utilized for affordable, fast, and noninvasive healthcare applications [14]. PPG is used for detecting SpO_2 in various studies and some of them are implemented as wearable devices [15]–[19]. PPG has also been used for drowsiness detection specially during car driving [20]–[24]. In addition, for glucose level detection[25]–[28], respiration rate [17], [29], [30], hemoglobin prediction [31]–[33], stress detection [34]–[36] PPG signals have been used by researchers.

Berwal et al. [15] have proposed a method for improving oxygen saturation estimation accuracy by denoising the infrared and red signals. They have considered the green PPG signal as a reference for baseline wander removal. Entropy, kurtosis, and signal-to-noise ratio have been considered for detecting the signal quality of the signal. They are hopeful about their designed system performance to provide with 1% variance in detecting oxygen saturation. Fachrurazi et al. [16] have developed a wearable pulse oximeter for estimating oxygen saturation. They used a MAX30100 PPG sensor and a microprocessor that processes the PPG signal and sends the oxygen saturation data to android device via bluetooth. It shows an accuracy of 99.72% in predicting oxygen

saturation. Krizea et al. [17] have developed a wearable platform for various health parameter checking including heart rate, respiration rate, and oxygen saturation. The hardware components are implemented on a PCB surface. The system uses a PPG sensor, microcontroller, accelerometer, and a power supply. They have used an IIR Butterworth bandpass filter for denoising the PPG signal. They predicted oxygen saturation by the ratio of AC and DC components of the red and infrared light of the PPG sensor. They achieved a mean percentage error of 0.8% in detecting oxygen saturation. Braun et al. [18] have designed an ear pulse oximeter for oxygen saturation detection. They evaluated their system for 16 healthy subjects and 20 other hypoxemic patients. The results show almost the same output in detecting oxygen saturation with a standard pulse oximeter. Tham et al. [19] have developed an IOT-based health monitoring device for measuring oxygen saturation. They also used the ratio of AC and DC components of red and infrared light to detect oxygen saturation.

Rundo et al. have done multiple studies on drowsiness detection from PPG signals. In [20], the authors proposed a driving assistance system based on an ad-hoc designed biosensor that samples the PPG signal of the driver and correlates it with attention level. They used a 1D Temporal dilated convolution neural network to classify the driver's attention level and achieved an accuracy of 98.71% for the drowsy driver and 99.03% for the wakeful driver. From [21] it is found from the same authors that they have used a 3D semantic segmentation deep network with ad-hoc 1D Temporal dilated convolution neural network and embedded the system on STA1295 Accordo5 core. In this method, they achieved 98.78% accuracy for the drowsy driver and 99.13% for the wakeful driver. In [22], an embedded time-domain hyper-filtering approach is designed which is combined with a 1D Temporal Convolutional architecture with a progressive dilation setup. It has achieved 96% accuracy in drowsiness detection. Again, in [23], the authors designed an embedded platform based on the STA1295 core for drowsiness detection. For analysis, they used data from 40 subjects. Though their system is able to detect drowsiness the performance analysis of their system is lacking. In [24], the author suggests an embedded perceptual ADAS system that uses the well-known hyper-spectral approach, often used to process

2D images, as inspiration for a novel and patented PPG signal processing technique termed "hyper-filtering". The proposed method has achieved an accuracy of 98.71% accuracy in drowsy driver detection.

PPG has been studied for glucose level estimation also. Hina et al. [25] used ensembled boosted trees to detect glucose levels from PPG signal. They designed a preprocessor for the removal of baseline wander and motion artifacts. The system has been implemented in a 180nm CMOS technology which requires an area of 4.5mm^2 and consumes $208\mu\text{w}$ power. It shows a relative difference of 5.83% in glucose level prediction. The same author designed a glucose monitoring system using support vector regression with fine gaussian kernel [26]. In this study also, they used a 180nm CMOS technology which requires an area of 4.0mm^2 and consumes 1.62mw power. It shows a mean absolute relative difference of 7.62%. Mahmud et al. [27] proposed a cost-effective glucose estimation system based on PPG. They used a PPG sensor, galvanic skin response, and temperature sensor to collect data and fed these in a CNN model. However, the device is yet to be explored for testing on a large scale. In [28], Hammour et al. have developed an in-ear blood glucose prediction system. It uses a PPG sensor which is embedded in an earbud. 4 subjects have been used for this study which has achieved an accuracy of 82% in blood glucose level prediction.

The respiration rate is also detected from the PPG signal. Park et al. have designed an earphone-type device for detecting respiration rate from PPG signal [29]. The noise of the PPG signal is removed by denoising the long short-term memory encoder. Gradient element, heart rate, and envelope are extracted from the preprocessed signal as features that are used to design a regression model. The system shows an error of 8.95% in predicting respiration rate. Prasetyo et al. have designed a respiration rate estimation system from PPG signal [30]. They used a PPG sensor to detect changes in heartbeat frequencies. An information filter has been used for denoising the PPG signals. The respiration rate has been detected by the device algorithm and spirometer. Their system has shown an accuracy of 80% compared with the spirometer.

Oxygen hemoglobin is also related to PPG signals as several studies suggested.

In [31], Munadi et al. have designed a non-invasive system for detecting hemoglobin from PPG signals. They used a PPG sensor and a microcontroller for processing the signal. They used the K- nearest neighbor algorithm to achieve 94.01% accuracy and the artificial neural network provided an accuracy of 92.45% in detecting oxygen hemoglobin levels in the blood. Pintavirooj et al. [32] used an optical technique to measure hemoglobin concentration from PPG signal. The hemoglobin concentration will also help to detect anemia disease. They measured the hemoglobin concentration by the modified Beer-Lambert law. An android app is also developed for monitoring glucose concentration. Their system achieved an accuracy of 90.9%. Olakanmi et al. have designed a device for measuring blood hemoglobin based on the hypothesis that the HbO_2/Hb mixture in a given volume of blood significantly absorbs and transmits light in the red and NIR regions of the electromagnetic spectrum [33]. They used a photo spectroscopic sensor and arduino with a display for the hardware implementation. The system achieved an accuracy of 65.07% in detecting hemoglobin levels. However, the system has also detected anemia patients with an accuracy of 93.3%. Mitro et al. designed an AI-enabled smart wristband for detecting stress from PPG signal [34]. The PPG sensor collects the PPG data which goes through a bandpass filter for denoising. The denoised signal is used for extracting four types of features and the SVM algorithm is used for the classifier. The authors have achieved 91% accuracy for the WESAD dataset while 76% accuracy has been achieved for an independent dataset. Nath et al. have designed a smart wristband for detecting stress [35]. However, they used 3 other signals along with PPG for stress detection. Electrodermal activity, blood volume pulse, and skin temperature are also used with PPG signals in their study. They achieved an accuracy of 94% upon collecting the four signals from 40 subjects. Chaowadee et al. [36] have designed a prototype called stress warning unit for measuring stress index from PPG signal. Their system can predict 4 levels of stress based on the stress index value.

This study aims to design a hardware-based system for cardiovascular disease detection and heart rate and blood pressure estimation. In the following

sections, some of the previous works of application of PPG signal in detecting cardiovascular disease with heart rate and blood pressure estimation will be analyzed in depth.

2.2 Cardiovascular Disease Classification

Cardiovascular diseases (CVD), a group of disorders of the heart and blood vessels, are one of the leading causes of death worldwide, taking approximately 17.9 million lives each year [37], [38]. CVD is an umbrella term that covers a range of pathologies, including heart attack, hypertension, stroke, heart failure, myocardial infarction, cerebral infarction, and cerebrovascular disease. Delay in detection and, therefore late treatment can lead to death, which in recent years has increased with the spread of coronavirus. From March 2020 to March 2022, about 1,946,662 deaths have been reported by the National Centre for Health Statistics (NCHS) in the USA [39]. With the advancement in medical technology, it is expected to be in control though the lifestyle, food habits, and lack of physical activity have been worsening the situation. Despite recent developments in medication and management of CVDs, the challenge remains to detect CVDs due to the lack of an appropriate point-of-care system [40].

PPG has great potential to assess age-related changes in arterial stiffness, an accepted cardiovascular risk factor [41]. So, PPG signals have been analyzed for various cardiovascular disease identification. Cheng et al. achieved an accuracy of 98.21% in detecting atrial fibrillation from PPG signal [42]. In the study, the collected PPG is converted to a time-frequency chromatograph of $128 \times 1024 \times 3$ which is fed into convolution neural network (CNN) and long short-term memory (LSTM). They have achieved high accuracy and the model needs 0.00072195 s for atrial fibrillation recognition. Wang et al. used support vector machine (SVM) to detect cardiovascular diseases from PPG signal [43]. Allen et al. have studied to detect peripheral arterial disease (PAD) from PPG signal using a deep learning approach [44]. They have used AlexNet CNN, a deep learning method for detecting PAD into three classes: non-PAD, mild PAD, and major PAD. However, other CNN models were not analyzed in this study. Also,

the distribution of the three classes was unbalanced in their study. Fahoum et al. have detected coronary artery disease (CAD) from PPG signal collected from 360 subjects [45]. They have used the naïve bayes classifier and got an accuracy of 94.44%. Paradkar et al. also have studied the detection of CAD using the MIMIC II database [46]. They have used wavelet approach and got a sensitivity of 85% and specificity of 78%. The accuracy of their detection system is lacking in their study. Ave et al. have developed a device that works with a phone or tablet wirelessly through Bluetooth connection [47]. The system analyzes the PPG signal and gives the warning of cardiovascular disease in color code. However, the performance analysis and resource and power analysis of the system are lacking. Ramachandran et al. have cardiovascular risk level detection based on PPG signal [48]. The authors have used nine statistical features along with singular value decomposition and different wavelets and the study has achieved an accuracy of 97.24%. So far, PPG-based studies on cardiovascular disease detection have been analyzed. This thesis focused on classifying hypertension, cerebral infarction, and cerebrovascular disease from PPG signals. Hypertension is a common cardiovascular disease while the other two diseases are related to blood flow in the brain.

2.2.1 Hypertension

Hypertension is one of the leading cardiovascular diseases as the number of patients has almost doubled in recent years [49]. Hypertension is the medical term used to describe high blood pressure. High blood pressure causes the death of 7.6 million people around the world annually which is almost 13.5% of the total death [50]. High blood pressure affects more than 1 billion people worldwide and accounts for more than 20% of all cardiovascular diseases [51], [52]. Normal blood pressure is necessary to ensure the proper flow of blood from the heart to body organs and tissues. Blood pressure is related to many cardiovascular diseases. Hypertension is classified according to the blood pressure level. Another important parameter is heart rate which means the speed at which the heart beats. It is also an important indicator of overall health

Table 2.1. Hypertension Categories

Blood pressure category	Systolic Blood pressure (mm Hg)	And/ Or	Diastolic blood pressure (mm Hg)
Low	<90	Or	<60
Normal	<120	And	<80
Elevated	120-129	And	<80
Stage 1 hypertension	130-139	And	80-89
Stage 2 hypertension	>140	Or	>90
Hypertensive crisis	>180	And/Or	>120

as when the heart beats too fast or slow, that can be a vital sign of an unhealthy heart or other body problems. So, the detection of these heart parameters is essential for health condition analysis and to take immediate actions in case of emergency.

Normal blood pressure level, also known as normotension, is generally considered if SBP<120 mm Hg and DBP< 80 mm Hg [53]. If it exceeds a certain range, then it is called hypertension which is a multifactorial disease involving a broad array of risk factors and targets different organ injuries and cardiovascular events [54]. Blood pressure is classified into different stages according to the level. Table 2.1 shows the different stages of hypertension alongside their blood pressure level. Among the blood pressure category of Table 2.1; stage 1, stage 2, and hypertensive cases are considered as hypertension, while the elevated category can be considered a warning to future hypertension. Even though American Heart Association guidelines from 2017 advise lowering the threshold for hypertension from 140/90 to 130/80 mm Hg [55]. There are some research works on detecting hypertension from PPG signal which is related to blood pressure as well. Liang et al. used 10 PPG features and risk stratification approach for hypertension detection [56]. They achieved a maximum F1 score of 92.31% in the case of the normotension vs. hypertension trial. When compared to non-severe hypertension, the risk stratification technique performed better at identifying severe hypertension. Frederick et al. achieved a maximum of 80% accuracy using a deep learning model for detecting hypertension from PPG signal [57]. They have achieved a maximum accuracy of 80% for AvgPool_(VGG-16) approach. The detection accuracy of other approaches is not so high either. Martinez-Ríos et al. applied different machine

learning algorithms to detect hypertension from PPG signal [58]. They used 22 features and achieved an accuracy of 71.42% accuracy using the SVM classifier. Most of the features they have used are physical variables rather than features from the signals. Sadad et al. have used decision trees, naïve bayes, and support vector machines along with convolutional neural networks for detecting hypertension [59]. This is a multiclass classification approach for detecting 4 stages of hypertension. They have achieved 99.5% accuracy for the decision tree approach. Nour et al. also achieved 99.5% accuracy in hypertension detection using a decision tree approach from the same PPG BP dataset [60]. Welykholowa et al. have found that PPG along with another bio signal such as ECG can improve the accuracy of hypertension detection [61].

2.2.2 Cerebral Infarction

Cerebral infarction is a medical condition that occurs when the blood flow to the brain is interrupted by issues with the arteries that supply it. It is also called ischemic stroke, which leads to the death of brain cells due to deprivation of oxygen and other nutrients caused by a lack of blood supply. The brain receives less blood due to atherosclerosis, which is the buildup of fatty plaque in the blood vessels. This buildup may cause a blood clot or thrombus in an artery that supplies the brain or elsewhere in the body. A cerebral embolism can result from a piece of this clot breaking off and migrating to the blood vessels in the brain. People having high blood cholesterol may be affected by cerebral infarction. Being a frequently occurring disease, cerebral infarction is characterized by poor prognosis, high disability, and fatality rate [62]. 20% ischemic strokes are caused by cerebral infarction [63]. Risk factors for this condition include having diabetes, smoking, drinking too much alcohol, being overweight, and having a family history of heart disease. However, no study has been done yet to detect cerebral infarction from PPG signals.

2.2.3 Cerebrovascular Disease

Cerebrovascular disease is another type of CVD that represents a group of conditions that affect the blood flow and blood vessels in the brain. Blood vessel narrowing (stenosis), clot formation (thrombosis), artery blockage (embolism), blood vessel rupture (hemorrhage) etc. can be causes of this serious issue. Cerebrovascular disease is the fifth leading cause of death in the United States, causing 486 fatalities per million people [64]. The spread of coronavirus has increased the rate in recent years, and it has been found to be associated with cerebrovascular disease [65]–[67]. Zhu et al. have studied on detection of cerebrovascular disease detection from PPG signal using the wavelet transform method [68]. The study showed a good feasibility of detecting cerebrovascular disease in this method from PPG. Both cerebral infarction and cerebrovascular disease can lead to severe damage, while the ultimate result can cause death. Therefore, the detection of these diseases at an early stage is necessary.

2.2.4 Diabetes Detection

Another vital disease that is rapidly growing in the world is diabetes. It is a health condition that refers to the presence of high blood sugar. In this case, the body cannot make enough insulin or use it properly due to the incapability of beta cell production in the pancreas. Being a chronic disease, it tends to increase the risk of other diseases that negatively impact the brain, kidneys, eyes, and heart [69]. There are two main types of diabetes: type 1 and type 2. Type 1 diabetes is believed to be caused by an autoimmune reaction and develops early in life. As a result of the body's immune system attacking the insulin-producing islet cells in the pancreas, this condition prevents the pancreas from producing insulin. Type 2 diabetes develops over the course of many years and is related to lifestyle factors such as being inactive and carrying excess weight. In this type, the pancreas makes less insulin than used to, and the body becomes resistant to insulin. So, even though the body has insulin, it is unable to use it. Diabetes is correlated with cardiovascular diseases as people with diabetes are likely to

develop cardiovascular diseases 2 to 4 times more than others [70]. Detection and early-stage control of diabetes can prevent the build-up of cardiovascular diseases and help to grow consciousness about health. This study focuses on type 2 diabetes detection alongside cardiovascular diseases as the dataset provides PPG signals of patients with type-2 diabetes.

Some works have been done to detect diabetes from PPG signals. Prabha et al. have used a radial basis function (RBF) kernel SVM-based algorithm to detect diabetic mellitus from PPG signal [71]. They used PPG signals collected from 217 subjects. 104 MFFC features have been extracted and along with these, 3 physical features have been used for classification. An accuracy of 92.28% has been achieved by their system. Qawqzeh et al. have diagnosed diabetes from PPG signal using 3 predictors [72]. They have achieved 92.3% accuracy using the logistic regression method. However, there was an imbalance between diabetic and non-diabetic subjects used in the study. Susana et al. have achieved 98% accuracy in detecting diabetes from PPG signal using the ensemble bagged tree algorithm [73]. This work has used 400 raw datasets of blood glucose levels measured with PPG signal. Hettiarachchi et al. achieved an accuracy of 79% in predicting type 2 diabetes [74]. The authors have applied different machine learning algorithms, but linear discriminant analysis (LDA) achieved the maximum accuracy. Reddy et al. [75] have achieved 89% accuracy by SVM approach in detecting diabetes using 31 features from PPG signal.

2.3 Health Parameter Estimation

Various health parameters can be estimated upon analyzing the PPG signals. Oxygen saturation, body temperature, heart rate, and blood pressure are predicted from PPG signals. In this study, blood pressure and heart rate, two important health parameters are selected to be estimated from the PPG recordings.

2.3.1 Blood Pressure Estimation

The phrase "blood pressure" is crucial for tracking a person's health conditions. Blood pressure is a measurement of the force of the blood against the arteries [76]. It is necessary to monitor the blood pressure of heart disease-related patients regularly as uncontrolled high blood pressure can cause heart failure, kidney disease, eye disease, dementia, and other health issues. Both low and high blood pressure can cause serious issues in the human body. Even a healthy person can be a victim of high or low blood pressure with almost no or insignificant symptoms. Hence, blood pressure is an important health parameter that is necessary to check frequently.

PPG has been used in many studies for blood pressure detection. Yue et al. have used SVM method to predict blood pressure using 9 features from PPG signal [77]. Systolic pressure has a mean error + standard deviation of 11.6415 ± 8.2022 mmHg and diastolic pressure has a mean error + standard deviation of 7.617 ± 6.7837 mmHg. Samimi et al. have used 21 morphology features from PPG signal of 30 patients for blood pressure estimation [78]. They achieved a mean absolute error (MAE) of 3.32 for DBP and 7.41 for SBP. Slapnicar et al. have proposed a system for blood pressure detection based on PPG [79]. They used the MIMIC database for their study and achieved the lowest MAE of 8.57 mmHg for SBP and 4.42 mmHg for DBP using the ensemble of regression trees. There are some hardware-based blood pressure estimation works as well. Jeremy et al. implemented a digital system for estimating blood pressure using a fast digital chip of 3.97 mm^2 size and having a power consumption of 15.62 mW [80]. Their system achieved a maximum blood pressure error of ± 6 mm Hg from PPG signal of 8 patients. Bo et al. designed a cuffless blood pressure prediction device utilizing ECG and PPG signal [81]. The system is implemented in heterogeneous DSP and FPGA platforms though the accuracy and therefore the validation of the system is lacking. Rehman et al. designed a BP estimation processor which is implemented in a 180nm 1P6M CMOS process having an area of 3.45 mm^2 and $73 \mu\text{W}$ power consumption [82]. Sheeraz et al. have utilized Artix-7 FPGA to develop a blood pressure estimation system from the PPG signal of 25 subjects [83]. Using the decision tree algorithm, it has achieved

96.2% accuracy consuming 18.23 μ W power. However, this paper lacks the resource utilization analysis of the designed system.

2.3.2 Heart Rate Measurement

Heart rate is also an essential parameter for physiological and pathological condition analysis. Detection of abnormal heart rate may indicate various diseases. The heart generally pumps the blood at about 60 to 100 beats per minute (bpm). An irregular heartbeat indicates different complications in the heart. Tachycardia is characterized by a heart rate exceeding 100 bpm, and bradycardia by a heart rate below 60 bpm [84]. Different types of arrhythmias such as atrial fibrillation, atrial flutter, ventricular fibrillation etc. can be detected based on heart rate variability [85]. So, heart rate measurement can help to detect the arrhythmia types during emergency situations.

Heart rate prediction from PPG signals is also studied by researchers. Yuntong et al. [86] have combined signal processing and machine learning and achieved 5% error in heart rate prediction. The authors have used 10 to 20 features in their study for different trials. Attila et al. [87] used a convolution neural network for predicting heart rate. They have got MAE of 7.47 bpm for the WESAD dataset and an MAE of 7.65 bpm for PPG-DaLiA dataset. Chang et al. have used deep learning to design a heart rate detection approach which achieved an average absolute error of 1.61 bpm [88]. They used 12 records of PPG signals collected during various physical activities from the IEEE CUP training dataset. Using only 12 PPG recordings limits the validation of their study. Motin et al. achieved an average absolute error of 1.85 bpm for 23 PPG recordings during physical exercise [89]. They used Wiener filtering-based denoising algorithm to estimate heart rate. Karim et al. [90] have designed an FPGA-based heart rate calculation system using Xilinx system generator though the accuracy and performance analysis of their designed system is missing. Burrello et al. have designed a PPG-based heart rate monitoring system using microcontroller [91]. They have used temporal convolution network (TCN) and achieved an MAE of 3.84 bpm. However, TCN requires a large amount of data to be accurate and also they

trained their model based on two datasets. Ngoc-Thang et al. have developed a wearable device that uses a PPG sensor to collect PPG data and transfer to a microcontroller [92]. Microcontroller selects the high-quality PPG signal and a deep learning algorithm is implemented and the software-based design shows the estimated heart rate on the display. Kuo et al. have developed a wearable device based on sensor and Arduino for heart rate monitoring [93]. They applied a new Fuzzy algorithm in their system which can show the heart rate in mobiles through Bluetooth connection. Pamuk et al. have used a PPG sensor and a Raspberry Pi microcomputer to determine heart rate variability [94]. However, the preprocessing and heart rate determination was done at the software level. Also, they applied their system only on one subject for validation which is a major limitation in terms of generalization.

2.4 Hardware-based Implementation

Nowadays digital systems are developing and becoming popular due to their cost-effectiveness and their usage as a point-of-care device [95]. Many platforms are available for digital hardware-based designs like field programmable gate arrays (FPGA), complex programmable logic devices (CPLD), simple programmable logic devices (SPLD), microcontrollers, and others. There are some research works of implementing PPG signals for various purposes at the hardware level. Different sensors are commonly used for PPG data acquisition in different studies. Microcontroller has been used for heart rate and blood pressure estimation, hemoglobin prediction, drowsiness detection, and other applications [22], [91], [96], [97]. In [22] and [96], an embedded system for drowsiness detection of car drivers has been implemented using a microcontroller. In [91] and [97] microcontroller has been used to detect heart rate from PPG signal. Arduino is also used for hardware-based system design in some studies on the applications of PPG signals [98]–[101]. In [98], arduino has been used to implement a system for the detection of smokers and non-smokers from PPG signal. In [99], a pulse oximeter for measuring oxygen saturation is

developed using arduino. In [100] and [101] arduino has been used for health monitoring and continuous blood pressure measurement. Raspberry Pi is also used in a few applications like PPG signal compression, signal quality assessment, and detecting some bio parameters [94], [102]–[104]. In [94], Raspberry Pi is used to detect heart rate variability from PPG. In this study, 10-minute data of PPG signal has been recorded from a 24-year-old male and 5 time domain features have been extracted from the recorded signal. The change in these features according to different emotions is also studied. [102] and [104] have used Raspberry Pi for signal quality assessment and data reduction of PPG signal. [102] has achieved an accuracy of 97.09% in PPG signal quality assessment while [104] has achieved 95% compression ratio in data reduction. [103] have used this hardware system for blood pressure measurement. This study has used the MIMIC II and MIMIC III databases and extracted 20 features from the PPG signals. The authors have achieved a low latency and required less memory for this work.

In most cases, the hardware system is limited to acquiring the signal using a sensor and some preprocessing using microcontroller or Arduino. The main objectives have been achieved at the software level. However the nature of cardiovascular diseases requires a fully digital hardware system for quick identification and getting alerts about the disease. There are some studies that are fully hardware-implemented work based on CMOS processor or FPGA [80], [82], [83], [90]. However, these works sometimes lack performance or resource and power utilization analysis.

2.5 Summary and Implications

State-of-the-art- analysis verifies the use of PPG signals in multi-purpose applications. Health monitoring, oxygen saturation checking, stress detection, and drowsiness detection are common applications of PPG signals. PPG is also used for different cardiovascular disease detection such as hypertension, coronary artery disease, peripheral arterial disease, etc. Though there are some studies on hypertension detection from PPG signal they are done at the software

level. On the other hand, two important cardiovascular disease cerebral infarction and cerebrovascular disease detection from PPG signal has not been explored yet in previous studies. Hence, there is scope to detect these diseases from PPG. Diabetes is also detected from PPG by various researchers but they are at the software level. Blood pressure and heart rate estimation is another common application of the PPG signal. Again, most of these works are at the software level. Few works have been done at the hardware level based on PPG signal but they have some limitations in their studies as described in the literature review. Therefore, this study aimed to develop a hardware-based digital system for detecting hypertension, cerebral infarction, cerebrovascular disease, and diabetes. Furthermore, a system will be designed to detect heart rate and blood pressure from PPG.

Chapter 3: Software Framework

A software-based simulation framework is needed to benchmark a digital PPG processor, which is the final goal of this thesis. This section presents the methodology of the system at the software level. At first, a dataset is selected, and PPG recordings are selected. Then the selected signals go through a preprocessing stage consisting of filters. Features are extracted from the preprocessed signals and used for designing a suitable classifier.

3.1 Complete Methodology

This study aims to develop a hardware-based prototype for various disease detection and heart rate and blood pressure estimation. As software-based designs are commonly practised, the systems have been designed at the software level first. The overall methodology is shown in Fig. 3.1.

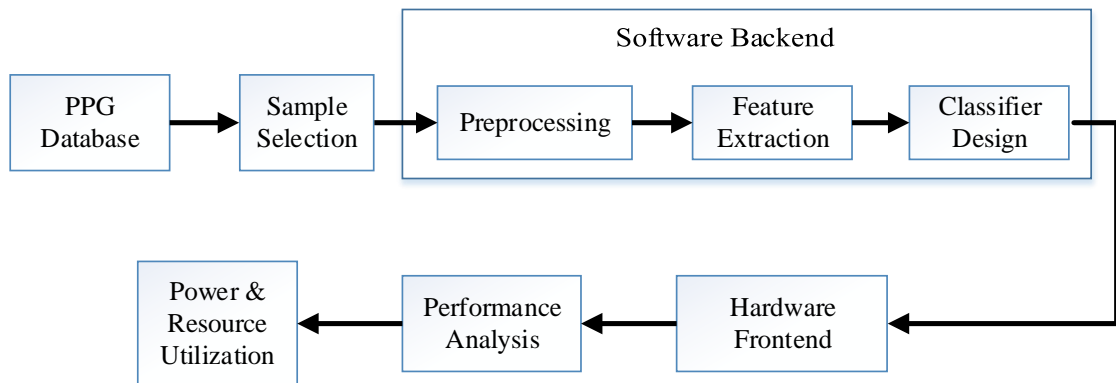


Fig. 3.1 Overall methodology of the study

It shows that the design procedure needs a PPG dataset to be selected first. From the dataset, proper signals are needed to be selected for disease detection. Then the selected dataset needs to be normalized. Then the normalized signals will go through a preprocessing stage for denoising the signals. Then the preprocessed signals will be used for feature extraction. The extracted features will be utilized

for classifier design. From the classifier, the disease will be detected, and heart rate and blood pressure will be estimated.

3.2 Dataset Selection

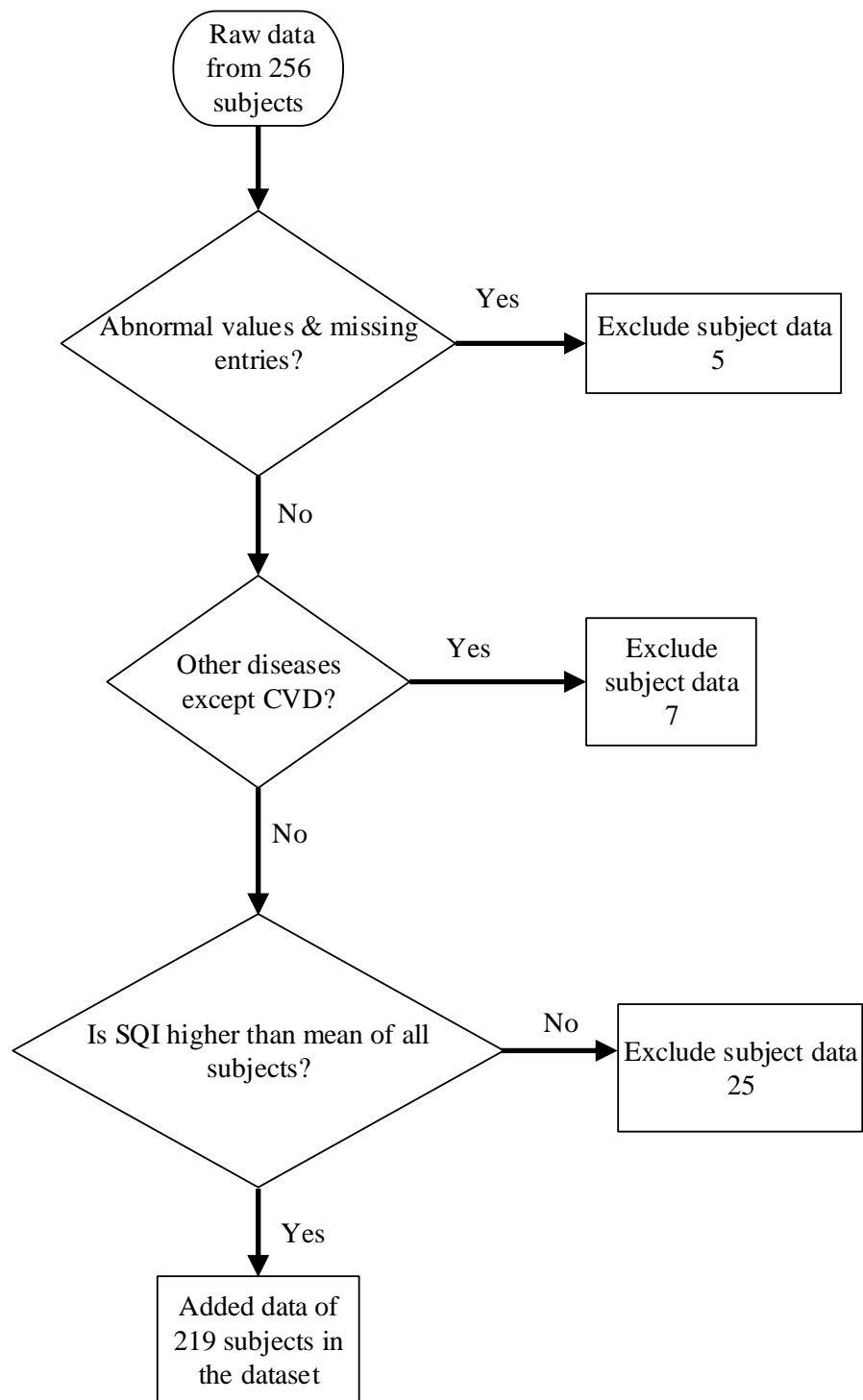


Fig. 3.2 PPG data acquisition process in the PPG BP dataset

For this study, an open-access “PPG BP Database” has been chosen [105]. The database contains 657 PPG data segments from 219 subjects. Among the subjects, 105 are males, and the rest are females. Their age covers the range of 20 to 89 years. A detailed description of the dataset is presented in Appendix A. The data selection process is shown in Fig. 3.2.

Each subject has 3 segments of PPG signal, each of 2.1 s in length. The dataset contains information on different CVDs like hypertension, cerebral infarction, cerebrovascular disease, and diabetes of the subjects. All the 3 segments went through a signal quality evaluation process. The signal quality index has been found to have a connection with the quality of the PPG waveform [106]. The signal quality index (SQI) of each signal was provided with the dataset. The SQI was measured after data collection to evaluate against the classification threshold of excellent, acceptable, or unfit PPG signals according to the following equation:

$$S_{SQI} = \frac{1}{N} \sum_{i=1}^N \left(x_i - \frac{\mu_x}{\sigma}\right)^3 \quad (3.1)$$

where, N is the sample number of the PPG signal, μ_x and σ are empirical estimates of the mean and standard deviation of x_i , respectively.

3.3 Segment Selection

The data set comprises various diseases, such as hypertension, diabetes, cerebral infarction, and cerebrovascular disease. It also includes blood pressure, heart rate, age, height, and body mass index (BMI) of the individual patient. According to the blood pressure level, hypertension has been labelled into four categories: normal, prehypertension, stage 1 hypertension, and stage 2 hypertension. Other diseases are labelled into 2 categories: normal or unhealthy. Cerebral infarction, cerebrovascular disease, hypertension, and type 2 diabetes have been chosen for the binary classification approach. Among the 219 subjects, 38 subjects were diagnosed with type 2 diabetes, 54 subjects were identified with stage 1 or stage 2 hypertension, 20 subjects were diagnosed with cerebral

Table 3.1. Sample selection from the database for the study

	Available in database	Selected for the study(SQI \geq 0.8)
Total subjects	219	
Available segments	657	331
Cerebral infarction	20 subjects 60 segments	23 segments
Cerebrovascular disease	25 subjects 75 segments	42 segments
Hypertension	54 subjects 162 segments	69 segments
Type 2 diabetes	38 subjects 114 segments	65 segments

infarction, and 25 subjects were identified with the problem of cerebrovascular disease. As each subject has PPG data of 3 segments, there are in total 114 segments for type 2 diabetes, 162 segments with hypertension, 60 segments with cerebral infarction, and 75 segments with cerebrovascular disease. However, the signal quality index is also considered for this study. As high-quality signals will help to provide the result more accurately, it is decided to consider only the signals having SQI equal to or greater than 0.8 for this study. In this process, 65 segments of subjects have been found to have type 2 diabetes, 69 segments with hypertension, 23 subjects with cerebral infarction, and 42 subjects with cerebrovascular disease. These PPG signal samples will be used for the detection of diseases through binary classification. Table 3.1 depicts the subject selection process for this study.

Again, for multiclass classification, combinations of different diseases have been considered. For this study, PPG signals having SQI equal to or above 0.8 have been considered. After screening through the dataset, 331 segments from 657 segments have been found to fulfil this criterion. From this list, it has been found that 165 segments belong to normal conditions, 17 segments have only diabetes mellitus type-2, 20 segments have only cerebral infarction, 32 segments with only cerebrovascular disease, 34 segments with stage 1 and 2 hypertension, 18 segments having hypertension and diabetes mellitus type-2, 4 segments with cerebrovascular disease and hypertension, 10 segments with cerebral infarction

and cerebrovascular disease, and 31 segments with diabetes mellitus type-2 and prehypertension. There are no segments for diabetes with cerebral infarction, diabetes mellitus type-2 with cerebrovascular disease, and cerebral infarction with hypertension. So, for developing a proper classifier with training and testing data, the cases having a minimum of 17 segments have been considered, as other cases have very few segments. A total of 7 classes have been found for this study. The segment selection process for the study is depicted in Fig. 3.3.

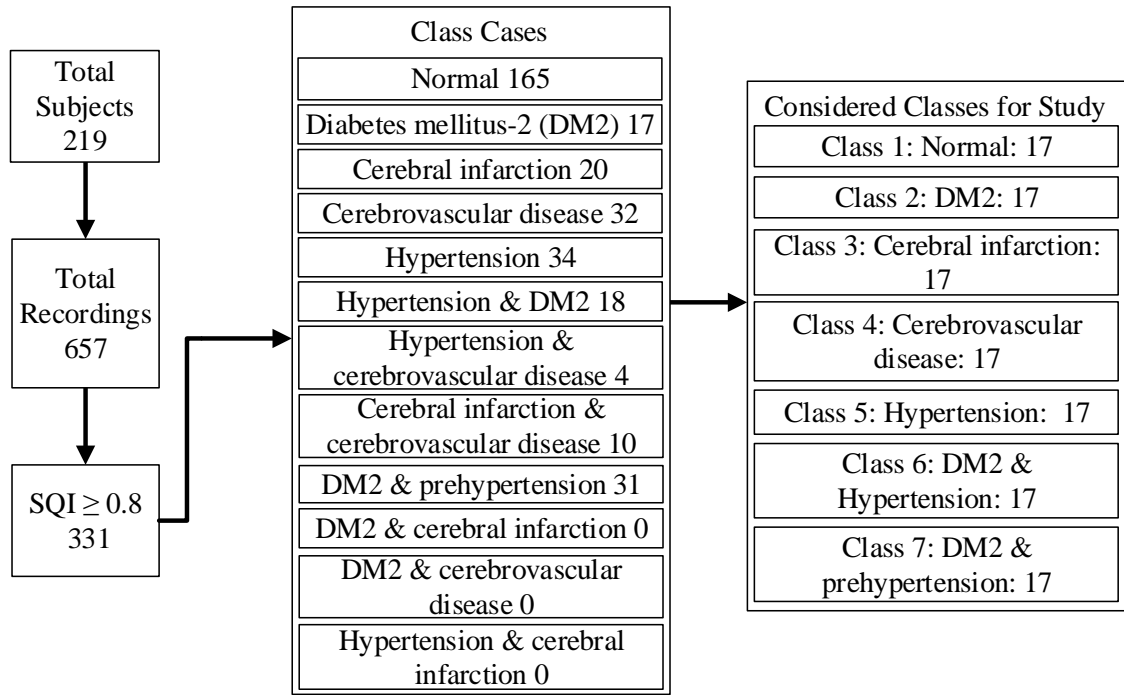


Fig. 3.3 Preprocessing stage of proposed the system

For the heart rate and blood pressure detection, all segments with SQI equal to or over 0.8 will also be considered.

3.4 Preprocessing

Biosignals are generally contaminated with different noises which hinder the proper analysis of the signal. PPG is also affected by various noises like motion artifacts, baseline wander, power line noise etc. [107]. To remove the noises, a preprocessor needs to be designed first. The signal is first normalised before giving input to the preprocessor, which is designed using low and high-pass filters. For the normalization, the signal is divided by the typical maximum

value of the PPG signal, which is 5 mV. The unit of the PPG signal amplitude is not given in the dataset. So considering the unit in μV the signals are divided by 5 mV or 5000 μV . As the PPG signal ranges from 0.5 to 15 Hz [108], removing the frequency component below 0.5 Hz and above 15 Hz from the signal is necessary. FIR and IIR filters are usually chosen to remove noises from digital systems. IIR filters become unstable, and the impulse response is not absolutely summable. Also, they are hard to implement using fixed-point arithmetic. So, FIR filters are selected for this study. FIR filter has the advantage of attaining an exact linear phase. They are simple to implement and also suited to multi-rate applications. The response of an FIR filter is as follows:

$$y(n) = \sum_{i=0}^N b_i x(n-i) \quad (3.2)$$

where, $x(n)$ is the input signal, $y(n)$ is the output signal, N is the order of the filter, & b_i is the impulse response at i_{th} instant for $0 \leq i \leq N$ of N_{th} order filter.

To remove the baseline wander noises a high pass filter of 0.5 Hz is designed while a low pass filter of 15 Hz has been developed to remove the high-frequency noises caused by electromyogram (EMG) and motion artifacts. Both the FIR filters have been designed in MATLAB, while the order of the filters has been selected so that the FFT of the preprocessed signals shows the removal of all undesired noises. In the case of the high pass filter order is 50, while for the low pass filter, the order is 81. Choosing lower filter orders does not attenuate the noise perfectly. The FFT response shows more noise spikes for filter orders lower than 50 and 81 for the high-pass and low-pass filters, respectively. Again, choosing a higher filter order number than the selected ones will require more resources, and thus, more power will be consumed.

3.5 Feature Extraction

The signals are used to extract various features for implementing them in the classifier later. In this study, it is necessary to choose the hardware-friendly

features. As the final target of this thesis is to implement the system in hardware, features must be chosen accordingly. For this purpose, nine statistical features: mean, mean absolute deviation (MAD), sum, absolute energy (AE), root mean square (RMS), standard deviation (SD), variance, skewness, and kurtosis are selected. These features are easy to implement in the FPGA board and consume less resources and power. Hence, they are selected for this study. The description of these features is given below:

Mean: Mean is the average value of all the samples in a signal. It can be expressed by the following equation:

$$mean, \bar{x} = \frac{1}{N} \sum_{i=1}^N x_i \quad (3.3)$$

Mean Absolute Deviation: The mean absolute deviation (MAD) is the mean or average difference between each data value and the mean of the dataset. The following equation presents it:

$$MAD = \frac{1}{N} \sum_{i=1}^N |x_i - \bar{x}| \quad (3.4)$$

Sum: Sum is the summation of all the samples of a signal. It is expressed by the following equation:

$$Sum = \sum_{i=1}^N x_i \quad (3.5)$$

Absolute signal energy: Absolute signal energy (AE) is a way to represent the strength of the data and is defined as follows:

$$AE = \sum_{i=1}^N x_i^2 \quad (3.6)$$

Root Mean Square: Root Mean Square (RMS) is the square root of the arithmetic

mean of the squares of a group value. It is defined by the following:

$$RMS = \sqrt{\frac{1}{N} \sum_{i=1}^N x_i^2} \quad (3.7)$$

Standard Deviation: Standard Deviation (SD) is a measure of the dispersion of the data in relation to the mean. The equation expresses it:

$$SD, \sigma = \sqrt{\frac{\sum_{i=1}^N (x_i - \bar{x})^2}{N}} \quad (3.8)$$

Variance: Variance means the variability that measures the spread between numbers in a dataset. It is defined as follows:

$$variance, \sigma^2 = \frac{\sum_{i=1}^N (x_i - \bar{x})^2}{N} \quad (3.9)$$

Skewness: Skewness is a measurement of the distortion of symmetrical distribution or asymmetry in a data set. It is expressed by:

$$Skewness = \frac{\sum_{i=1}^N (x_i - \bar{x})^3}{(N - 1) * \sigma^3} \quad (3.10)$$

Kurtosis: Kurtosis is a measure of the tailedness of a distribution. It is defined as:

$$Kurtosis = \frac{\sum_{i=1}^N (x_i - \bar{x})^4}{(N - 1) * \sigma^4} \quad (3.11)$$

Where, N is the total number of samples, x_i is the instant sample of a data recording, \bar{x} is the mean of a data recording, and σ is the standard deviation.

Along with these nine statistical features, two physical features: age and body mass index (BMI) have also been considered. These two physical features are available in the dataset. Here, BMI is an index of body fat measured based on

body weight and height. Its normal value is 18.5 to 25 [109]. A BMI below 18.5 is considered underweight, while over 25 is considered overweight. These two features are considered in these study as age, and BMI has a relation with developing different diseases [110].

3.6 Classifier

In machine learning, a classifier is an algorithm that automatically arranges or groups data into one or more of a set of "classes". Different classifiers are used in various classification studies according to need and application. Decision trees, naive bayes classifiers, k-nearest neighbours, support vector machines, and artificial neural networks are some commonly used machine learning algorithms. A supervised machine learning classification approach called a decision tree is used to create models with the structure of trees. It divides information into ever-finer categories. A series of probabilistic algorithms called Naive Bayes determines the likelihood that every given data point will fall into one or more of a set of categories. An algorithm for pattern recognition called K-nearest neighbours (k-NN) stores training data points and learns from them by figuring out how they relate to other data in an n-dimensional space. K-NN seeks to identify the k closest linked data points in future, unforeseen data. Artificial neural networks are built to function similarly to the human brain. The next algorithm is triggered when one algorithm or procedure successfully solves a problem. They link problem-solving processes in a chain of events.

This study aims to design a binary classification system to detect different cardiovascular diseases along with type 2 diabetes. Also, a multiclass classification system is designed to classify different combinations of cardiovascular diseases and type 2 diabetes. At last, heart rate and blood pressure are focused to be estimated from the PPG signals. The extracted features are given as input in the machine learning classification app, and the accuracy of different classifiers is determined. Linear SVM has shown the highest accuracy for binary and multiclass classification, while linear regression has achieved the highest accuracy for heart rate and blood pressure estimation.

So, for the binary and multiclass classification system, SVM classifier is selected to be applied while for the heart rate and blood pressure prediction analysis, a linear regression classifier will be used.

Binary classification is a popular classification method for which Support Vector Machine (SVM) is commonly used. Since its inception in the 1990s, it has been one of the most effective machine learning algorithms, mostly used for pattern identification [111]. SVM can be used for data that have an unknown distribution. It provides good accuracy and performs faster prediction compared to other classification strategies. It has the ability to perform well with small datasets. SVM is an easy-to-implement machine learning method that eliminates complexity in the hardware. When there is a large gap between the two classes, SVM performs reasonably well. It works well in high-dimensional space as well. SVM categorizes data points even when they are not otherwise linearly separable by mapping the data to a high-dimensional feature space. Once a separator between the categories is identified, the data are converted to enable the hyperplane representation of the separator. After that, traits of fresh data might be utilized to forecast the group to which a new record should belong. Also, it requires less memory because it uses a subset of training points in the decision phase. Considering the advantages of SVM specially the advantages provided for hardware implementation, it is chosen for binary and multiclass classification in this study.

The mathematical function used for the transformation is known as the kernel function. SVM uses different kernel functions such as:

- Linear
- Polynomial
- Radial basis function (RBF)
- Sigmoid

When the linear separation of the data is simple, a linear kernel function is advised. One of the other functions ought to be used in other circumstances.

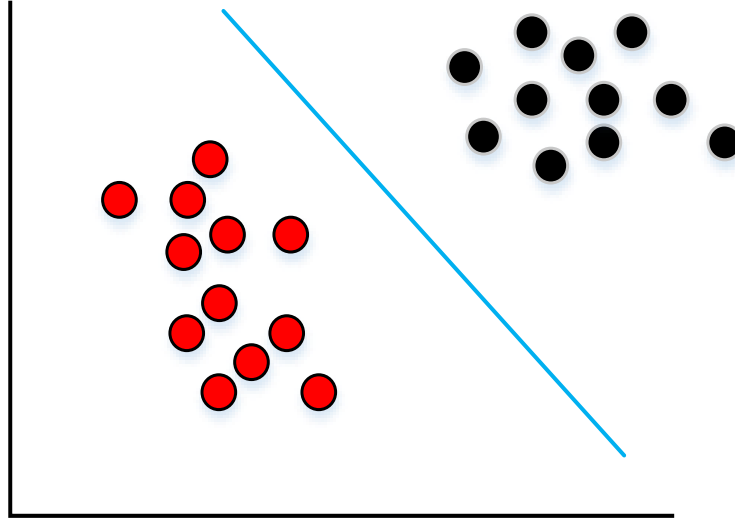


Fig. 3.4 Boundary between two categories defined by a hyperplane

The extracted features from the previous section have been used to train an SVM classifier. In this study, linear SVM has been used as it is simple and easy to implement in hardware platforms due to its simple function:

$$f(x) = x'\beta + b \quad (3.12)$$

where, x is an observation corresponding to a row of x indicating the features. b is the bias term, and β represents the weight values of the features.

The bias term b and the weight values are obtained upon training the data. For binary classification of hypertension, 69 segments with stage 1 or stage 2 hypertension segments have been selected from the dataset, along with 69 segments labelled normal. Similarly, for cerebral infarction, 23 segments of normal cases have been considered, with 23 segments with the disease, 42 segments of cerebrovascular disease, and 42 segments of normal PPG for this disease detection has been selected. And finally, for type II diabetes, 65 normal PPG segments have been taken, with 65 segments of diabetes selected in the segment selection process. In each disease detection case, 5-fold cross-validation has been applied where the dataset has been split into 5 folds, and for each fold, 80% data have been used for training, and the rest 20% have been for training. The classification has been done in Matlab at the software level. While training the data, the generated model provides the bias and weight values.

The SVM method is also used for disease identification in the multiclass operation. SVM does not, however, natively enable multiclass classification in its most basic form. It facilitates categorizing data points into two classes and using binary classification. The same method is applied to multiclass classification after dividing the multiclassification problem into numerous binary classification problems. It is intended to map data points to high-dimensional space to achieve mutual linear separation between every two classes. This technique, known as a One-to-One strategy, divides the multiclass classification problem into several binary classification problems. For each pair of classes, a binary classifier is needed. Another strategy is called One-to-Rest. In such a strategy, each class has a binary classifier as the breakdown. In the One-to-One technique, the points of the third class are ignored and a hyperplane is used to divide every two classes. This signifies that the present split solely considers the points of the two classes, as shown in Fig. 3.5. A hyperplane is required in the One-to-Rest technique in order to divide all classes from one another simultaneously. This indicates that all points are considered, and they are split into two groups: a group for class points and a group for all other points, as shown in Fig. 3.6.

In the multiclass detection approach, the one-to-rest SVM approach has been used for detecting the classes. The one-to-rest approach trains less number of classifiers than the one-to-one approach. Hence, the computational time will be faster and fewer resources and power will be utilized for the one-to-rest approach. There are seven classes in this multiclass detection study, so seven SVM classifiers are needed to design at this stage. In this study, for a particular classifier, 17 segments from that class and 17 others from all the other classes were for training and testing. 80% data have been used for training and 20% for testing for that particular classifier. So, a total of seven model functions for seven classifiers, along with the bias and weight values, have been generated in the software design.

Again, for heart rate and blood pressure detection, linear regression model has

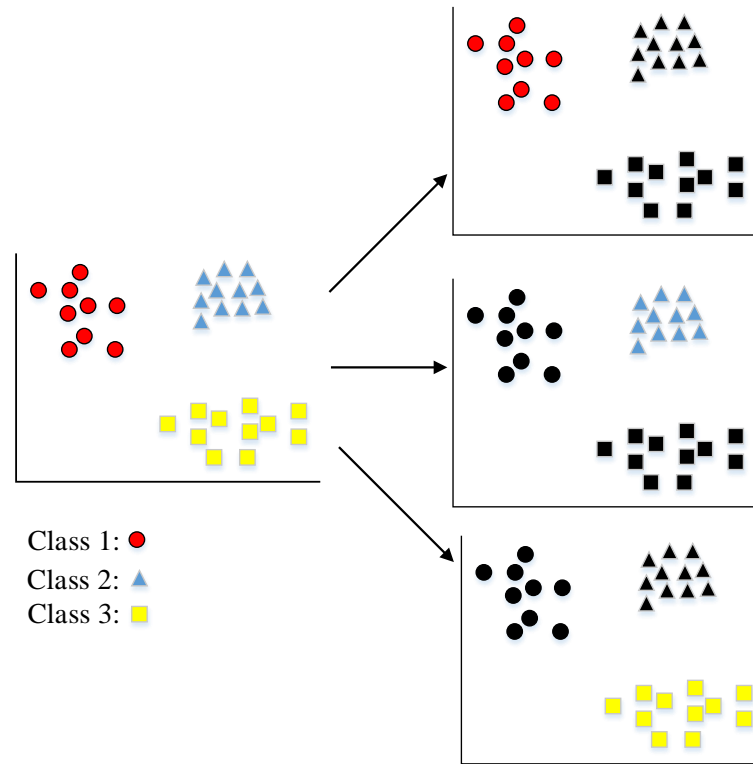


Fig. 3.5 One-to-one approach in multiclass SVM

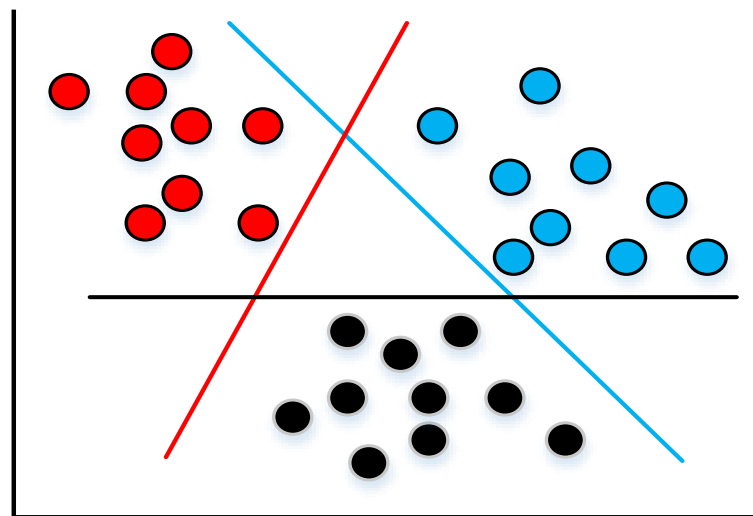


Fig. 3.6 One-to-rest approach in multiclass SVM

been chosen. For estimating or prediction of a variable, regression analysis is usually used [112]. Regression is one of the most significant supervised learning tasks. In regression, a series of records with X and Y values are present, and these values are used to train a function that may be used to predict Y from an unknown X . To perform regression, the value of Y needs to be determined. In

order to predict continuous Y in the case of regression, given X as independent features, a function is needed. There are various regression models for estimation and prediction studies, such as linear regression, logistic regression, polynomial regression, random forest, etc. However, linear regression is the simplest algorithm among them. It is less complex than other approaches and hence easy to implement at the hardware level. Because it enables the measuring of anticipated effects and the modelling of those effects against one or more input variables, linear regression is commonly used in mathematical analysis [113]. The link between the variables is shown by a slanted straight line provided by the linear regression model as shown in Fig. 3.7.

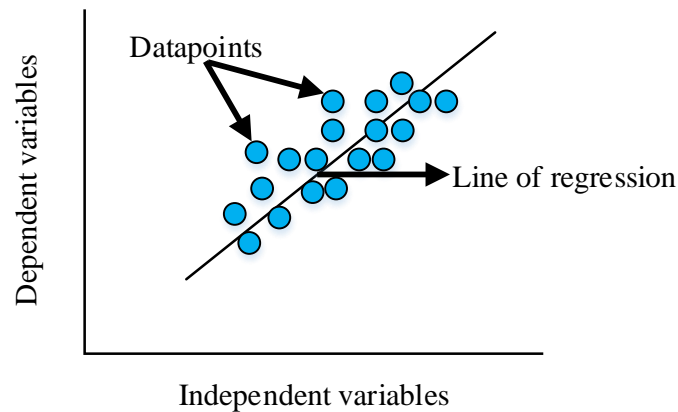


Fig. 3.7 A simple linear regression process

Simple linear regression and multiple linear regression are two different types of linear regression. In the case of simple linear regression, the estimated value or the dependent variable is measured using a single independent variable. It is expressed by:

$$y = a + bx \quad (3.13)$$

where, y represents the dependent or estimated value, a represents the intercept of error value, b is the slope or regression coefficient, and x is the independent value.

Again, for multiple linear regression, there is more than one independent

variable on which the estimated value depends. It is expressed by the following:

$$y = b_0 + b_1x_1 + b_2x_2 + + b_mx_m \quad (3.14)$$

where, y is the estimated value, b_0 is the intercept, $b_1, b_2, b_3, ..., b_m$ are regression coefficient, and $x_1, x_2, x_3, ..., x_m$ are the independent variables or the feature values.

As nine features have been extracted from the PPG signal, multiple linear regression will be applied in this study for heart rate and blood pressure estimation. Different combinations of the extracted features will be used in the linear regression model to determine the most optimized features for the prediction study. Predicting the most accurate heart rate and blood pressure values from a minimum number of features will ensure using the least resources and the lowest power consumption.

Chapter 4: Hardware Architecture

After designing the systems at the software level, it is necessary to develop a hardware architecture for implementing the system. This section provides the system architecture design for FPGA implementation. Xilinx system generator has been used for the system architecture design. The Xilinx zedboard zynq-7000 and the zedboard ultrascale+ have been used for the implementation of the systems. The design procedure of the preprocessor, feature extractor, and classifier are presented in this chapter.

4.1 Methodology for Hardware Design

In this stage, the system developed at the software level in Chapter 3, has to be implemented at the hardware level. The overall process is shown in Fig. 4.1. Like the software design, segments for further processing need to be selected at first. In the next stage, a proper tool selection is required for the hardware design. Then it is necessary to normalize the signals and pass them through a preprocessing stage. The preprocessing stage will denoise the signals. The preprocessed signal will be used for feature extraction. The extracted features will be used for classifier design. The classifier will give the ultimate results by providing the disease detection result or estimating the heart rate and blood pressure.

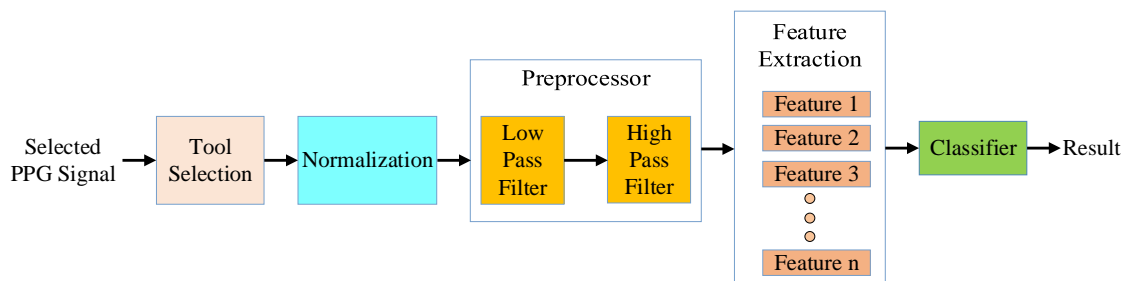


Fig. 4.1 Overall methodology of hardware design

4.2 Device selection

The system has to be designed at the hardware level to fulfill the purpose of the study. Hardware-based digital and embedded systems are becoming more popular due to their multifunction capability, low cost, and high-performance accuracy [114]. Digital hardware systems can be implemented in various devices such as field programmable gate array (FPGA), complex programmable logic devices (CPLD), simple programmable logic devices (SPLD), microcontrollers, and others [115]. FPGA has been chosen for this study as it is simple and easy to design as well as has the advantage of reprogrammable functionality [116]. FPGA contains more logic blocks than CPLD or SPLD. It allows greater customization and more complex processes than CPLD and SPLD. Also, microcontroller provides reprogramming of firmware, but FPGA has the advantage of changing the functionality of both hardware and firmware. FPGA has the advantage of hardware acceleration as it can be used to accelerate workloads and gain significant benefits. Parallel computing is another advantage of the FPGA. It allows to handle multiple workloads without sacrificing performance. This enables one to work on different stages of tasks concurrently, which cannot be done with GPUs. Smaller board space, power efficiency, and reliability are also reasons for choosing FPGA in this study. Zedboard zynq-7000 has been primarily targeted for developing the proof of concept of this system. However, in case the zedboard zynq-7000 fails to provide the necessary resources, zynq ultrascale+ will be utilized for the design. Both the FPGA board offer embedded system design and development at low cost and provide the advantage of long life.

4.2.1 Zedboard zynq-7000

It is a low-cost development board for Xilinx. Everything required to develop a design for Linux, Android, Windows, or other OS is included on this board. Additionally, a number of expansion connectors provide simple user access to the processing system and programmable logic inputs and outputs. It Utilizes

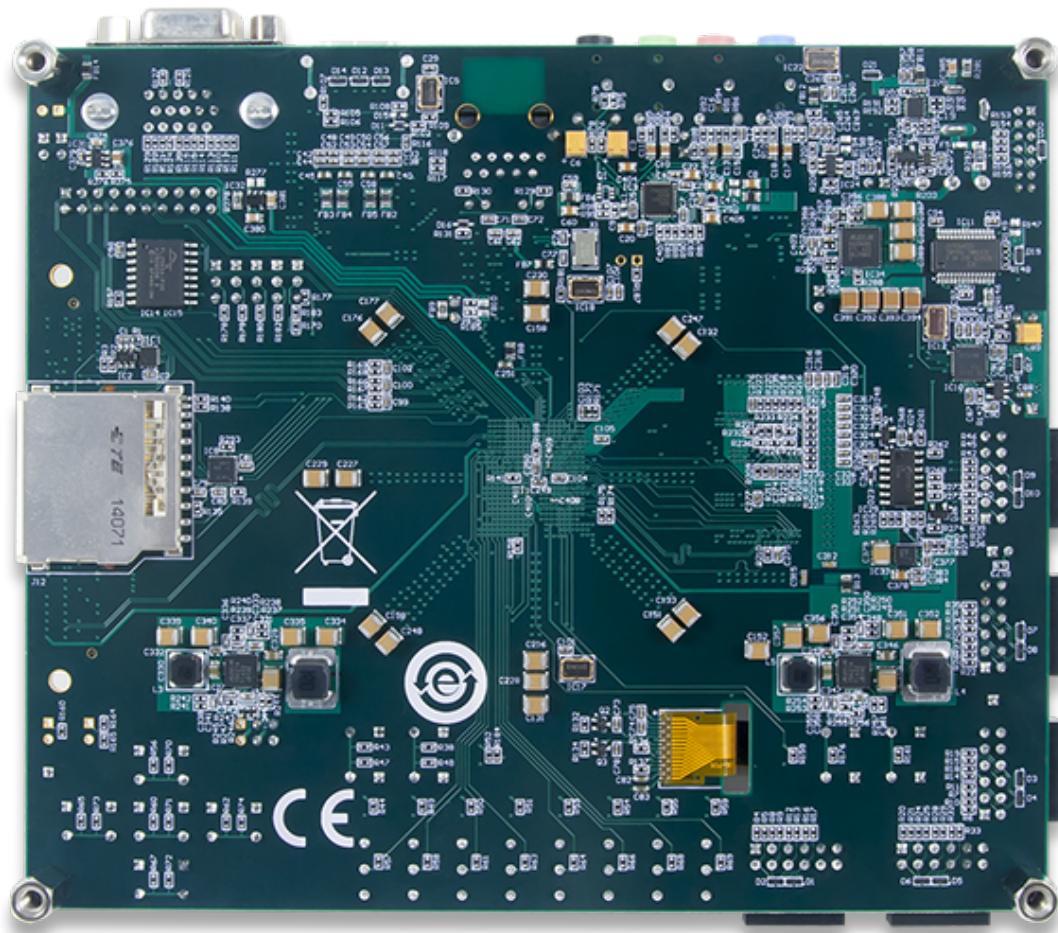


Fig. 4.2 Zynq-7000 FPGA board structure

the tightly integrated ARM (Advance RISC Machine) processing system and 7-series programmable logic of the Zynq-7000 AP SoC to build innovative and potent designs for the ZedBoard. Target applications include embedded ARM processing, software acceleration, video processing, motor control, Linux/Android development, and general Zynq-7000 all-programmable SoC (system-on-a-chip) prototyping.

It contains four major blocks.

- Application processor unit (APU)
- Memory interfaces
- I/O peripherals
- Interconnect

The APU includes Dual-core or single-core ARM Cortex-A9 MPCores. The memory interface unit includes dynamic and static memory controller modules. The dynamic memory controller supports DDR3, DDR3L, DDR2, and LPDDR2 memories. The I/O peripherals unit contains the data communication peripherals. The APU, memory interface unit and the IOP are all connected to each other and to the PL through a multilayered ARM AMBA AXI interconnect. The interconnect is non-blocking and supports multiple simultaneous master-slave transactions.



Fig. 4.3 Zynq-ultrascale+ FPGA board structure

4.2.2 Zynq Ultrascale+

Xilinx Zynq UltraScale+™ Multiprocessors feature 64-bit processor scalability, combining real-time control with soft and hard engines for graphics, video, waveform, and packet processing. The multiprocessor systems-on-chip devices are constructed on a platform with a common real-time processor and programmable logic. Three different models of Xilinx UltraScale+

Multiprocessors (dual-core, quad-core, and video code-c) are available. Devices with dual-core application processors are ideal for sensor fusion and industrial motor control. Devices with quad-core application processors perform exceptionally well in the data center, aerospace, and defence applications. Devices with video codecs are useful for surveillance, multimedia, and automated driving assistance systems in automobiles.

It uses Arm Cortex-A53-based application processing unit (APU). CPU frequency is up to 600 MHz. The programmable logic block has 36Kb block ram, 288Kb dual port ultra ram, dsp blocks, I/O blocks, and video encoder/decoder. Zynq ultrascale+ FPGA board has more resources than the zedboard zynq-7000 FPGA board. However, zynq ultrascale+ is more costly than zynq-7000. Therefore, zynq-7000 will be primarily used for the design implementations. If the resources of this board are insufficient, then the ultrascale+ FPGA will be utilized for the implementation.

4.3 Design Tool Selection

For the hardware prototype design Xilinx system generator (XSG) has been selected. It is a MATLAB Simulink add-on that enables the development of architecture-level FPGA designs using graphical block programming. Xilinx FPGAs are heterogeneous compute platforms that include Block RAMs, DSP Slices, PCI Express support, and programmable fabric. They enable parallelism and pipelining of applications across the entire platform as all of these compute resources can be used simultaneously. In XSG, hardware description language is used to assemble FPGA building blocks into a circuit that performs a specific task, making the programming different from typical high-level languages. The two most popular hardware description languages are VHDL and Verilog. In XSG the system is designed in Matlab Simulink and then synthesized the design into an FPGA. The next sections present the hardware design procedure. Screenshots of actual designs of the different subsystems in the Xilinx system generator are presented in Appendix B.

4.4 Normalization

Normalization is the process of reducing data redundancy in a dataset and improving data integrity. The main objective of database normalization is to eliminate redundant data, minimize data modification errors, and simplify the query process. Ultimately, normalization goes beyond simply standardizing data, and can even improve workflow, increase security, and lessen costs.

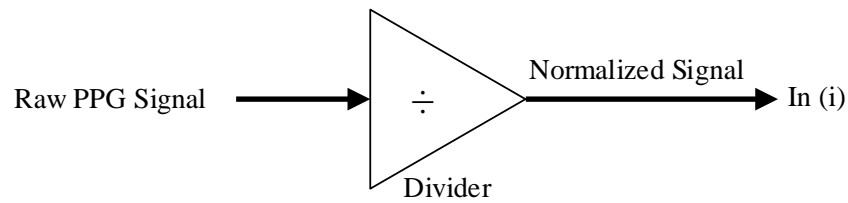


Fig. 4.4 Normalization of the raw PPG signal

The raw PPG signal is first normalized using a divider. The signal amplitude is divided by a high-value number to get the normalized signal. The high-value number can be the maximum amplitude of the PPG signal or a higher value than the maximum amplitude. The typical maximum value of the PPG signal is 5 mV. The unit of the PPG signal amplitude is not given in the dataset. So considering the unit in μV the signals are divided by 5 mV or 5000 μV . The procedure is shown in Fig. 4.4 where the input is the raw PPG signal, and the output is the normalized signal indicated by In(i) in the figure, which is the input to the preprocessor in the next stage.

4.5 Preprocessor Subsystem

The processes executed for software-level design will be followed in this case also. At first, the normalized signal passes through a high pass filter of 0.5 Hz and then a low pass filter of 15 Hz, designed in the Xilinx system generator using the FDA tool. Filter orders are kept the same, 50 and 81, respectively, for the high and low pass filters, as per software design. FFT filters are designed for the hardware-based preprocessing system. The response of both the high and low

pass filters follows the equation:

$$y(n) = \sum_{i=0}^N b_i x(n - i) \quad (4.1)$$

where, $x(n)$ is the input signal, $y(n)$ is the output signal, N is the order of the filter, & b_i is the impulse response at i_{th} instant for $0 \leq i \leq N$ of N_{th} order filter.

The high and low pass filters can be designed using different filtering methods. In the FDAtools, several filtering techniques such as equiripple, least square, constrained least square, barlett, rectangular, hann, hamming etc. These filtering techniques have been applied to design the high and low pass filters. For each filtering technique, the resource and power utilization have been found to get the optimized resource utilization technique. After the resource utilization analysis, the best filtering technique will be chosen for the optimized design. The resource utilization and filter type selection are explained in detail in Chapter 5.

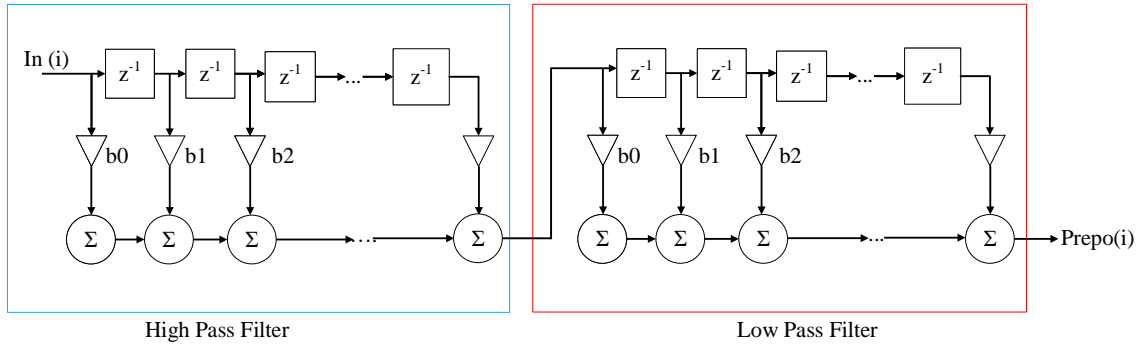


Fig. 4.5 Preprocessing stage of proposed the system

The preprocessor design is shown in Fig. 4.5. Here, $b_0, b_1, b_2, a_1, a_2, \dots$ are filter coefficients. The $In(i)$ is the normalized PPG signal, and the $Prepo(i)$ is the output of the preprocessor.

4.6 Feature Extractor

In the next step, the features are needed to be extracted from the hardware design. The system architecture has been designed to extract the features that are already selected at the software level. Various mathematical and logic blocks are used for

the implementation. The system architectures for feature extraction in the Xilinx system generator have been depicted in Fig. 4.6-4.15.

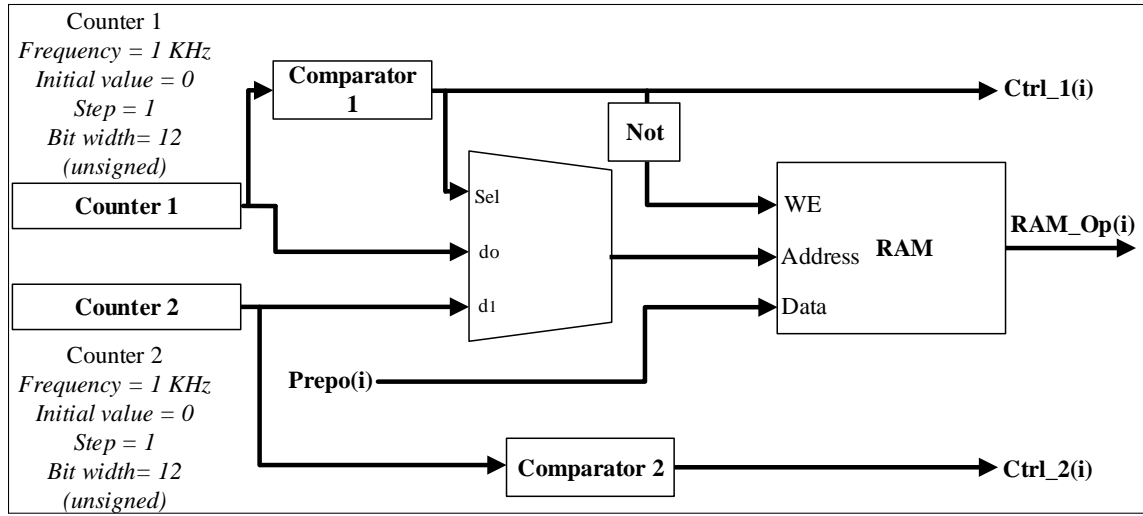


Fig. 4.6 Memory and control subsystem for feature extraction

In Fig. 4.6, a multiplexer (mux) and a RAM are used to store the input signal data in a memory which will be utilized in further feature extraction blocks. The output of the preprocessor, $prepo(i)$ is input to the data port of the RAM. Two counters having the same frequency are used. Counter 1 starts counting from zero, and it passes through a logic comparator. It continues to count till the total sample number of a PPG signal is 2100, and during that period, it keeps the writing enable (WE) disabled due to the not gate. The logical comparator 1 also controls the selector switch. When the counter follows the comparator 1 logic, it is selected to d_0 , and when the comparator logic breaks, it is selected to d_1 , which is controlled by counter 2. Counter 2 is enabled and starts saving the data in the proper address after the comparator 1 logic breaks, when counter 1 exceeds counting 2100, enabling the (WE) port. Counter 2 counts to 4200, controlled by the logical comparator 2 and stores the 2100 sample of a PPG signal in the RAM address. The counters passing through the comparator's logic blocks create two control signals mentioned as $Ctrl_1(i)$ and $Ctrl_2(i)$. These control signals are used during feature extractions.

In Fig. 4.7, all the sample values of $prepo(i)$ signal are added using an

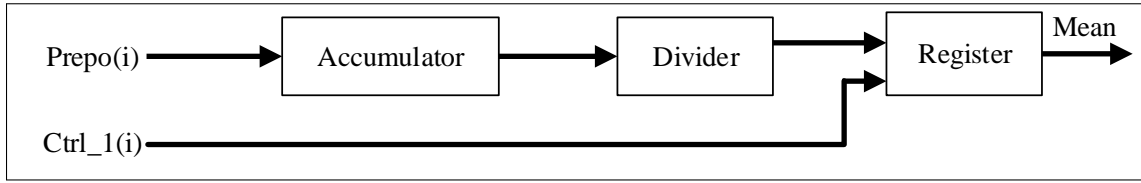


Fig. 4.7 Mean feature extraction in hardware level

accumulator, which is later divided by the total number of samples to generate the mean value of the signal. The control signal $ctrl_1(i)$ helps to store the value in a register.

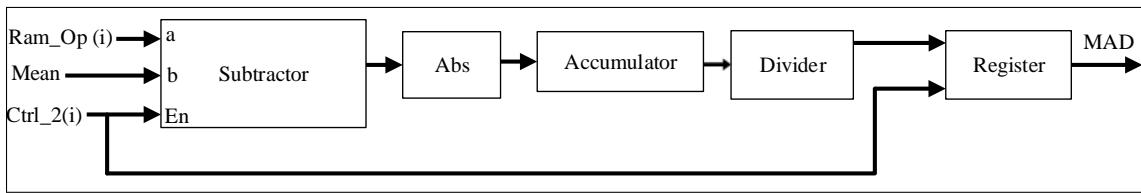


Fig. 4.8 MAD extraction in Xilinx system genrator

To determine the mean average deviation (MAD), the sample values of a signal, $RAM_Op(i)$, are recalled from the RAM and the mean value is subtracted from each of the sample value of the signal using the block mentioned as Subtractor in Fig. 4.8. Then, the absolute value, indicated by the Abs block in Fig. 4.8, of the subtraction is added using an accumulator and later divided by the total number of samples to generate MAD. The feature is stored in a register using the $Ctrl_2(i)$ signal.

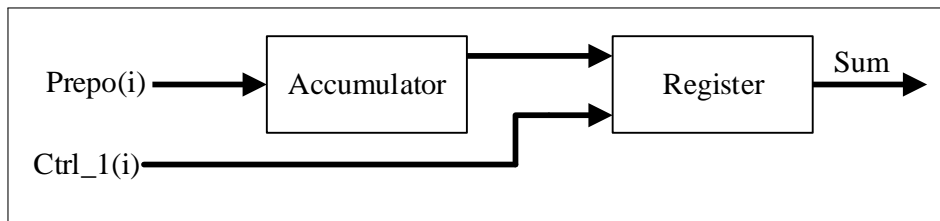


Fig. 4.9 SUM extraction in the hardware design

In Fig. 4.9 the result of the accumulator gives the sum output shown. In the case of extracting AE, it is needed to square each sample value of $prepo(i)$, and for the summation of the squared values, an accumulator is used in Fig. 4.10. $Ctrl_1(i)$ is also used to store the sum and AE value in a register.

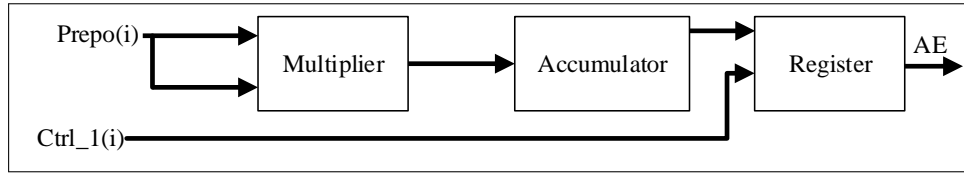


Fig. 4.10 AE extraction for the FPGA design

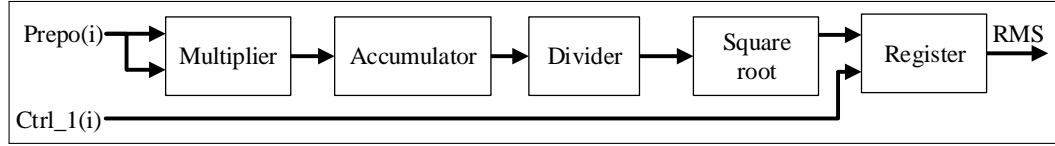


Fig. 4.11 RMS extraction in Xilinx system generator

In Fig. 4.11, the sample values of $prepo(i)$ are squared using a multiplier block and then added using an accumulator. The result is divided by the total number of sample values and later square rooted for generating RMS value which is stored in a register and $Ctrl_1(i)$ is used for controlling this.

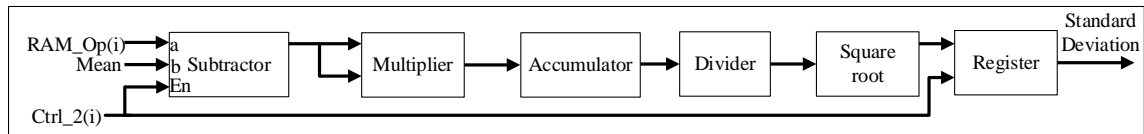


Fig. 4.12 Standard deviation extraction for FPGA design

For determining the standard deviation mean value of each $prepo(i)$ signal is subtracted from all the samples and squared. The squared values are added using an accumulator followed by a divider dividing the accumulator output by the total number of samples. Later the result of the divider is root squared to get the standard deviation of the input signal as shown in Fig. 4.12. The extraction of the feature called variance is almost the same process as extracting standard deviation except for the root square process. After determining the variance, a root square block is used to determine the standard deviation. A register is used to store the standard deviation of the input PPG signal. The process is shown in Fig. 4.13.

In the case of skewness, the mean value of a PPG signal is subtracted from the sample values preserved in the RAM, $RAM_Op(i)$. Then the same result is

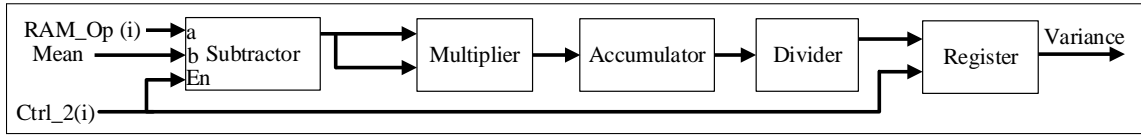


Fig. 4.13 Variance extraction for classifier design

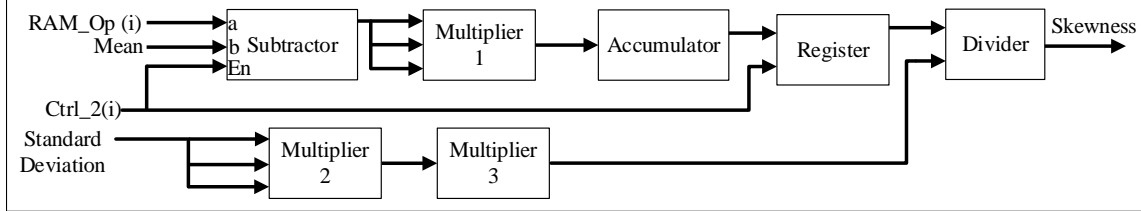


Fig. 4.14 Skewness extraction at the hardware level

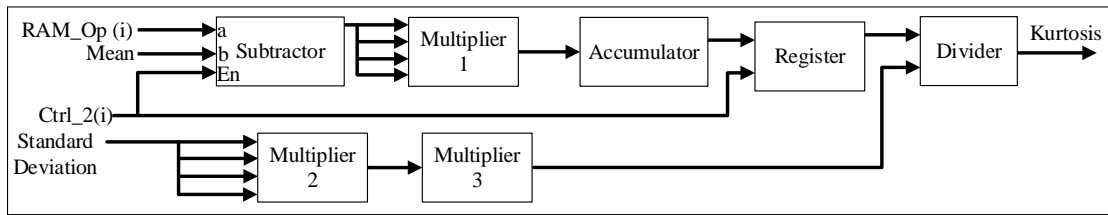


Fig. 4.15 Kurtosis extraction for hardware design

multiplied three times and added to an accumulator. The standard deviation, extracted previously, is multiplied three times and then multiplied with 1 less than the total number of samples. This multiplication output divides the accumulator output to get the skewness value. For kurtosis, the process is almost the same, except here, it is necessary to multiply the values four times instead of three times, as in the case of determining skewness. In the case of standard deviation, variance, skewness, and kurtosis, the Ctrl.2(i) signal is used to control registers that store the values respectively.

The overall extraction of all the features is shown in Fig. 4.16. The different colour boxes indicate the individual feature extraction in this figure. The design uses accumulators, dividers, multipliers, absolute blocks, and square blocks for different operations. Also, it needs registers for storing the features.

4.7 Classification Subsystem

At this stage, it is necessary to design a classifier to achieve the purposes of the study. One classifier is needed for a binary classification for detecting individual

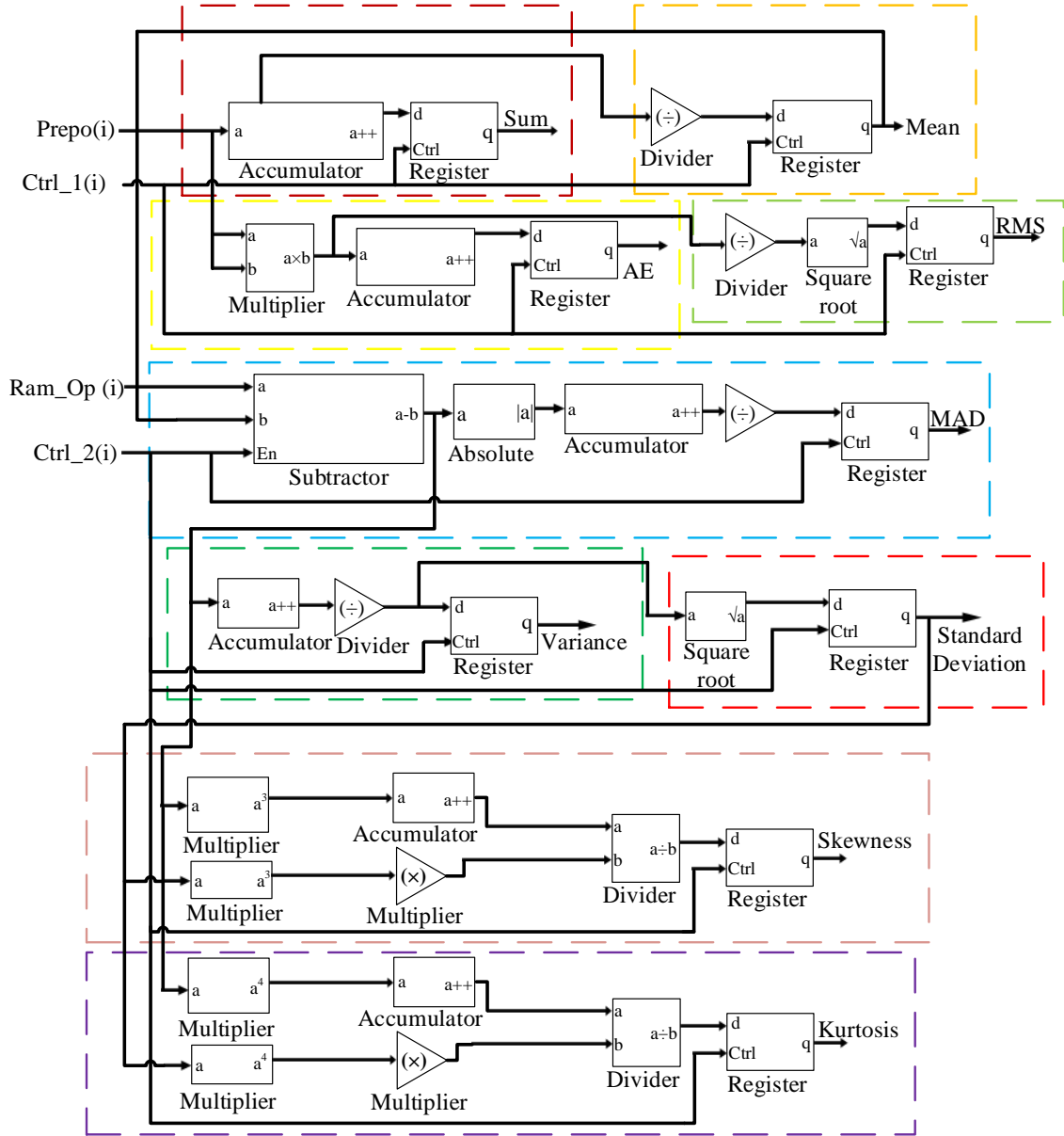


Fig. 4.16 Complete feature extraction process in Xilinx system generator

diseases, and another for multiclass classification. Also, to predict heart rate and blood pressure another classifier needs to be designed. Binary SVM and multiclass SVM classifiers are designed for binary and multiclass classification analyses, while linear regression classifier has been designed for heart rate and blood pressure estimation.

4.7.1 Classifier for Binary Classification

The extracted features have to be utilized for developing a classifier to classify the PPG signal for the detection of diseases. For this, SVM classifier has been

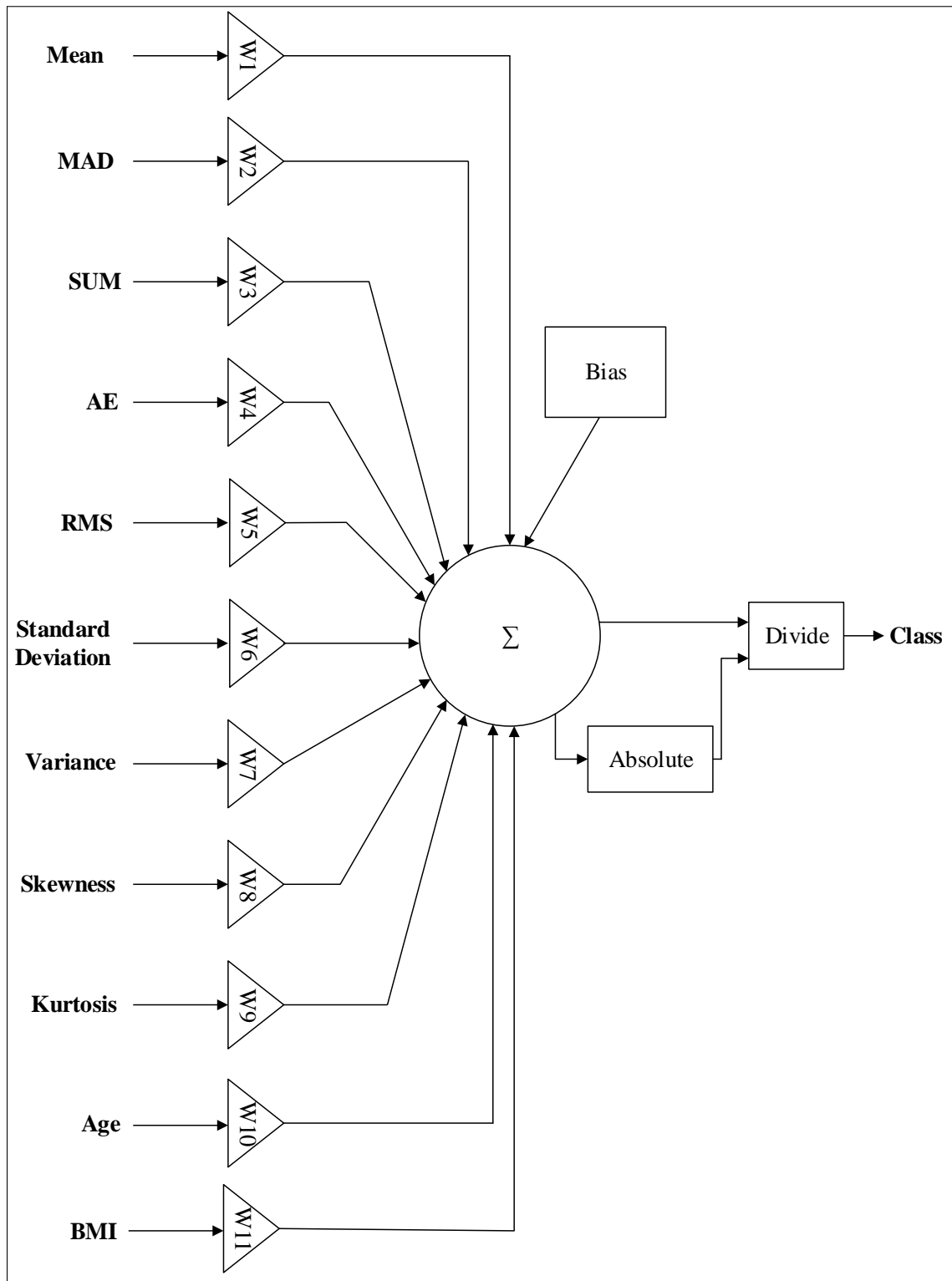


Fig. 4.17 SVM Classifier for binary classification

chosen as it is easy and simple to implement in hardware due to its simple function. There will be one SVM classifier for each disease for binary classification of diseases. The total classifier system architecture designed in the Xilinx system generator is shown in Fig. 4.17. The weight values (w_1, w_2, \dots, w_{11})

and bias values (b) are chosen from the model found in Matlab by training the dataset at the software level as mentioned in Chapter 3. The extracted features are multiplied by the weight values and added together. Finally, the bias value is added and the total summation is divided by the absolute value of the sum.

$$class = \frac{f(x)}{|f(x)|} \quad (4.2)$$

If it results in 1, it is considered a normal case and if the result is -1 , it is considered a signal of a subject of a particular disease.

4.7.2 Classifier Design for Multiclass Classification

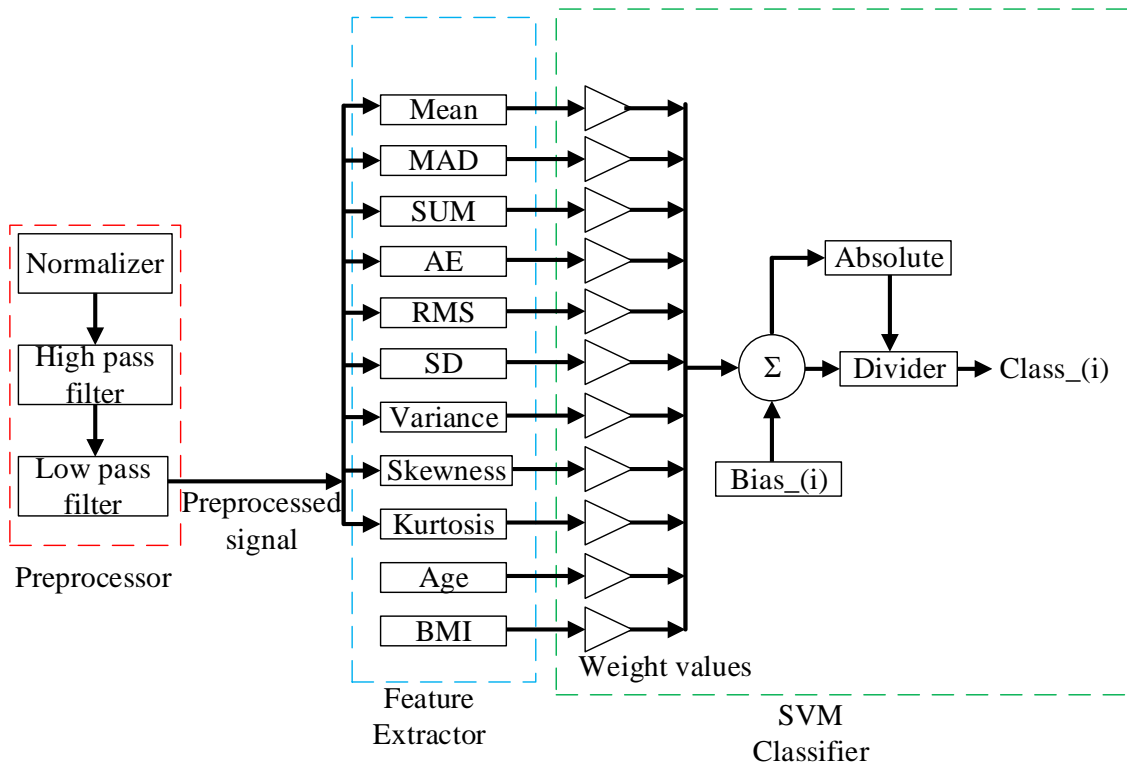


Fig. 4.18 Individual SVM classifier architecture for multi-class classification

For multiclass classification also, SVM classifier is used. In this study, seven classes have been used, so it is required to design seven SVM classifiers as the binary SVM classifier. The system block for this case is presented in Fig. 4.18. The figure shows the preprocessing stage design to a single SVM classifier design. Seven similar SVM classifiers are designed in the same pattern. All the

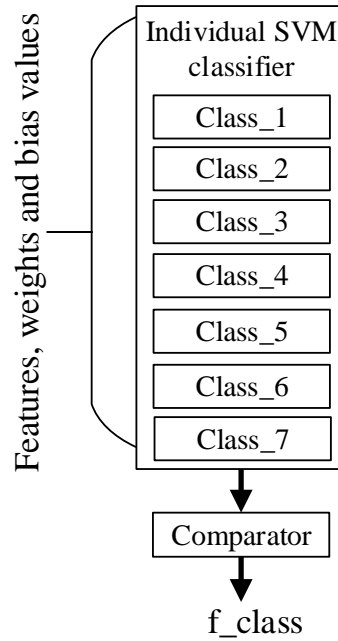


Fig. 4.19 Comparator in multiclass classification

Algorithm 1: Algorithm for class prediction

```

if class_1 = -1 then
  | f_class = 1
else if class_2 = -1 then
  | f_class = 2
else if class_3 = -1 then
  | f_class = 3
else if class_4 = -1 then
  | f_class = 4
else if class_5 = -1 then
  | f_class = 5
else if class_6 = -1 then
  | f_class = 6
else
  | f_class = 7
end
  
```

class results will go to a comparator which compares the classes of all classifiers to show the final class of the signal. It is shown in Fig. 4.19. The comparator checks the output of all the classifiers and then gives the final class output. The comparator gives the result by the Algorithm 1.

The comparator logic is implemented to determine the actual class between the seven classes. It checks the output of the seven classifiers. If the class 1 output is

-1 then the comparator gives the output f_{class} 1 indicating the PPG segment belongs to normal or class 1. If the output of classifier 1 is 1, it checks the next classifier's output. If the output of the second classifier is -1 then the comparator gives an output of 2. Similarly, it shows the output of other classes if their respective classifier output results in -1. When multiple classifiers show the same -1 output, the comparator checks the classifier outputs and provides the result according to the algorithm.

4.7.3 Classifier Design for BP and Heart Rate Estimation

A linear regression classifier is designed for heart rate and blood pressure estimation. The regression coefficients and intercept value needed for the system development are taken from the software design in Chapter 3. Nine statistical features have been extracted in this study. Different numbers of features are used to predict the heart rate and blood pressure from PPG signals. At first, 3 features are used and then in the next steps, the number of features is increased by 1. For increasing a new feature, it has been ensured that the new feature requires fewer resources than the other features. Upon trying these combinations of features, it has been found that using 5 features: mean, MAD, sum, AE, and RMS gives the best results for heart rate and blood pressure estimation. It is shown in the result section in Chapter 5. The system architecture is shown in Fig. 4.20.

The linear regression model can be designed such that a single classifier model can provide the output of heart rate, systolic blood pressure, and diastolic blood pressure. It is necessary to design three linear regression classifiers for these three parameter estimations in a single system. Each class's regression coefficients and intercepts must be implemented in their respective classifiers. However, it will take a lot of resources, and thus power consumption will be much higher. Hence, a single health parameter estimation system is designed in this study.

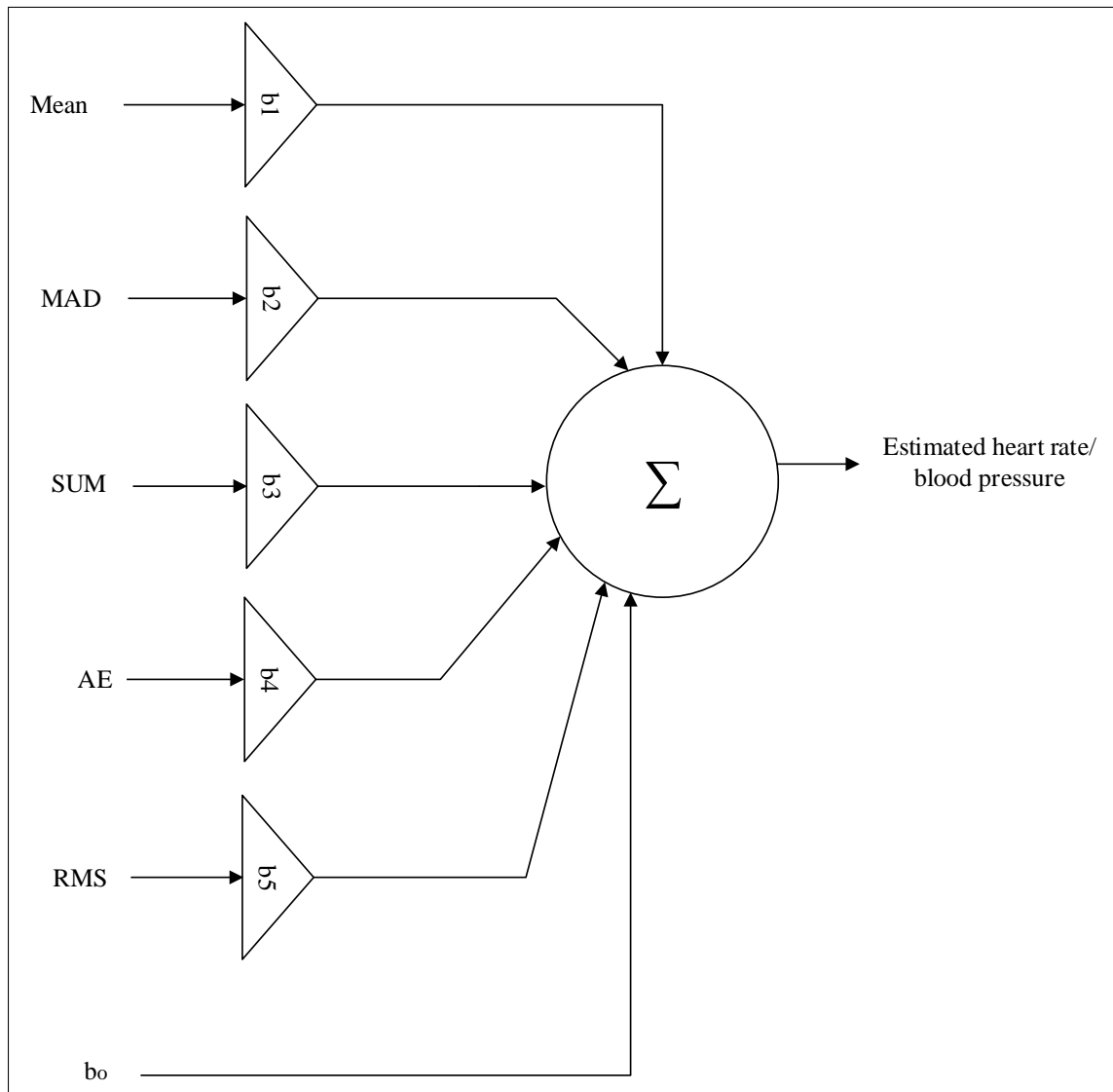


Fig. 4.20 Linear regression classifier for heart rate and BP estimation

Chapter 5: Performance Analysis

Analyzing the system performance of the design system both at the software and hardware level is necessary for the validation of the systems. It will also provide a distinction between the performances of the FPGA-based system and the software system. This section represents the results of the software system developed in Chapter 3 and the Hardware prototype designed in Chapter 4. The performance of the preprocessor, feature extractor, classifier, and prediction system is analyzed.

5.1 Results of Preprocessing Subsystem

As biosignals are contaminated with different noises preprocessing stage must remove them before further analysis of the signal. The preprocessor is designed with a low-pass filter and a high-pass filter. Different filtering techniques have been applied for quantitative analysis. Resource utilization of the designed system for various filtering techniques has been determined. After analyzing all the filtering techniques, these have appeared to be the best regarding resource utilization and power consumption. The overall resource utilization for different

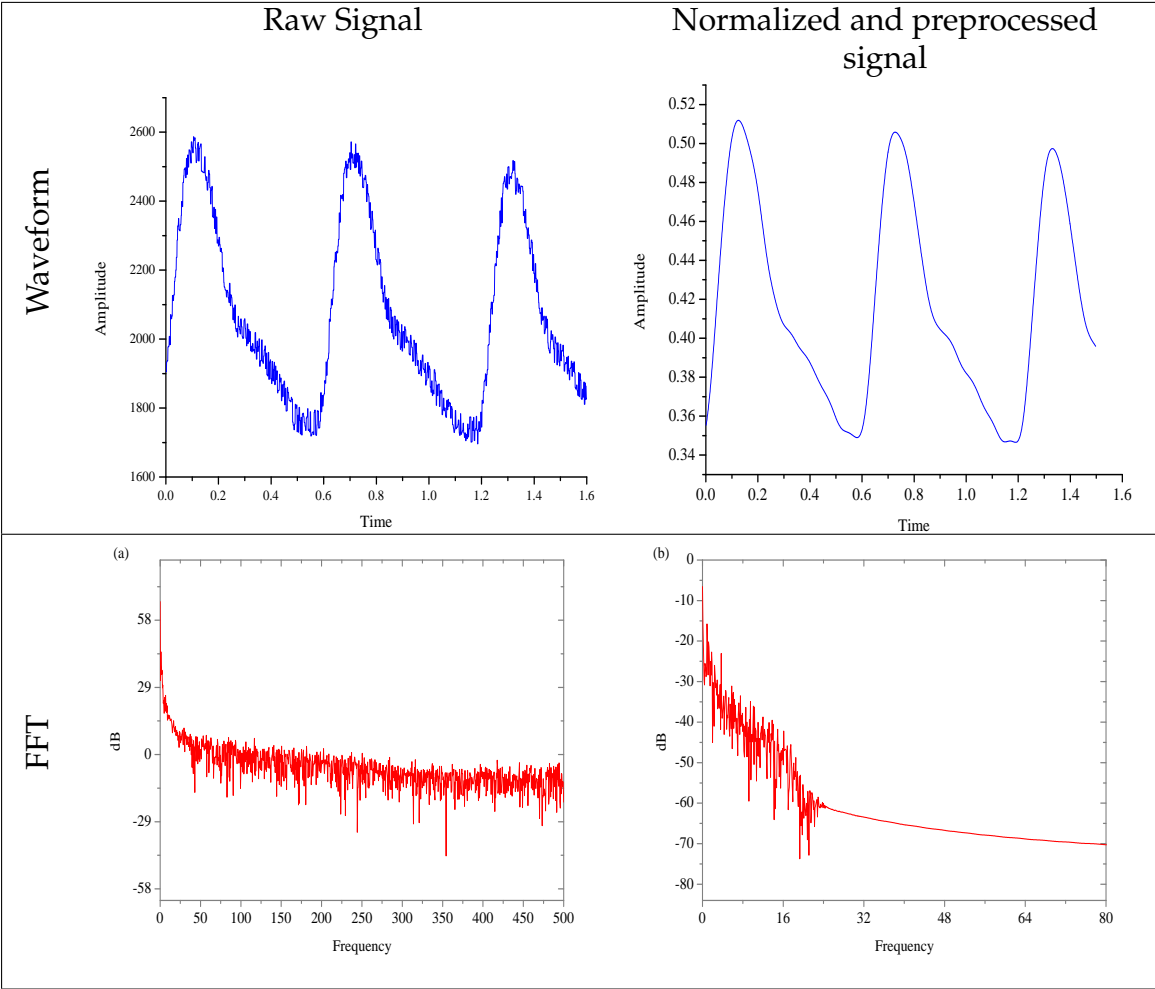
Table 5.1. Resource utilization for different filtering approaches

Filter Design for PPG Preprocessor		Resource Utilization				
High Pass Filter	Low Pass Filter	LUT	LUTRAM	Flipflop	DSP	I/O
Kaiser	Kaiser	2700	2513	5315	112	65
Least Square	Least Square	2717	2513	5320	112	65
Constrained Least square	Constrained Least square	2700	2513	5315	112	65
Equiripple	Equiripple	2719	2513	5322	112	65
Barlett	Barlett	2719	2513	5322	112	65
Rectangular	Rectangular	2700	2513	5315	112	65
Hann	Hann	2712	2513	5318	112	65
Hamming	Hamming	2698	2501	5277	112	65

techniques is presented in Table 5.1. From the resource analysis, it is seen that the hamming window requires the least amount of logic elements, and thus the

on-chip power consumption will be the lowest among all filtering techniques for the PPG preprocessor. The use of I/O, and DSP is the same for all the different filtering techniques. The amount of LUTRAM required is also the same for all the techniques except the hamming window. However, different numbers of LUT and flip-flops are required by them. As the hamming window requires the lowest number of resources for the preprocessor system, hence it is selected for the hardware system design. So, the next results are analyzed based on the Hamming window filtering technique. These filters have successfully removed the noises so, higher order filters are avoided for minimum resource and power utilization.

Table 5.2. Preprocessing stage performance



The PPG signal from the database is given input to the preprocessing stage designed in the Xilinx system generator. The high and low pass filters remove the undesired noises from the signal. In Table 5.2, it can be seen that the raw

PPG signal is noisy which is noise-free in the case of preprocessed signal after passing through the filter. Also, the signal is normalized first before giving input to the preprocessing stage.

In the software stage, the FFT analysis of the preprocessed signal shows the removal of noises. In the hardware stage, noise removal is also evident in the FFT response of the signals. The FFT of raw PPG signal and preprocessed PPG signal is shown in Table 5.2. It is evident from the figure that noises contaminate the raw PPG signal, and noise spikes are found all over the frequency range. After passing the normalized signal through the filters, the noises are removed. It can be seen that at the hardware level, the designed preprocessor output has very little amount of noise above 15 Hz and above 20 Hz, noise is almost fully suppressed.

5.2 Performance of Feature Extractor

The feature extractor subsystem extracts nine statistical features. To verify the extracted features, they are compared with features extracted in software simulation. The Pearson correlation coefficient and root-squared error (RSE) values are determined for statistical analysis.

The most popular method for determining a linear correlation between two variables is the Pearson correlation coefficient (r). It is expressed by the following equation:

$$r = \frac{1}{n-1} \left(\frac{\sum x \sum y (x - \bar{x})(y - \bar{y})}{S_x S_y} \right) \quad (5.1)$$

where, r is Pearson correlation coefficient, n is the total number of compared data, \bar{x} and \bar{y} are the average of x and y values, x values are considered software data and y values are considered hardware data, S_x & S_y are corresponding standard deviations.

In the study, nine features have been used, which are extracted from the designed subsystem. The Pearson correlation coefficients of these features are presented in Table 5.3 and Fig. 5.1. A Pearson correlation coefficient value close to 1 indicates

higher accuracy [117]. The Table shows that all the extracted features from the 331 PPG recordings by the subsystem have a Pearson correlation coefficient above 0.97. This validates the feature extractor design of this study.

Table 5.3. Pearson correlation coefficient for extracted features for 331 PPG recordings

Feature	Pearson correlation coefficient
Mean	0.9982
MAD	0.9893
Sum	0.9793
AE	0.9812
RMS	0.9882
Standard deviation	0.9791
Variance	0.9832
Skewness	0.9783
Kurtosis	0.9884

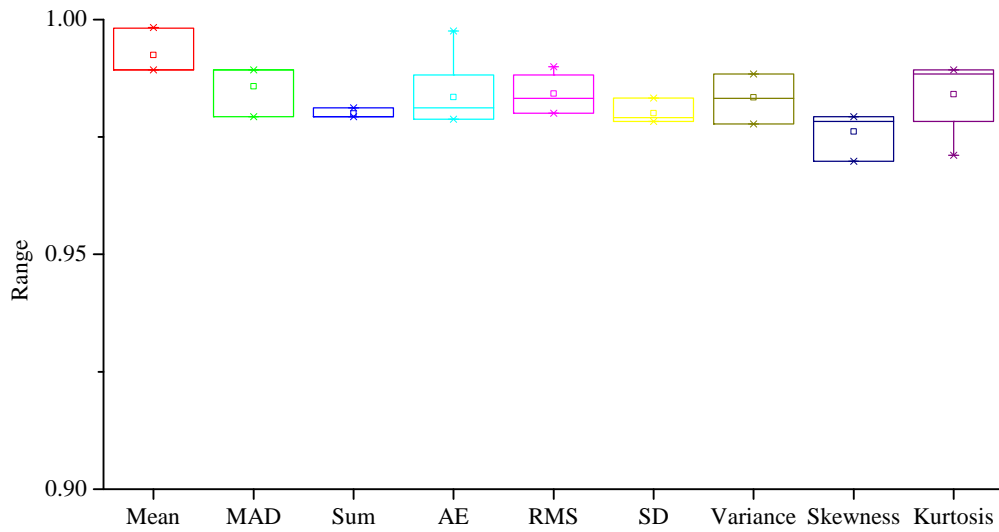


Fig. 5.1 Pearson Correlation coefficient for extracted software and hardware features

Another metric is root squared error (RSE), one of the common methods for gauging how well a model predicts quantitative data. It is expressed by:

$$RSE = \sqrt{(X - Y)^2} \quad (5.2)$$

where, X represents software outcome, Y represents hardware outcome. RSE Value closer to 0 indicates higher accuracy. Fig. 5.2 shows the boxplot of RSE data for the extracted features. The “x” sign indicates the outlier, and “-”

indicates the range of minimum and maximum data points considered. A closer value to 0 indicates higher accuracy. In the figure, all the RSE values of the features are close to 0. The Pearson correlation coefficient and the RSE values validate the feature extraction subsystem design in the hardware level.

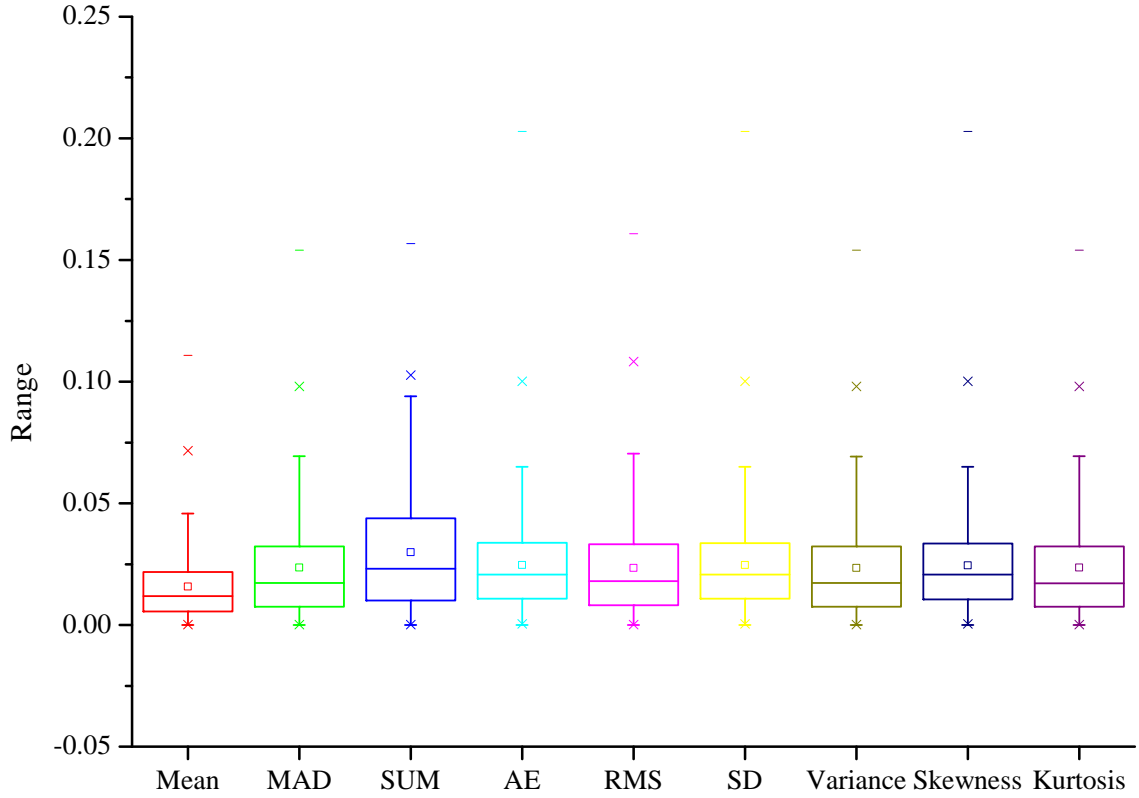


Fig. 5.2 Boxplot of RSE for different features

5.3 Performance of the classifier

Three classifiers have been designed, as explained in Chapter 4. It is needed to analyze the performance of these classifier subsystems to validate the designs. The first system is designed for the purpose of binary classification of different cardiovascular diseases. The designed prototype gives the result of 1 or -1 in the final stage. In the second classifier, the classifier gives the output from class 1 to class 7 upon processing the PPG signal. For these two classifiers, it is required to determine the true positive (TP), false positive (FP), true negative (TN), and false

negative (FN) cases from the system.

True Positive (TP): Normal instances correctly identified as normal

False Negative (FN): Normal instances that are identified as abnormal

True Negative (TN): Abnormal instances that are identified as abnormal

False Positive (FP): Abnormal instances that are identified as normal

Various parameters are checked to analyze the system performance of a machine learning classifier. These are discussed below which will be used to check the system performance of the designed classifiers in detecting various diseases.

How well a machine learning model can identify positive examples is measured by its sensitivity. It is often referred to as recall or true positive rate (TPR). It is expressed by eqn. 5.3.

$$Sensitivity = \frac{TP}{TP + FN} * 100 \quad (5.3)$$

The capacity of the algorithm or model to forecast a true negative for each possible category is referred to as specificity. It is defined by eqn. 5.4.

$$Specificity = \frac{TN}{TN + FP} * 100 \quad (5.4)$$

The accuracy in machine learning is a measurement statistic that compares the proportion of accurate predictions made by a model to all predictions made. The following equation determines it:

$$Accuracy = \frac{TN + TP}{TN + TP + FN + FP} * 100 \quad (5.5)$$

Eqn. 5.6 shows the error rate, which measures how far a model deviates from the genuine model in its predictions.

$$Err = \frac{FN + FP}{TN + TP + FN + FP} * 100 \quad (5.6)$$

A false alarm rate is calculated as the ratio of false alerts to all other non-events. It is expressed by eqn. 5.7

$$FA = \frac{FP}{TN + FP} * 100 \quad (5.7)$$

Precision indicates the proportion of positive identifications that are actually correct. It is determined by the following equation:

$$Precision = \frac{TP}{TP + FP} * 100 \quad (5.8)$$

The F-measure, commonly called the F1 score, is a metric used to assess how well a machine learning model performs. The harmonic mean of precision and recall is used to calculate the F-measure, giving each the same weight. It enables the evaluation of a model that accounts for both precision and recall using a single score, which is useful for characterizing the model's performance. It is expressed by eqn. 5.9

$$F - measure = 2 * \frac{Sensitivity * Precision}{Sensitivity + Precision} * 100 \quad (5.9)$$

The necessary confusion matrices for measuring these parameters are presented in Fig. 5.3. It can be seen from the confusion matrices that using the physical features: age and BMI, along with nine statistical features provides the better result. The total number of true positives and true negatives has increased for 11 features. So, it has improved the classification performance for each disease detection if it is compared with the performance in the case of using only the nine statistical features. Hence, the accuracy and classification parameters have improved. Therefore, the results are analyzed for 11 features for the binary classifier performance analyses. We can see the total number of true positives and true negatives has increased by 2 for hypertension. For cerebral infarction and cerebrovascular disease, it has increased by 1. For diabetes, the total number of true positives and negatives has increased by 6. So, for all the diseases, the accuracy will be better for 11 features.

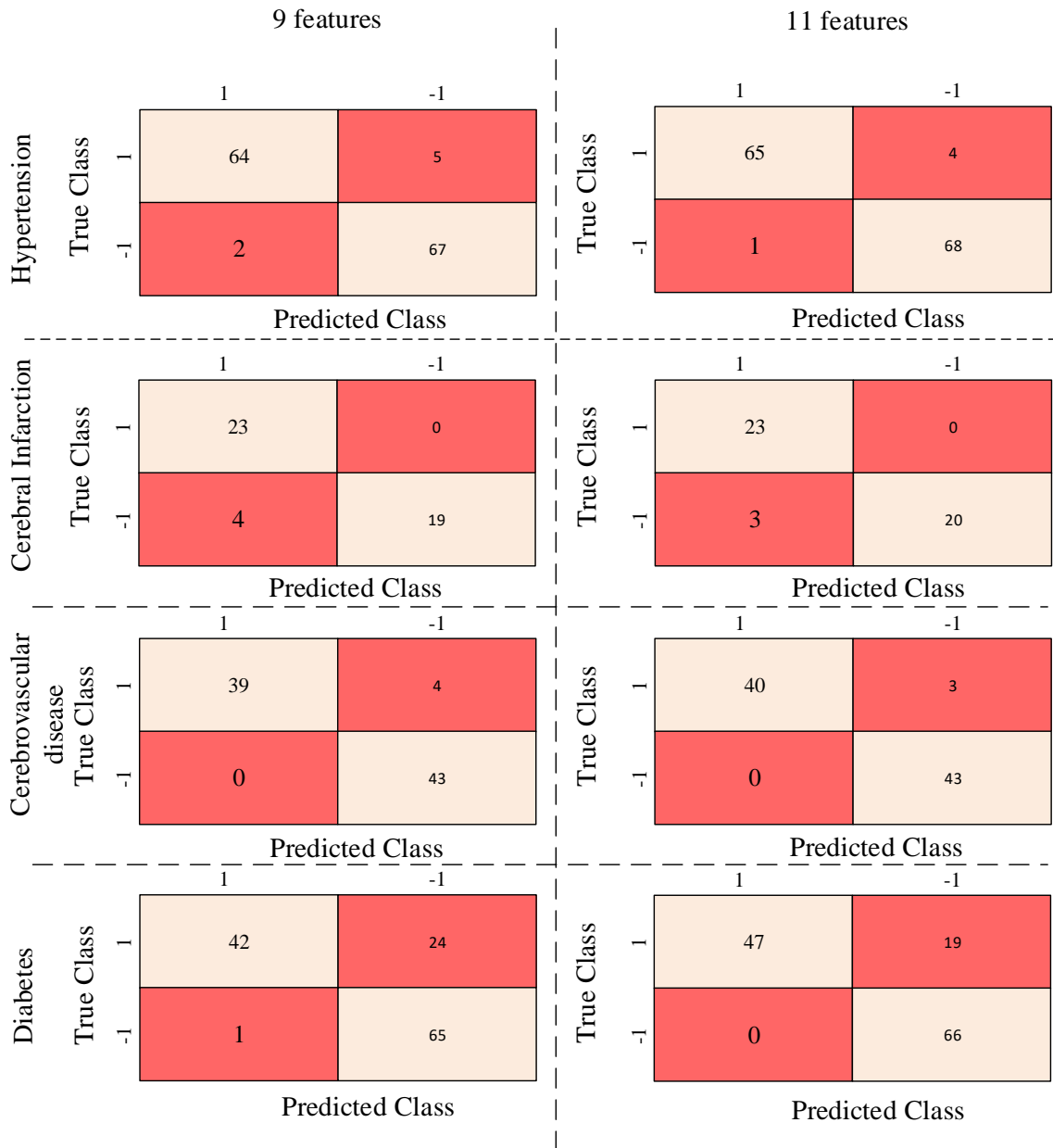


Fig. 5.3 Confusion matrix for binary classification using 9 and 11 features

5.3.1 Hypertension Detection

The performance of the designed binary SVM classifier for hypertension is analyzed in this section. In the software level design, 5-fold cross-validation has been applied. It resulted in 98.5% accuracy in detecting hypertension. For hardware-level implementation, nine statistical features and two physical features are used. The performance of the classifier using these features is determined using Eqn. 5.3 to Eqn. 5.9 and presented in Table 5.4.

Table 5.4. Confusion matrix and classifier performance for hypertension detection

Performance parameter	Rate	Confusion matrix	
Sensitivity	94.2%	<div> <div>True Class</div> <div> <div>1</div> <div>-1</div> </div> <div> <div>1</div> <div>-1</div> </div> <div>Predicted Class</div> </div>	<div> <div>1</div> <div>-1</div> </div>
Specificity	98.55%		
Accuracy	96.37%		
Error rate	3.63%		
False alarm	1.45%		
Precision	98.48%		
F-measure	96.29%		

5.3.2 Cerebral Infarction Detection

In the case of cerebral infarction, an accuracy of 96.05% has been achieved using 9 statistical and 2 physical features with 5-fold cross-validation in the software design. The confusion matrix and classifier performances for cerebral infarction detection with nine statistical features are presented in Table 5.5.

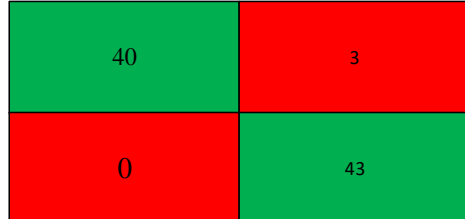
Table 5.5. Confusion matrix and classifier performance for cerebral infarction detection

Performance parameter	Rate	Confusion matrix	
Sensitivity	100%	<div> <div>True Class</div> <div> <div>1</div> <div>-1</div> </div> <div> <div>1</div> <div>-1</div> </div> <div>Predicted Class</div> </div>	<div> <div>1</div> <div>-1</div> </div>
Specificity	86.96%		
Accuracy	93.48%		
Error rate	6.53%		
False alarm	13.04%		
Precision	88.46%		
F-measure	93.48%		

5.3.3 Cerebrovascular Disease Detection

For cerebrovascular disease detection at the software level, an accuracy of 98.33% has been achieved from the SVM classifier using 11 features with 5-fold cross-validation. The confusion matrix for cerebrovascular disease detection is presented in Table 5.6.

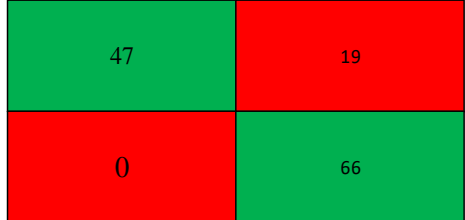
Table 5.6. Confusion matrix and classifier performance for cerebrovascular disease detection

Performance parameter	Rate	Confusion matrix	
Sensitivity	95.24%		
Specificity	97.62%		
Accuracy	96.43%		
Error rate	3,57%		
False alarm	2.38%		
Precision	97.56%		
F-measure	96.39%		
		Predicted Class	

5.3.4 Diabetes Detection

For diabetes detection using 5-fold cross-validation in Matlab, 97.17% accuracy is achieved. At the hardware level, the classifier is tested with the selected recordings. The confusion matrix for diabetes detection with eleven features is presented in Table 5.7.

Table 5.7. Confusion matrix and classifier performance for type-2 diabetes mellitus detection

Performance parameter	Rate	Confusion matrix																	
Sensitivity	81.54%	<div><div><div>1</div><div>-1</div></div><div><div>1</div><div>-1</div></div></div>  <tr><td>Specificity</td><td>95.38%</td></tr> <tr><td>Accuracy</td><td>88.46%</td></tr> <tr><td>Error rate</td><td>11.54%</td></tr> <tr><td>False alarm</td><td>4.61%</td></tr> <tr><td>Precision</td><td>94.64%</td></tr> <tr><td>F-measure</td><td>87.6%</td></tr> <tr><td colspan="2"></td><td colspan="2">Predicted Class</td></tr>		Specificity	95.38%	Accuracy	88.46%	Error rate	11.54%	False alarm	4.61%	Precision	94.64%	F-measure	87.6%			Predicted Class	
Specificity	95.38%																		
Accuracy	88.46%																		
Error rate	11.54%																		
False alarm	4.61%																		
Precision	94.64%																		
F-measure	87.6%																		
		Predicted Class																	

A comparison showing the performance parameters for all the disease detection in the binary classifiers is presented in Table 5.8. It shows that all the classifiers have an accuracy of over 85% and over 90% for 3 cardiovascular diseases. On average, the accuracy of the binary classifiers is 93.69%.

Table 5.8. System performance analysis for binary classification

	Hypertension	Cerebral infarction	Cerebrovascular diseases	Diabetes
Sensitivity	94.2%	100%	95.24%	81.54%
Specificity	98.55%	86.96%	97.62%	95.38%
Accuracy	96.37%	93.48%	96.43%	88.46%
Err	3.63%	6.52%	3.57%	11.54%
FA	1.45%	13.04%	2.38%	4.61%
Precision	98.48%	88.46%	97.56%	94.64%
F-1 score	96.29%	93.88%	96.39%	87.6%

5.3.5 Multiclass Classification

In the case of multiclass classification, 7 classes have been considered. The classifier is developed based on the SVM classifier. A comparator gives the output of different classes after analyzing the PPG signal. The confusion matrix for this case is shown in Fig. 5.4. Here, among the different classes the

True Class	Normal	17	0	0	0	0	0	
	Diabetes	0	15	0	0	0	1	1
	Cerebral Infarction	0	0	12	2	2	1	0
	Cerebrovascular Disease	0	0	0	13	2	2	0
	Hypertension	0	0	0	0	11	4	2
	Hypertension & Diabetes	0	3	0	0	1	13	0
	Diabetes & Prehypertension	0	1	0	0	0	2	14
		Normal	Diabetes	Cerebral Infarction	Cerebrovascular Disease	Hypertension	Hypertension & Diabetes	Diabetes & Prehypertension
		Predicted Class						

Fig. 5.4 Confusion matrix for multiclass classification

developed system can predict all the 17 normal cases accurately. In the case of diabetes, it can predict 15 accurately. 12, 13, 11, 13, and 14 cases are accurately

predicted for cerebral infarction, cerebrovascular disease, hypertension, hypertension with diabetes and prehypertension with diabetes, respectively. So, It has an accuracy of 100% for class 1, 88.24% for predicting class 2, 70.58% for class 3, 76.47% for class 4 and class 6, 64.71% for class 5, and 82.35% for class 7. The overall accuracy of this system is approximately 80%.

5.3.6 Heart Rate and Blood Pressure Estimation Classifier

Linear regression algorithm has been used for estimating blood pressure and heart rate. A different number of features have been utilized to check the result. It has been started from 3 features: mean, sum, AE and the mean absolute error (MAE) and standard deviation have been checked for each case. Then one feature has been added and the system performance has been checked again. This has been continued for all the nine statistical features. When a feature is increased for accuracy, the feature requiring fewer logic blocks during design has been given priority. The heart rate and blood pressure for different feature combinations are measured following the multiple linear regression equation:

$$y = b_o + b_1x_1 + b_2x_2 + \dots + b_mx_m \quad (5.10)$$

where, y is the estimated value, b_o is the intercept, $b_1, b_2, b_3, \dots, b_m$ are regression coefficients, and $x_1, x_2, x_3, \dots, x_m$ are the independent variables or the feature values.

The performance in heart rate and blood pressure estimating for different feature combinations is shown in Table 5.9.

Table 5.9 shows that for all cases, using 5 features gives the best result. Using only three features, the worst result is achieved. By using 5 features, the $MAE \pm SD$ for heart rate estimation is 3.05 ± 1.99 beat per minute. In the case of systolic and diastolic blood pressure, they are 4.79 ± 2.74 and 3.52 ± 2.33 , respectively.

Table 5.9. Performance analysis for different features

Heart Rate			Blood Pressure			
features			SBP		DBP	
	MAE	SD	MAE	SD	MAE	SD
3	4.33	2.18	6.3	2.4	5.14	2.87
4	3.75	2.14	5.72	2.88	4.51	2.98
5	3.05	1.99	4.79	2.74	3.52	2.33
6	3.29	2.15	4.99	2.97	4.12	3.13
7	3.45	2.67	5.39	3.06	4.34	2.76
8	3.38	2.54	5.07	2.99	3.94	2.88
9	3.56	2.27	5.33	3.18	4.22	3.02

5.4 Resource and Power Utilization Analysis

The system has been implemented in the Xilinx system generator primarily targeting Zedboard Zynq xc7z020-1clg484. It utilizes look-up table (LUT), lookup table random access memory (LUTRAM), flip flop (FF), block random access memory (BRAM), digital signal processing (DSP), input/output (IO), global buffer (BUFG). These resources consume power for their operation. The resource utilization of the various systems designed is presented in this section. Also, the amount of power required by the designed prototype is analyzed in this section.

5.4.1 Binary Classification Architecture

For the binary classifier, a SVM classifier is designed. The system with eleven features performs better than the other designs with nine features. Hence, the better system has been selected for resource and power utilization analysis.

Table 5.10. Zedboard Resource utilization for binary classifier

Resource	Utilization	Available	Utilization percentage
LUT	20349	53200	38.23%
LUTRAM	501	17400	2.88%
FF	3990	106400	3.75%
BRAM	7.50	140	5.35%
DSP	134	220	60.9%
I\O	65	200	32.5%
BUFG	1	32	3.12%

The resource utilization considering eleven features is presented in Table 5.10. It is evident from Table 5.10 that, the Zedboard zynq 7000 FPGA board has enough resources for this system design.

Due to the requirement of these resources, the system will require some power to operate these logic blocks. The power consumption by the binary system is depicted in Fig. 5.5.

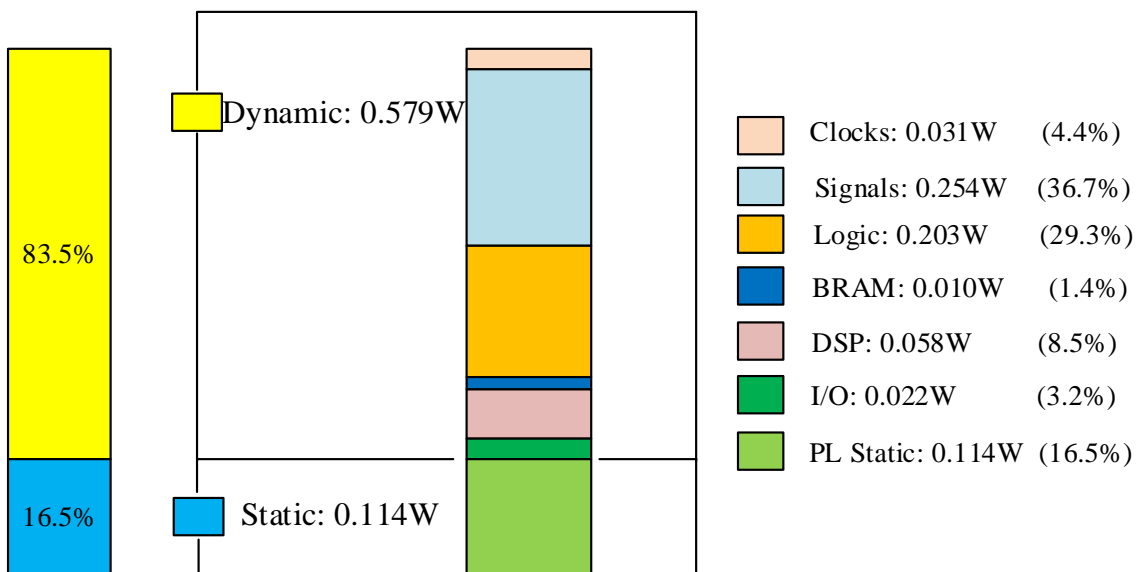


Fig. 5.5 Power Utilization for the binary classifier in Zedboard

As shown in Fig. 5.5, the system requires a total of 0.693 W power, among which 0.579 W is dynamic power and 0.114 W is static power. Static power is the power supplied when the design is configured but no activity is applied. It is the minimum power that is required while the design operates. On the other hand, dynamic power is the power that is required when the device is running an application. 83.5% of the dynamic power is distributed for different logic operations where signals and logic blocks consume maximum power. This system requires maximum power for signals and logic portion.

5.4.2 Multiclass Classification Architecture

For the multiclass classifier, seven SVM classifiers have been designed. Due to the high amount of logic blocks required during the design procedure, it will

have more resource utilization than the binary classification process. The system requires more DSP than available in Zedboard zynq. Hence, zynq ultrascale+ have been selected for this design in FPGA. The resource analysis is presented in Table 5.11.

Table 5.11. Zynq Ultrascale+ Resource utilization analysis for multiclass classification

Resource	Utilization	Available	Utilization percentage
LUT	49168	230400	21.34%
LUTRAM	501	101760	0.5%
FF	8783	460800	1.9%
BRAM	7.5	312	2.4%
DSP	270	1728	15.62%
I\O	258	360	71.67%
BUFG	1	544	0.18%

It can be seen from Table 5.11 that, the amount of LUT, LUTRAM, Flipflop, BRAM, and BUFG required for this design are available in zedboard zynq. However, the amount of DSP and Input-Output (I\O) blocks required for this design are more than the number available in this board. However, zynq ultrascale+ board has an available number of blocks for DSP and I\O. Also, other resources are available in increased numbers on this board. Due to the increased number of SVM classifiers in this design, it requires more resources. So, it will require more power to operate. The power consumption by the multiclass classifier system is depicted in Fig. 5.6.

This system requires 0.807 W of power as dynamic power which is 57.51% of total power. The rest 42.49% is static power which is about 0.596 W. In this system static power is required for processing system (PS) and programmable logic (PL). In this system, maximum power is consumed for PL static case.

5.4.3 Heart Rate and Blood Pressure Estimation Architecture

For the heart rate and blood pressure estimation, linear regression classifier has been used. Also, in this case, 5 features are used. So, the number of required

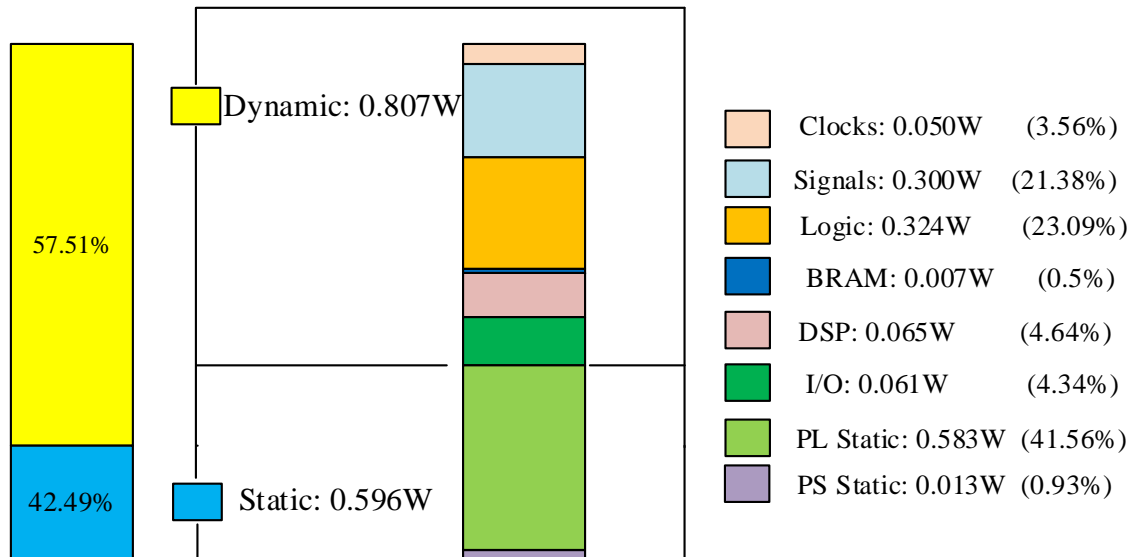


Fig. 5.6 Power Utilization for the multiclass classifier in zynq Ultrascale+

resources will be less than in other designs. The heart rate and blood pressure are measured following the multiple linear regression equation:

$$y = b_0 + b_1x_1 + b_2x_2 + \dots + b_mx_m \quad (5.11)$$

where, y is the estimated value, b_0 is the intercept, $b_1, b_2, b_3, \dots, b_m$ are regression coefficients, and $x_1, x_2, x_3, \dots, x_m$ are the independent variables or the feature values.

The resource utilization for this stage is shown in Table 5.12.

Table 5.12. Resource utilization analysis of the developed prototypes in zedboard

Resource	Utilization	Available	Utilization percentage
LUT	9903	53200	18.61%
LUTRAM	466	17400	2.68%
FF	2536	106400	2.38%
BRAM	7.50	140	5.35%
DSP	74	220	33.64%
IO	65	200	32.5%
BUFG	1	32	3.12%

It is evident from Table 5.12 that, this system requires the least amount of logic blocks. As the zynq 7000 FPGA board has enough resources required for this system, this board has been used in this design. The power requirement will also

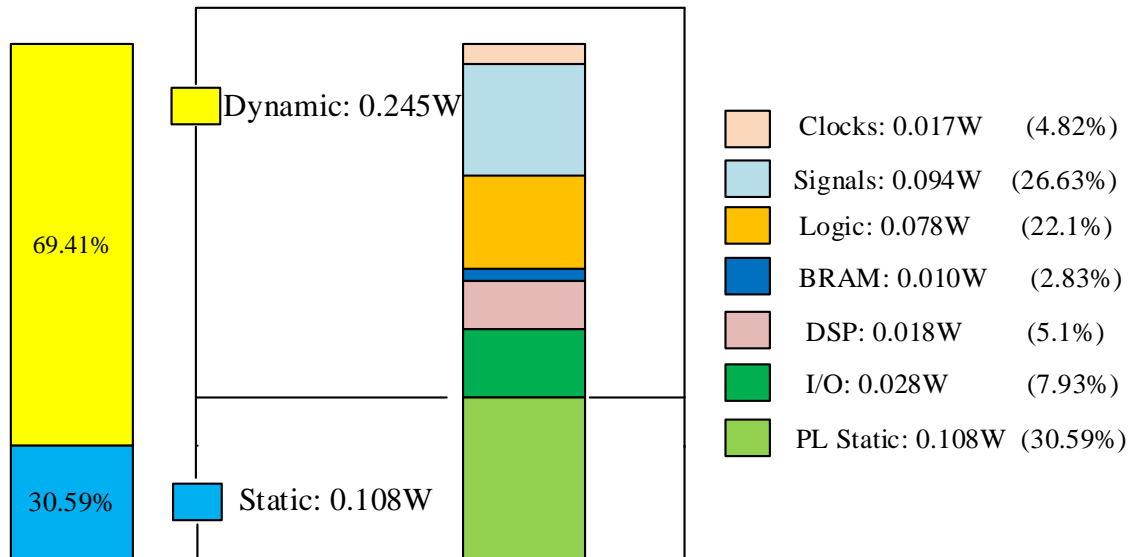


Fig. 5.7 Zedboard power Utilization for heart rate and blood pressure estimation

be less for this system with fewer resources. The power consumption by the prediction system is depicted in Fig. 5.7.

So, the system requires 0.353 W of power, among which 0.245 W is dynamic power and 0.108 W is static power. In this case, also, maximum power is required for static operation.

5.5 Comparative Study

The designed system performance needs to be compared with the previous works to show their efficacy.

A comparison study of cardiovascular disease detection from PPG signal is shown in Table 5.13.

From Table 5.13 it is seen that different types of cardiovascular disease classification have been done from PPG signal. However, to the best of my knowledge, this is the first work to detect cerebral infarction and cerebrovascular disease from PPG. This study has detected these diseases from PPG signals with significant accuracy. Also, hypertension has been classified from PPG signals and the detection accuracy is better than most of the works on

hypertension classification from PPG signals.

A part of this study also includes a multiclass classification study to detect various combinations of cardiovascular diseases including diabetes. However, previously the maximum study was done for binary classification. Only [59] has done a multiclass classification of different hypertension stages. Again, considering the number of features used in previous studies it can be seen that fewer features have been used in this study than most of the works. It should be noted that the works that have used fewer features have achieved lower accuracy. Also, most of the previous works are done at the software level while the designed systems in this thesis have developed the classification or detection system both at the software and hardware level. In both software and hardware based studies this study has shown significantly improved accuracy than the previous studies.

Considering the accuracy of the classification systems of the previous works it also illustrates that the developed prototypes have achieved significantly more accuracy than most of the works. It can be seen from Table 5.13 that some of the works did not provide their system accuracy. Instead, these works have provided the F1-score, sensitivity and specificity results. However, the designed systems have overcome them in those parameters also. [59] has achieved more accuracy in detecting hypertension. However, it is done at the software level, while the system in this study is developed at the hardware level. Also, this work has utilized 30 features, while only 11 features have been used for this system design.

Therefore, this study has advantages over previous studies in terms of using fewer features and achieving higher accuracy even at the hardware level, along with classifying two cardiovascular diseases which were not explored before to the best of my knowledge.

Table 5.13. Comparative study on CVD detection from PPG

Reference	Dataset	Disease type	Features used	Design level	Method	Accuracy
Wang et al. [43]	Collected data	CVDs	4	Software	SVM	78.84%
Allen et al. [44]	Collected data		–	Software	AlexNet Deep learning	88.9%
Fahoum et al. [45]	Collected data	Coronary artery disease	14	Software	Naive Bayes	94.44%
Paradkar et al. [46]	MIMIC II	Coronary artery disease	45	Software	SVM	85% sensitivity, 78% specificity
Liang et al. [56]	PPG BP	Hypertension	10	Software	Risk stratification	91.31% F1 score
Frederick et al. [57]	PPG BP	Hypertension	–	Software	CNN	80%
Martinez et al. [58]	PPG BP	Hypertension	22	Software	SVM	71.42%
Sadad et al. [59]	PPG BP	Hypertension	30	Software	Decision tree	99.5%
Evdochim et al. [118]	PPG BP	Hypertension	4	Software	Quadratic SVM	72.9%
Proposed work-Binary		Hypertension Cerebral infarction Cerebrovascular disease	11	Hardware		96.37%
	PPG BP				SVM	93.48%
						96.47%
Proposed work-Multiclass	PPG BP	Hypertension, cerebral infarction, cerebrovascular disease, diabetes mellitus type -2 and their combinations (7 class)	11	Hardware	SVM	79.83%

Table 5.14. Comparative study for diabetes classification from PPG

Reference	Dataset	Features used	Design level	Method	Accuracy
Prabha et al. [71]	C. Salamea	107	Software	RBF Kernel based SVM	92.38%
Qawqzeh et al. [72]	Collected data	3	Software	Logistic Regression	92.3%
Susana et al. [73]	Gold standard dataset	–	Software	Ensemble Bagged Trees	98%
Hettiarachchi et al.[74]	PPG BP dataset	4	Software	Linear Discriminant Analysis	79%
Reddy et al. [75]	IAIMS research	31	Software	SVM	89%
This work	PPGBP	11	Hardware	SVM	88.46%

The diabetes mellitus type-2 classification is also performed on the binary SVM classifier system. Its performance is compared with some previous studies on the detection of diabetes from PPG signal in Table 5.14.

It can be seen from Table 5.14 that, the previous works on diabetes detection have been done at the software level. In this study, a hardware-based system is designed for type-2 diabetes mellitus classification. Considering the number of used features, it can be seen that the designed system uses fewer features than some of the previous works. Different classification methods have been applied for diabetes detection from PPG signals. This system uses SVM for diabetes detection. The [75] has also used SVM for diabetes classification and achieved slightly higher accuracy. But it has used more features than the proposed work and done at the software level.

Though most of the previous works have better accuracy than the proposed work, the proposed system is designed at the hardware level. To the best of my knowledge, it is the first hardware-based work for type-2 diabetes mellitus classification from PPG.

Table 5.15. Comparison study of heart rate estimation from PPG

Reference	Dataset	Subjects /segments	Implementation level	Method	MAE (bpm)	SD	Error Rate
Zhang et al. [86]	IPSC	12 subjects	Software	Signal processing & ML	–	–	5%
Reiss et al. [87]	WESAD	15 subjects	Software	CNN	7.65	–	–
Change et al. [88]	IEEE Cup Training dataset	12 segments	Software	DCNN	1.61	–	–
Motin et al. [89]	IEEE Cup Training dataset	23 segments	Software	Weiner filtering	1.85	–	–
Islam et al. [119]	–	12 subjects	Software	Time-frequency domain approach	1.16	± 1.74	–
Proposed work	PPG BP Dataset	331 recordings	Hardware	Linear Regression	3.05	± 1.98	4.04%

Again, the heart rate estimation performance is compared with previous studies in Table 5.15. Here also, most of the works are done at the software level. There is a hardware-based implementation using FPGA for predicting heart rate [89]. However, it has not provided any performance analysis of the developed system. In this study, the system's performance has been analyzed evaluating its error percentage in predicting the heart rate. Also, the power consumption analysis and resource analysis are done in this study. It is seen that the number of subjects considered for different studies is lower than the this study. 331 recordings from 153 subjects have been considered for this proposed work which validates the system more. Also, the algorithm that has been implemented, linear regression, is not used in those previous studies. Though the mean absolute error of the proposed system is higher than some of the works, as a cuffless and non-invasive method along with the hardware implementation, this system has shown significant results in predicting heart rate.

The blood pressure estimation system is compared with previous studies in Table 5.16. There are some works utilizing digital chips for predicting blood pressure [79], [80]. However, the detection algorithm is implemented at the software level in those works. Other previous works are also done at the software level. In this case also, the proposed system has been developed considering more subjects than other works. Also, fewer features have been used than most of the previous works. The previous studies have used different machine learning algorithms like SVM, ANN, and CNN, but in this study, a system has been designed using linear regression. In previous studies, system performance analysis or resource and power consumption analysis of the designed system is lacking. Furthermore, the proposed work outperforms most of the works in blood pressure prediction accuracy though it is developed at the hardware level.

Table 5.16. Comparison study of blood pressure estimation from PPG

Reference	Database /Segments	Features	Implementation level	Method	SBP (mmHg)			DBP (mmHg)		
					MAE	SD	Error	MAE	SD	Error
Zhang et al. [77]	Vital signs dataset	9	Software	SVM	11.64	± 8.20	-	7.617	± 6.78	-
Samimi et al. [78]	Vital signs dataset	21	Software	ANN	7.41	10.4	-	3.32	4.89	-
Slapnicar et al. [79]	MIMIC	13	Software	Regression	8.57	-	-	4.42	-	-
Wang et al. [80]	Collected data	3	Hardware	-	3.27	3.27	-	1.21	1.97	-
Kurylyak et al. [120]	MIMIC	21	Software	ANN	3.80	± 3.46	-	2.21	± 2.09	-
Schlesinger et al. [121]	MIMIC	-	Software	CNN	5.95	-	-	3.41	-	-
Proposed work	PPG BP dataset	9	Hardware	Linear Regression	4.79	± 2.74	3.77%	3.52	± 2.33	4.8%

5.6 Key Findings

The key findings of this study are presented below:

- The study has designed an implementation of FPGA-based binary classification of several cardiovascular diseases: hypertension, cerebral infarction, and cerebrovascular disease from PPG signal.
- Though there are some previous works on hypertension detection, they are done at the software level. The implemented system has been designed at the hardware level with 96.37% accuracy. Also, to the best of my knowledge, there are no previous works on classifying PPG signal for cerebral infarction and cerebrovascular diseases. So, it is the first of its kind in this regard. The designed system detects cerebral infarction with 93.48% accuracy and cerebrovascular disease with 96.47%.
- The study also classifies PPG signal for the detection of type-2 diabetes. In this case also, no FPGA-based previous implementation work has been found. The system detects diabetes with 88.46% accuracy. To the best of my knowledge, it is the first PPG-based hardware implemented type-2 diabetes detection work.
- This study also checks the feasibility of multiclass classification of PPG signals. There are few studies on the multiclass classification of hypertension based on software-based PPG signals. However in this study, a combination of four diseases have been considered for multiclass classification and achieved an accuracy of 79.83% from the FPGA implementation.
- The study also focuses on blood pressure and heart rate estimation from PPG signal with FPGA implementation. It is analyzed for hardware implementation, while the previous works are done at the software level. Compared to traditional wearable devices, the designed system can also detect some cardiovascular diseases and diabetes which is one of the uniquenesses of this study.

Chapter 6: Conclusions

The overall methodologies and findings of this study are presented in this chapter. It summarizes the discussion of the methodology and results section. In addition, this chapter contains general, key findings, and limitations along with the significance of the study. The future study subsection will present the researchers interested in this topic with some suggestions to work with.

6.1 Conclusions

Photoplethysmogram is a biosignal that can be acquired in a non-invasive manner with the use of a simple sensor. It is an electrical signal that acts according to the change in the volume of blood supply. It has been studied for various purposes by researchers which include different disease detection, health condition monitoring, and health parameter estimation. In this study, the aim is to detect several cardiovascular diseases: hypertension, cerebral infarction, and cerebrovascular disease along with diabetes from PPG signal. In addition, predicting heart rate and blood pressure from PPG is another objective of the study. State-of-the-art research presents most of the detection or classification or estimation studies of PPG signals are at the software level. So, the target has been to implement a hardware-based system for detecting the diseases. FPGA is chosen for its advantage over other hardware-based platforms. Xilinx system generator has been used for the design procedure and Zedboard zynq 7000 board has been targetted primarily for implementation. The binary classification system and the heart rate and blood pressure estimation system have been successfully implemented using this FPGA. However, for the multiclass classification, more resources have been required by the system. So, zynq ultrascale+ FPGA board has been targeted for the multiclass classification approach. All system performances have been individually analyzed in the study. Furthermore, the power utilization analysis

has been done, which verifies the efficacy of the systems as power-efficient devices.

6.2 Limitations

The study has been tried to design with the best level to get maximum performance with optimized resource and power utilization. However, still some limitations are there which are as follows:

- Different disease detection systems have been developed and tested based on one dataset only. It is needed to test and verify for other datasets also.
- There are not enough data in some cases, for example, in the case of cerebrovascular disease, we have selected only 23 segments to work with. More data will undoubtedly validate the system design more strongly.
- Three systems are designed in this study for multiple purposes. We could develop all the systems in a single design, but due to resource limitations of the FPGA board, all the systems had to be designed separately.
- Though we have achieved satisfactory accuracy in detecting hypertension, cerebral infarction and cerebrovascular disease, the detection accuracy of diabetes is below 90%.
- The multiclass classification system has an accuracy of 79.83%, which is also not up to the mark.
- The power consumption analysis of various designs has shown the static power consumption, which is the power needed during the design operation, but no activity is applied. It consumes a lot of power in all the cases. Specially, for the multiclass classification system, it is 42.49% of total power and 30.59% in case of heart rate and blood pressure estimation.

6.3 Future Scopes

The designed systems can be utilized and improved for future studies. There are scopes to develop wearable devices, smart healthcare systems, and point-of-care

systems using FPGA-based designs.

The developed prototype can be extended further to design wearable devices such as smartwatches, fitness trackers etc. Heart rate and blood pressure measurements are important health parameters for checking the condition of patients or during physical exercise. The designed system can be implemented to develop wearable systems to detect these parameters from the PPG signal instantly.

Smart healthcare systems are now a need in the modern world. Automatic disease detection can save millions of lives from early departure. So, a smart healthcare system based on FPGA-based designs can be handy. The developed prototype can be improvised to detect disease or alarming symptoms of disease and will pave the way for early treatment.

Point-of-care system can be implemented too using the designed prototypes. A POC will monitor the condition of a patient and give information about important health parameters to the doctors and relatives. It will also alarm the patient during severe conditions. Thus the hidden symptoms of the disease can be detected instantly and necessary steps for treatment can be made.

There is an opportunity to improve the designed systems from several perspectives too. There is scope to increase the accuracy of the systems designed in the Xilinx system generator. In particular, the multiclass classifier system has an accuracy of 79.83% and the diabetes mellitus type-2 detection system has an accuracy of 88.46%. These accuracies can be improved further.

Also, the system can be extended to detect other cardiovascular diseases. PPG is verified to detect various cardiovascular diseases from the literature review and also this study validates this more. So, PPG can be further studied to detect other types of diseases in the future.

The system has been developed and tested based on one dataset only. In the future, other PPG datasets can be combined to validate the system more firmly. It will also ensure the incorporation of more PPG recordings to design the system.

The power consumption analysis of various designs has shown the static power consumption, which is the power needed during the design operation, but no

activity is applied. It consumes a lot of power in all the cases. Specially, for the multiclass classification system, it is 42.49% of total power and 30.59% in the case of heart rate and blood pressure estimation. So, future studies can be done to reduce the static power consumption along with the total system power consumption.

The binary classification system, multiclass classification system and the blood pressure and heart rate estimation system have been developed on individual system designs. All the designs can be developed on the same system but it will utilize more resources and more power will be needed. So, it can be analyzed in future studies to develop all the systems in a single architecture with less resource and power utilization.

There is scope to validate the system more by collecting practical data from patients of the considered cardiovascular diseases and testing the designed systems with those data.

It can be further improved to develop medical equipment for treatment purposes and laboratory use in the future. The system will help doctors to detect various diseases quickly and validate different test results. Also, cardiac patients will get early treatment and will have a better chance of procurement.

Bibliography

- [1] A. A. Alian and K. H. Shelley, "PPG in clinical monitoring," *Eds. Academic Press*, 2022, pp. 341–359. doi: <https://doi.org/10.1016/B978-0-12-823374-0.00006-2>.
- [2] T. Y. Abay and P. A. Kyriacou, "Photoplethysmography for blood volumes and oxygenation changes during intermittent vascular occlusions," *J. Clin. Monit. Comput.*, vol. 32, no. 3, pp. 447–455, 2018, doi: [10.1007/s10877-017-0030-2](https://doi.org/10.1007/s10877-017-0030-2).
- [3] M. Elgendi, "On the Analysis of Photoplethysmogram Signal," *Curr. Cardiol. Rev.*, vol. 8, no. c, pp. 14–25, 2012.
- [4] J. Allen, "Photoplethysmography and its application in clinical physiological measurement," *Physiol. Meas.*, vol. 28, no. 3, p. R1, Feb. 2007, doi: [10.1088/0967-3334/28/3/R01](https://doi.org/10.1088/0967-3334/28/3/R01).
- [5] R. Shriram, M. Sundhararajan, and N. Daimiwal, "Application of high & low brightness LEDs to human tissue to capture photoplethysmogram at a finger tip," *2014 Int. Conf. Conver. Technol. I2CT 2014*, pp. 3–7, 2014, doi: [10.1109/I2CT.2014.7092340](https://doi.org/10.1109/I2CT.2014.7092340).
- [6] A. R. Kavsaotlu, K. Polat, and M. Hariharan, "Non-invasive prediction of hemoglobin level using machine learning techniques with the PPG signal's characteristics features," *Appl. Soft Comput. J.*, vol. 37, pp. 983–991, 2015, doi: [10.1016/j.asoc.2015.04.008](https://doi.org/10.1016/j.asoc.2015.04.008).
- [7] M. DeMarco et al., "Enhanced Photochemical Activity and Ultrafast Photocarrier Dynamics in Sustainable Synthetic Melanin Nanoparticle-

- Based Donor-Acceptor Inkjet-Printed Molecular Junctions,” *Nanoscale*, p., 2023, doi: 10.1039/D3NR02387G.
- [8] B. Desai and U. Chaskar, “Comparison of optical sensors for non-invasive hemoglobin measurement,” in *2016 International Conference on Electrical, Electronics, and Optimization Techniques (ICEEOT)*, 2016, pp. 2211–2214. doi: 10.1109/ICEEOT.2016.7755085.
- [9] M. M. Wagner, W. R. Hogan, and R. M. Aryel, “The Healthcare System.”, *Elsevier Inc.*, 2006. doi: 10.1016/B978-012369378-5/50008-9.
- [10] M. L. Bates et al., “Sex differences in cardiovascular disease and dysregulation in Down syndrome,” *Am. J. Physiol. Circ. Physiol.*, vol. 324, no. 4, pp. H542–H552, 2023, doi: 10.1152/ajpheart.00544.2022.
- [11] G. W. Jones, “Impact of COVID-19 on mortality in Asia,” *Asian Popul. Stud.*, vol. 19, no. 2, pp. 131–147, 2023, doi: 10.1080/17441730.2023.2193476.
- [12] J. Park, H. S. Seok, S. S. Kim, and H. Shin, “Photoplethysmogram Analysis and Applications: An Integrative Review,” *Front. Physiol.*, vol. 12, no. March, pp. 1–23, 2022, doi: 10.3389/fphys.2021.808451.
- [13] S. Huthart, M. Elgendi, D. Zheng, G. Stansby, and J. Allen, “Advancing PPG Signal Quality and Know-How Through Knowledge Translation—From Experts to Student and Researcher,” *Front. Digit. Heal.*, vol. 2, no. December, 2020, doi: 10.3389/fdgth.2020.619692.
- [14] M. A. Almarshad, M. S. Islam, S. Al-Ahmadi, and A. S. Bahammam, “Diagnostic Features and Potential Applications of PPG Signal in Healthcare: A Systematic Review,” *Healthc.*, vol. 10, no. 3, pp. 1–28, 2022, doi: 10.3390/healthcare10030547.
- [15] D. Berwal, A. Kuruba, A. M. Shaikh, A. Udupa, and M. S. Baghini, “SpO₂ Measurement: Non-Idealities and Ways to Improve Estimation Accuracy in Wearable Pulse Oximeters,” *IEEE Sens. J.*, vol. 22, no. 12, pp. 11653–11664, 2022, doi: 10.1109/JSEN.2022.3170069.

- [16] M. Fachrurazi, M. H. Barri, and R. A. Piramathi, "Design of Wearable Pulse Oximeter Based on Android with Bluetooth Low Energy Communication Using Artificial Neural Network," *2021 Int. Conf. Data Sci. Its Appl. ICoDSA 2021*, pp. 263–268, 2021, doi: 10.1109/ICoDSA53588.2021.9617472.
- [17] M. Krizea, J. Gialelis, G. Protopsaltis, C. Mountzouris, and G. Theodorou, "Empowering People with a User-Friendly Wearable Platform for Unobtrusive Monitoring of Vital Physiological Parameters," *Sensors*, vol. 22, no. 14, 2022, doi: 10.3390/s22145226.
- [18] F. Braun et al., "Evaluation of a novel ear pulse oximeter: Towards automated oxygen titration in eyeglass frames," *Sensors (Switzerland)*, vol. 20, no. 11, pp. 1–11, 2020, doi: 10.3390/s20113301.
- [19] O. Y. Tham, M. A. Markom, A. H. A. Bakar, E. S. M. M. Tan, and A. M. Markom, "IoT Health Monitoring Device of Oxygen Saturation (SpO₂) and Heart Rate Level," *Proceeding - 1st Int. Conf. Inf. Technol. Adv. Mech. Electr. Eng. ICITAMEE 2020*, pp. 128–133, 2020, doi: 10.1109/ICITAMEE50454.2020.9398455.
- [20] F. Rundo, R. Emanuele Sarpietro, and S. Battiato, "Bio-inspired Embedded System for Intelligent Driving Assistance in the Next Generation Cars," *2022 AEIT Int. Annu. Conf. AEIT 2022*, pp. 1–6, 2022, doi: 10.23919/AEIT56783.2022.9951723.
- [21] F. Rundo, R. Leotta, and S. Battiato, "Real-Time Deep Neuro-Vision Embedded Processing System for Saliency-based Car Driving Safety Monitoring," *2021 4th Int. Conf. Circuits, Syst. Simulation, ICCSS 2021*, pp. 218–224, 2021, doi: 10.1109/ICCSS51193.2021.9464177.
- [22] F. Rundo, C. Spampinato, S. Battiato, F. Trenta, and S. Conoci, "Advanced 1D temporal deep dilated convolutional embedded perceptual system for fast car-driver drowsiness monitoring," *2020 AEIT Int. Conf. Electr. Electron. Technol. Automotive, AEIT Automot. 2020*, 2020, doi: 10.23919/aeitautomotive50086.2020.9307400.

- [23] F. Rundo, S. Conoci, S. Battiato, F. Trenta, and C. Spampinato, "Innovative saliency based deep driving scene understanding system for automatic safety assessment in next-generation cars," *2020 AEIT Int. Conf. Electr. Electron. Technol. Automotive, AEIT Automot. 2020*, 2020, doi: 10.23919/aeitautomotive50086.2020.9307425.
- [24] F. Rundo, "Perceptive Advanced Car-driver Drowsiness Monitoring Neuro-Embedded System," *Eliv 2021*, no. 2384, pp. 317–330, 2021, doi: 10.51202/9783181023846-317.
- [25] A. Hina, S. Minto, and W. Saadeh, "A 208 μ W PPG-based Glucose Monitoring SoC using Ensembled Boosted Trees," *20th IEEE Int. Interreg. NEWCAS Conf. NEWCAS 2022 - Proc.*, pp. 241–245, 2022, doi: 10.1109/NEWCAS52662.2022.9842163.
- [26] A. Hina and W. Saadeh, "A Noninvasive Glucose Monitoring SoC Based on Single Wavelength Photoplethysmography," *IEEE Trans. Biomed. Circuits Syst.*, vol. 14, no. 3, pp. 504–515, 2020, doi: 10.1109/TBCAS.2020.2979514.
- [27] T. Mahmud et al., "Non-invasive Blood Glucose Estimation Using Multi-sensor Based Portable and Wearable System," *2019 IEEE Glob. Humanit. Technol. Conf. GHTC 2019*, pp. 1–5, 2019, doi: 10.1109/GHTC46095.2019.9033119.
- [28] G. Hammour and D. P. Mandic, "An In-Ear PPG-Based Blood Glucose Monitor: A Proof-of-Concept Study," *Sensors*, vol. 23, no. 6, p. 3319, Mar. 2023, doi: 10.3390/s23063319.
- [29] S. H. Park, S. J. Choi, and K. S. Park, "Advance continuous monitoring of blood pressure and respiration rate using denoising auto encoder and LSTM," *Microsyst. Technol.*, vol. 28, no. 10, pp. 2181–2190, 2022, doi: 10.1007/s00542-022-05249-0.
- [30] R. B. Prasetyo, K. S. Choi, and G. H. Yang, "Design and implementation of respiration rate measurement system using an information filter on an embedded device," *Sensors (Switzerland)*, vol. 18, no. 12, 2018, doi: 10.3390/s18124208.

- [31] R. Munadi, S. Sussi, N. Fitriyanti, and D. N. Ramadan, "Non-Invasive Hemoglobin Monitoring Device Using K-Nearest Neighbor and Artificial Neural Network Back Propagation Algorithms," *Int. J. Electron. Telecommun.*, vol. 68, no. 1, pp. 13–18, 2022, doi: 10.24425/ijet.2022.139842.
- [32] C. Pintavirooj, B. Ni, C. Chatkobkool, and K. Pinijkij, "Noninvasive portable hemoglobin concentration monitoring system using optical sensor for anemia disease," *Healthc.*, vol. 9, no. 6, 2021, doi: 10.3390/healthcare9060647.
- [33] O. Olakanmi, M. Benyeogor, H. Alabi, and S. Kumar, "Bi-spectral Photoplethysmographic Non-invasive Device for Real-Time Monitoring of Blood Haemoglobin Level," *International Journals of Science and Engineering investigations*, vol. 9, no. 97, March, 2020.
- [34] N. Mitro et al., "AI-Enabled Smart Wristband Providing Real-Time Vital Signs and Stress Monitoring," *Sensors*, vol. 23, no. 5, pp. 1–26, 2023, doi: 10.3390/s23052821.
- [35] R. K. Nath and H. Thapliyal, "Smart Wristband-Based Stress Detection Framework for Older Adults with Cortisol as Stress Biomarker," *IEEE Trans. Consum. Electron.*, vol. 67, no. 1, pp. 30–39, 2021, doi: 10.1109/TCE.2021.3057806.
- [36] N. Chaowadee, P. Lertsiriyothin, T. Phuangkhemkhao, and T. Chanwimalueang, "Reinforced Learning in Children through a Stress Warning Unit," *2021 2nd Inf. Commun. Technol. Conf. ICTC 2021*, pp. 386–389, 2021, doi: 10.1109/ICTC51749.2021.9441507.
- [37] M. R. Meenal and S. M. Vennila, "Bidirectional Recurrent Network and Neuro-fuzzy Frequent Pattern Mining for Heart Disease Prediction," *SN Comput. Sci.*, vol. 4, no. 4, p. 379, 2023, doi: 10.1007/s42979-023-01711-6.
- [38] V. Mani et al., "Multiplexed sensing techniques for cardiovascular disease biomarkers - A review," *Biosens. Bioelectron.*, vol. 216, p. 114680, 2022, doi: <https://doi.org/10.1016/j.bios.2022.114680>.

- [39] L. Han et al., "Excess cardiovascular mortality across multiple COVID-19 waves in the United States from March 2020 to March 2022," *Nat. Cardiovasc. Res.*, vol. 2, no. 3, pp. 322–333, 2023, doi: 10.1038/s44161-023-00220-2.
- [40] N. A. Mohamed, I. Marei, S. Crovella, and H. Abou-Saleh, "Recent Developments in Nanomaterials-Based Drug Delivery and Upgrading Treatment of Cardiovascular Diseases," *Int. J. Mol. Sci.*, vol. 23, no. 3, 2022, doi: 10.3390/ijms23031404.
- [41] J. Allen, K. Overbeck, G. Stansby, A. Murray, "A. Photoplethysmography Assessments in Cardiovascular Disease," *Measurement and Control*, 2006;39(3):80-83. doi:10.1177/002029400603900303.
- [42] P. Cheng, Z. Chen, Q. Li, Q. Gong, J. Zhu, and Y. Liang, "Atrial fibrillation identification with PPG signals using a combination of time-frequency analysis and deep learning," *IEEE Access*, vol. 8, pp. 172692–172706, 2020, doi: 10.1109/ACCESS.2020.3025374.
- [43] Y. Wang, "Identification of Cardiovascular Diseases Based on Machine Learning," *ACM Int. Conf. Proceeding Ser.*, vol. 1, no. 1, pp. 531–536, 2022, doi: 10.1145/3570773.3570855.
- [44] J. Allen, H. Liu, S. Iqbal, D. Zheng, and G. Stansby, "Deep learning-based photoplethysmography classification for peripheral arterial disease detection: A proof-of-concept study," *Physiol. Meas.*, vol. 42, no. 5, 2021, doi: 10.1088/1361-6579/abf9f3.
- [45] A. S. Al Fahoum, A. O. Abu Al-Haija, and H. A. Alshraideh, "Identification of Coronary Artery Diseases Using Photoplethysmography Signals and Practical Feature Selection Process," *Bioengineering*, vol. 10, no. 2, 2023, doi: 10.3390/bioengineering10020249.
- [46] N. Paradkar and S. Roy Chowdhury, "Coronary artery disease detection using photoplethysmography," *Proc. Annu. Int. Conf. IEEE Eng. Med. Biol. Soc. EMBS*, pp. 100–103, 2017, doi: 10.1109/EMBC.2017.8036772.

- [47] A. Ave, H. Fauzan, S. R. Adhitya, and H. Zakaria, "Early detection of cardiovascular disease with photoplethysmogram(PPG) sensor," *Proc. - 5th Int. Conf. Electr. Eng. Informatics Bridg. Knowl. between Acad. Ind. Community, ICEEI 2015*, pp. 676–681, 2015, doi: 10.1109/ICEEI.2015.7352584.
- [48] D. Ramachandran, V. Ponnusamy Thangapandian, and H. Rajaguru, "Computerized approach for cardiovascular risk level detection using photoplethysmography signals," *Meas. J. Int. Meas. Confed.*, vol. 150, p. 107048, 2020, doi: 10.1016/j.measurement.2019.107048.
- [49] B. Zhou et al., "Worldwide trends in hypertension prevalence and progress in treatment and control from 1990 to 2019: a pooled analysis of 1201 population-representative studies with 104 million participants," *Lancet*, vol. 398, no. 10304, pp. 957–980, 2021, doi: 10.1016/S0140-6736(21)01330-1.
- [50] H. Arima et al., "Mortality patterns in hypertension," *Journal of hypertension*, vol. 29, Suppl 1 (2011): S3-7, doi:10.1097/01.hjh.0000410246.59221.b1
- [51] M. H. Forouzanfar et al., "Global burden of hypertension and systolic blood pressure of at least 110 to 115mmHg, 1990-2015," *JAMA - J. Am. Med. Assoc.*, vol. 317, no. 2, pp. 165–182, 2017, doi: 10.1001/jama.2016.19043.
- [52] S. Yusuf et al., "Modifiable risk factors, cardiovascular disease, and mortality in 155722 individuals from 21 high-income, middle-income, and low-income countries (PURE): a prospective cohort study," *Lancet*, vol. 395, no. 10226, pp. 795–808, 2020, doi: 10.1016/S0140-6736(19)32008-2.
- [53] S. T. Hardy et al., "Maintaining Normal Blood Pressure Across the Life Course: The JHS," *Hypertension*, vol. 77, no. 5, pp. 1490–1499, 2021, doi: 10.1161/HYPERTENSIONAHA.120.16278.
- [54] O. Reges et al., "Decision Tree-Based Classification for Maintaining Normal Blood Pressure throughout Early Adulthood and Middle Age: Findings from the Coronary Artery Risk Development in Young Adults (CARDIA) Study," *Am. J. Hypertens.*, vol. 34, no. 10, pp. 1037–1041, 2021, doi: 10.1093/ajh/hpab099.

- [55] I. I. Chan, M. K. Kwok, and C. M. Schooling, "The total and direct effects of systolic and diastolic blood pressure on cardiovascular disease and longevity using Mendelian randomisation," *Sci. Rep.*, vol. 11, no. 1, pp. 1–9, 2021, doi: 10.1038/s41598-021-00895-2.
- [56] Y. Liang, Z. Chen, R. Ward, and M. Elgendi, "Hypertension assessment using photoplethysmography: A risk stratification approach," *J. Clin. Med.*, vol. 8, no. 1, 2019, doi: 10.3390/jcm8010012.
- [57] G. Frederick, Y. T, and B. T. A, "PPG Signals for Hypertension Diagnosis: A Novel Method using Deep Learning Models," 2023, [Online]. Available: <http://arxiv.org/abs/2304.06952>
- [58] E. Martinez-Ríos, L. Montesinos, and M. Alfaro-Ponce, "A machine learning approach for hypertension detection based on photoplethysmography and clinical data," *Comput. Biol. Med.*, vol. 145, no. January, p. 105479, 2022, doi: 10.1016/j.combiomed.2022.105479.
- [59] T. Sadad, S. A. C. Bukhari, A. Munir, A. Ghani, A. M. El-Sherbeeney, and H. T. Rauf, "Detection of Cardiovascular Disease Based on PPG Signals Using Machine Learning with Cloud Computing," *Comput. Intell. Neurosci.*, vol. 2022, 2022, doi: 10.1155/2022/1672677.
- [60] M. Nour and K. Polat, "Automatic Classification of Hypertension Types Based on Personal Features by Machine Learning Algorithms," *Math. Probl. Eng.*, vol. 2020, pp. 1–14, 2020, doi: 10.1155/2020/2742781.
- [61] K. Welykholowa et al., "Multimodal photoplethysmography-based approaches for improved detection of hypertension," *J. Clin. Med.*, vol. 9, no. 4, 2020, doi: 10.3390/jcm9041203.
- [62] Z. Sun, Q. Xu, G. Gao, M. Zhao, and C. Sun, "Clinical observation in edaravone treatment for acute cerebral infarction," *Niger. J. Clin. Pract.*, vol. 22, no. 10, pp. 1324–1327, 2019, doi: 10.4103/njcp.njcp_367_18 .

- [63] Y. Zhao, X. Zhang, X. Chen, and Y. Wei, "Neuronal injuries in cerebral infarction and ischemic stroke: From mechanisms to treatment (Review)," *Int. J. Mol. Med.*, vol. 49, no. 2, pp. 1–9, 2022, doi: 10.3892/ijmm.2021.5070.
- [64] Centers for Disease Control and Prevention [CDC], "Underlying Cause of Death 2018-2021, Single Race Results," *National Center for Health Statistics. National Vital Statistics System, Mortality 2018-2021 on CDC WONDER Online Database*. 2021. [Online].
- [65] Y. Li et al., "Acute cerebrovascular disease following COVID-19: a single center, retrospective, observational study," *Stroke Vasc. Neurol.*, vol. 5, no. 3, pp. 279–284, 2020, doi: 10.1136/svn-2020-000431.
- [66] Goldberg MF, Goldberg MF, Cerejo R, Tayal AH, "Cerebrovascular Disease in COVID-19," *AJNR Am J Neuroradiol*, 2020 Jul;41(7):1170-1172. doi: 10.3174/ajnr.A6588.
- [67] G. Aggarwal, G. Lippi, and B. Michael Henry, "Cerebrovascular disease is associated with an increased disease severity in patients with Coronavirus Disease 2019 (COVID-19): A pooled analysis of published literature," *Int. J. Stroke*, vol. 15, no. 4, pp. 385–389, 2020, doi: 10.1177/1747493020921664.
- [68] X. Zhu, J. Liu, and Y. Zha, "Application of photoplethysmography signal in diagnosis of cerebrovascular disease and its extraction method based on Wavelet Transform," *J. Phys. Conf. Ser.*, vol. 2031, no. 1, 2021, doi: 10.1088/1742-6596/2031/1/012002.
- [69] P. Theerthagiri, A. U. Ruby, and J. Vidya, "Diagnosis and Classification of the Diabetes Using Machine Learning Algorithms," *SN Comput. Sci.*, vol. 4, no. 1, p. 72, 2022, doi: 10.1007/s42979-022-01485-3.
- [70] S. Lathief and S. E. Inzucchi, "Approach to diabetes management in patients with CVD," *Trends Cardiovasc. Med.*, vol. 26, no. 2, pp. 165–179, 2016, doi: <https://doi.org/10.1016/j.tcm.2015.05.005>.
- [71] A. Prabha, J. Yadav, A. Rani, and V. Singh, "Non-invasive Diabetes Mellitus Detection System using Machine Learning Techniques," *Proc. Conflu.* 2021

- 11th Int. Conf. Cloud Comput. Data Sci. Eng., pp. 948–953, 2021, doi: 10.1109/Confluence51648.2021.9377138.
- [72] Y. K. Qawqzeh, A. S. Bajahzar, M. Jemmali, M. M. Otoom, and A. Thaljaoui, “Classification of Diabetes Using Photoplethysmogram (PPG) Waveform Analysis: Logistic Regression Modeling,” *Biomed Res. Int.*, vol. 2020, 2020, doi: 10.1155/2020/3764653.
- [73] E. Susana, K. Ramli, H. Murfi, and N. H. Aprianoro, “Non-Invasive Classification of Blood Glucose Level for Early Detection Diabetes Based on Photoplethysmography Signal,” *Inf.*, vol. 13, no. 2, 2022, doi: 10.3390/info13020059.
- [74] C. Hettiarachchi and C. Chitraranjan, “A machine learning approach to predict diabetes using short recorded photoplethysmography and physiological characteristics”, *Springer International Publishing*, vol. 11526 LNAI, 2019, doi: 10.1007/978-3-030-21642-9_41.
- [75] V. R. Reddy, A. D. Choudhury, S. Jayaraman, N. K. Thokala, P. Deshpande, and V. Kaliaperumal, “PerDMCS: Weighted fusion of PPG signal features for robust and efficient diabetes mellitus classification,” *Heal. 2017 - 10th Int. Conf. Heal. Informatics, Proceedings; Part 10th Int. Jt. Conf. Biomed. Eng. Syst. Technol. BIOSTEC 2017*, vol. 5, pp. 553–560, 2017, doi: 10.5220/0006297205530560.
- [76] B. Zhou, P. Perel, G. A. Mensah, and M. Ezzati, “Global epidemiology, health burden and effective interventions for elevated blood pressure and hypertension,” *Nat. Rev. Cardiol.*, vol. 18, no. 11, pp. 785–802, 2021, doi: 10.1038/s41569-021-00559-8.
- [77] Y. Zhang and Z. Feng, “A SVM method for continuous blood pressure estimation from a PPG signal,” *ACM Int. Conf. Proceeding Ser.*, vol. Part F1283, pp. 128–132, 2017, doi: 10.1145/3055635.3056634.
- [78] Samimi H, Dajani HR, “A PPG-Based Calibration-Free Cuffless Blood Pressure Estimation Method Using Cardiovascular Dynamics”, *Sensors (Basel)*, 2023 Apr, 21;23(8):4145, doi: 10.3390/s23084145.

- [79] G. Slapničar, M. Luštrek, and M. Marinko, "Continuous blood pressure estimation from PPG signal," *Inform.*, vol. 42, no. 1, pp. 33–42, 2018.
- [80] J. H. S. Wang, M. H. Yeh, P. C. P. Chao, T. Y. Tu, Y. H. Kao, and R. Pandey, "A fast digital chip implementing a real-time noise-resistant algorithm for estimating blood pressure using a non-invasive, cuffless PPG sensor," *Microsyst. Technol.*, vol. 26, no. 11, pp. 3501–3516, 2020, doi: 10.1007/s00542-020-04946-y.
- [81] B. Liang et al., "Live demonstration: A support vector machine based hardware platform for blood pressure prediction," *Proc. - 2016 IEEE Biomed. Circuits Syst. Conf. BioCAS 2016*, vol. 7, p. 130, 2016, doi: 10.1109/BioCAS.2016.7833744.
- [82] A. Rehman, M. A. Bin Altaf, and W. Saadeh, "A 73 μ W single channel Photoplethysmography-based Blood Pressure Estimation Processor," *Proc. - IEEE Int. Symp. Circuits Syst.*, vol. 2022-May, pp. 2318–2322, 2022, doi: 10.1109/ISCAS48785.2022.9937690.
- [83] M. Sheeraz, A. R. Aslam, N. Hafeez, H. Heidari, and M. A. Bin Altaf, "A Wearable High Blood Pressure Classification Processor Using Photoplethysmogram Signals through Power Spectral Density Features," *Proceeding - IEEE Int. Conf. Artif. Intell. Circuits Syst. AICAS 2022*, pp. 198–201, 2022, doi: 10.1109/AICAS54282.2022.9869847.
- [84] P. Kansara, R. Dhar, R. Shah, D. Mehta, and P. Raut, "Heart Rate Measurement," *J. Phys. Conf. Ser.*, vol. 1831, no. 1, 2021, doi: 10.1088/1742-6596/1831/1/012020.
- [85] A. A. Khan, G. Y. H. Lip, and A. Shantsila, "Heart rate variability in atrial fibrillation: The balance between sympathetic and parasympathetic nervous system," *Eur. J. Clin. Invest.*, vol. 49, no. 11, pp. 0–3, 2019, doi: 10.1111/eci.13174.
- [86] Y. Zhang et al., "PPG-based Heart Rate Estimation with Efficient Sensor Sampling and Learning Models," *Proc. - 24th IEEE Int. Conf. High Perform.*

- Comput. Commun. 8th IEEE Int. Conf. Data Sci. Syst. 20th IEEE Int. Conf. Smart City 8th IEEE Int. Conf. Dep*, pp. 1971–1978, 2022, doi: 10.1109/HPCC-DSS-SmartCity-DependSys57074.2022.00294.
- [87] A. Reiss, I. Indlekofer, P. Schmidt, and K. Van Laerhoven, “Deep PPG: Large-scale heart rate estimation with convolutional neural networks,” *Sensors (Switzerland)*, vol. 19, no. 14, pp. 1–27, 2019, doi: 10.3390/s19143079.
 - [88] X. Chang, G. Li, G. Xing, K. Zhu, and L. Tu, “DeepHeart: A Deep Learning Approach for Accurate Heart Rate Estimation from PPG Signals,” *ACM Trans. Sens. Networks*, vol. 17, no. 2, pp. 1–18, 2021, doi: 10.1145/3441626.
 - [89] M. A. Motin, C. K. Karmakar, and M. Palaniswami, “PPG Derived Heart Rate Estimation during Intensive Physical Exercise,” *IEEE Access*, vol. 7, no. c, pp. 56062–56069, 2019, doi: 10.1109/ACCESS.2019.2913148.
 - [90] K. Meddah, M. Kedir-Talha, and H. Zairi, “FPGA-based system for heart rate calculation based on PPG signal,” *2017 5th Int. Conf. Electr. Eng. - Boumerdes, ICEE-B 2017*, vol. 2017-Janua, pp. 1–5, 2017, doi: 10.1109/ICEE-B.2017.8192157.
 - [91] A. Burrello et al., “Embedding Temporal Convolutional Networks for Energy-efficient PPG-based Heart Rate Monitoring,” *ACM Trans. Comput. Healthc.*, vol. 3, no. 2, 2022, doi: 10.1145/3487910.
 - [92] B. Ngoc-Thang, T. M. Tien Nguyen, T. T. Truong, B. L. H. Nguyen, and T. T. Nguyen, “A dynamic reconfigurable wearable device to acquire high quality PPG signal and robust heart rate estimate based on deep learning algorithm for smart healthcare system,” *Biosens. Bioelectron. X*, vol. 12, no. August, p. 100223, 2022, doi: 10.1016/j.biosx.2022.100223.
 - [93] T. H. Kuo, C. M. Teng, M. F. Wu, and C. Y. Wen, “An adaptive heart rate monitoring algorithm for wearable healthcare devices,” *Electron.*, vol. 10, no. 17, 2021, doi: 10.3390/electronics10172092.

- [94] Z. Pamuk and C. Kaya, "Detection of Heart Rate Variability from Photoplethysmography (PPG) Signals Obtained by Raspberry Pi Microcomputer," *Sak. Univ. J. Comput. Inf. Sci.*, vol. 5, no. 1, pp. 104–120, 2022, doi: 10.35377/saucis...1024414.
- [95] A. Chowdhury, D. Das, R. C. C. Cheung, and M. H. Chowdhury, "Hardware/Software Co-design of an ECG- PPG Preprocessor: A Qualitative & Quantitative Analysis," in *2023 International Conference on Electrical, Computer and Communication Engineering (ECCE)*, 2023, pp. 1–6. doi: 10.1109/ECCE57851.2023.10101536.
- [96] F. Rundo, C. Spampinato, S. Conoci, F. Trenta, and S. Battiato, "Deep bio-sensing embedded system for a robust car-driving safety assessment," *2020 AEIT Int. Conf. Electr. Electron. Technol. Automotive, AEIT Automot. 2020*, 2020, doi: 10.23919/aeitautomotive50086.2020.9307409.
- [97] M. Risso et al., "Robust and Energy-Efficient PPG-Based Heart-Rate Monitoring," *2021 IEEE International Symposium on Circuits and Systems (ISCAS), Daegu, Korea*, 2021, pp. 1-5, doi: 10.1109/ISCAS51556.2021.9401282.
- [98] B. Haryadi, P. H. Chang, Akrom, A. Q. Raharjo, and G. Prakoso, "Poincare plots to analyze photoplethysmography signal between non-smokers and smokers," *Int. J. Electr. Comput. Eng.*, vol. 12, no. 2, pp. 1565–1570, 2022, doi: 10.11591/ijece.v12i2.pp1565-1570.
- [99] M. A. K. Altayeb, A. Abdelrahman, M. A. Bashir, and O. A. Bashir, "Cost-effective Design of Pulse Oximeter using a Recycled SPO2 Sensor and Arduino Microcontroller," *Proc. 2020 Int. Conf. Comput. Control. Electr. Electron. Eng. ICCCEEE 2020*, pp. 0–5, 2021, doi: 10.1109/ICCCEEE49695.2021.9429681.
- [100] P. U. Pulsesensor, A. Golparvar, O. Khorsand, and A. Panahi, "An Arduino-based Remote Health Monitoring and Alert System with Fingertip Photoplethysmography Using PulseSensor," no. June 2022, pp. 0–6, 2021.

- [101] C. B. D. Kuncoro, W. J. Luo, and Y. Der Kuan, "Wireless Photoplethysmography Sensor for Continuous Blood Pressure Biosignal Shape Acquisition," *J. Sensors*, vol. 2020, 2020, doi: 10.1155/2020/7192015.
- [102] P. Prasun, S. Mukhopadhyay, and R. Gupta, "Real-time multi-class signal quality assessment of photoplethysmography using machine learning technique," *Meas. Sci. Technol.*, vol. 33, no. 1, 2022, doi: 10.1088/1361-6501/ac2d5b.
- [103] M. S. Roy, R. Gupta, and K. Das Sharma, "BePCon: A Photoplethysmography-Based Quality-Aware Continuous Beat-to-Beat Blood Pressure Measurement Technique Using Deep Learning," *IEEE Trans. Instrum. Meas.*, vol. 71, pp. 1–9, 2022, doi: 10.1109/TIM.2022.3212750.
- [104] A. B. Abdelaziz et al., "Photoplethysmography Data Reduction Using Truncated Singular Value Decomposition and Internet of Things Computing," *Electron.*, vol. 12, no. 1, 2023, doi: 10.3390/electronics12010220.
- [105] Y. Liang, Z. Chen, G. Liu, and M. Elgendi, "A new, short-recorded photoplethysmogram dataset for blood pressure monitoring in China," *Sci. Data*, vol. 5, pp. 1–7, 2018, doi: 10.1038/sdata.2018.20.
- [106] R. Krishnan, B. Natarajan, and S. Warren, "Two-stage approach for detection and reduction of motion artifacts in photoplethysmographic data," *IEEE Trans. Biomed. Eng.*, vol. 57, no. 8, pp. 1867–1876, 2010, doi: 10.1109/TBME.2009.2039568.
- [107] S. Li, L. Liu, J. Wu, B. Tang, and D. Li, "Comparison and Noise Suppression of the Transmitted and Reflected Photoplethysmography Signals," *Biomed Res. Int.*, vol. 2018, 2018, doi: 10.1155/2018/4523593.
- [108] Á. Solé Morillo, J. Lambert Cause, V. E. Baciú, B. da Silva, J. C. Garcia-Naranjo, and J. Stiens, "PPG EduKit: An Adjustable Photoplethysmography Evaluation System for Educational Activities," *Sensors*, vol. 22, no. 4, pp. 1–22, 2022, doi: 10.3390/s22041389.

- [109] Y. C. Chooi, C. Ding, and F. Magkos, "The epidemiology of obesity," *Metabolism*, vol. 92, pp. 6–10, 2019, doi: <https://doi.org/10.1016/j.metabol.2018.09.005>.
- [110] C. J. Chang, C. H. Wu, W. J. Yao, Y. C. Yang, J. S. Wu, and F. H. Lu, "Relationships of age, menopause and central obesity on cardiovascular disease risk factors in Chinese women," *Int. J. Obes.*, vol. 24, no. 12, pp. 1699–1704, 2000, doi: 10.1038/sj.ijo.0801457.
- [111] S. Karamizadeh, S. M. Abdullah, M. Halimi, J. Shayan, and M. J. Rajabi, "Advantage and drawback of support vector machine functionality," *I4CT 2014 - 1st Int. Conf. Comput. Commun. Control Technol. Proc.*, no. I4ct, pp. 63–65, 2014, doi: 10.1109/I4CT.2014.6914146.
- [112] D. Maulud and A. M. Abdulazeez, "A Review on Linear Regression Comprehensive in Machine Learning," *J. Appl. Sci. Technol. Trends*, vol. 1, no. 4, pp. 140–147, 2020, doi: 10.38094/jastt1457.
- [113] H.-I. Lim, "A Linear Regression Approach to Modeling Software Characteristics for Classifying Similar Software," *IEEE 43rd Annual Computer Software and Applications Conference (COMPSAC)*, 2019, pp. 942–943
- [114] G. Dere, 'Biomedical Applications with Using Embedded Systems', *Data Acquisition - Recent Advances and Applications in Biomedical Engineering. IntechOpen*, Mar. 17, 2021. doi: 10.5772/intechopen.96070.
- [115] W. F. Samayoa, M. L. Crespo, A. Cicuttin, and S. Carrato, "A Survey on FPGA-based Heterogeneous Clusters Architectures," *IEEE Access*, vol. 11, no. June, pp. 67679–67706, 2023, doi: 10.1109/ACCESS.2023.3288431.
- [116] S. Gandhare and B. Karthikeyan, "Survey on FPGA Architecture and Recent Applications," in *2019 International Conference on Vision Towards Emerging Trends in Communication and Networking (ViTECoN)*, 2019, pp. 1–4. doi: 10.1109/ViTECoN.2019.8899550.
- [117] M. H. Chowdhury, A. B. M. Eldaly, S. K. Agadagba, R. C. C. Cheung and L. L. H. Chan, "Machine Learning Based Hardware Architecture

- for DOA Measurement From Mice EEG,” in *IEEE Transactions on Biomedical Engineering*, vol. 69, no. 1, pp. 314–324, Jan. 2022, doi: 10.1109/TBME.2021.3093037.
- [118] L. Evdochim, D. Dobrescu, S. Halichidis, L. Dobrescu, and S. Stanciu, “Hypertension Detection Based on Photoplethysmography Signal Morphology and Machine Learning Techniques,” *Appl. Sci.*, vol. 12, no. 16, 2022, doi: 10.3390/app12168380.
- [119] M. T. Islam, I. Zabir, S. T. Ahamed, M. T. Yasar, C. Shahnaz, and S. A. Fattah, “A time-frequency domain approach of heart rate estimation from photoplethysmographic (PPG) signal,” *Biomed. Signal Process. Control*, vol. 36, pp. 146–154, 2017, doi: 10.1016/j.bspc.2017.03.020.
- [120] Y. Kurylyak, F. Lamonaca, and D. Grimaldi, “A Neural Network-based method for continuous blood pressure estimation from a PPG signal,” *Conf. Rec. - IEEE Instrum. Meas. Technol. Conf.*, pp. 280–283, 2013, doi: 10.1109/I2MTC.2013.6555424.
- [121] O. Schlesinger, N. Vigderhouse, D. Eytan, and Y. Moshe, “Blood Pressure Estimation From PPG Signals Using Convolutional Neural Networks And Siamese Network,” in *ICASSP 2020 - 2020 IEEE International Conference on Acoustics, Speech and Signal Processing (ICASSP)*, 2020, pp. 1135–1139. doi: 10.1109/ICASSP40776.2020.9053446.

Appendices

Appendix A: Description of the Dataset

Data Descriptor: A new, shortrecorded photoplethysmogram dataset for blood pressure monitoring in China

Open clinical trial data provide a valuable opportunity for researchers worldwide to assess new hypotheses, validate published results, and collaborate for scientific advances in medical research. Here, we present a health dataset for the non-invasive detection of cardiovascular disease (CVD), containing 657 data segments from 219 subjects. The dataset covers an age range of 20–89 years and records of diseases including hypertension and diabetes. Data acquisition was carried out under the control of standard experimental conditions and specifications. This dataset can be used to carry out the study of photoplethysmograph (PPG) signal quality evaluation and to explore the intrinsic relationship between the PPG waveform and cardiovascular disease to discover and evaluate latent characteristic information contained in PPG signals. These data can also be used to study early and noninvasive screening of common CVD such as hypertension and other related CVD diseases such as diabetes.

This PPG and BP (PPG-BP) database integrates the deidentified, comprehensive clinical data of patients admitted to the Guilin People’s Hospital in Guilin, China. The openness of the data allows clinical studies to explore and improve the understanding of relationships between cardiovascular health and PPG signals, with the final goal of creating a simple, effective non-invasive detection technology that is easy to use and wearable. This dataset has been collected from 219 subjects, aged 21–86 years, with a median age of 58 years. Males accounted for 48%. The dataset covers several diseases including hypertension, diabetes, cerebral infarction, and insufficient brain blood supply.

Experimental design and data acquisition:

The dataset collection program involved acquiring information on the basic

physiology of individuals, extracting information on cardiovascular diseases from hospital electronic medical records, collecting PPG waveform signals, and detecting instant arterial blood pressure at the same time. The data acquisition was conducted at the Guilin People's Hospital. A customized portable hardware platform was designed, and consisted of a PPG sensor probe, microcontroller, and a matching app. Data were transmitted via Bluetooth. The PPG sensor model was SEP9AF-2 (SMPLUS Company, Korea), which contains dual LED with 660nm (Red light) and 905 nm (Infrared) wavelengths, with a sampling rate of 1 kHz and 12-bit ADC, and the hardware filter design is 0.5–12Hz bandpass. The microcontroller model was MSP430FG4618 (Texas Instruments company, USA) embedded on the probe's board to configure the ADC, fetch the data and send the data to the matching app via Bluetooth. Waveform data is collected using a set of customized probes and a matching app that was developed based on Android Studio. The PPG detection probe used the infrared light and transmission method to collect fingertip PPG waveform data. These real-time data are transmitted to the matching app via Bluetooth. The app can control the detection probe, display the real-time waveform, and conduct a signal quality assessment of the PPG waveform in order to save the high-quality PPG wave segment. The arterial blood pressure is measured using the Omron HEM-7201 (Omron Company, Kyoto, Japan) upper arm blood pressure monitor.

The study was approved by the ethics committee of the Guilin People Hospital and the Guilin University of Electronic Technology in China. All participants gave written and informed consent before the study. They were compensated monetarily at 10 Yuan/h. Participants answered questions about age, gender, height, and weight and all initial data acquisition was conducted in a private, and comfortable clinical room.

Before beginning with signal collected, each individual was asked to sit in an office chair in the most comfortable posture and to relax their arms on an empty desk. Each individual had 10 min to adapt to the environment and adjust their breathing after entering the data collection room. The specific collection settings were as follows: The PPG signal was collected at the fingertip of the left index finger, the arterial blood pressure was collected from the right forearm, all of

which was completed within three minutes. The arterial blood pressure measurement was performed by the hospital nurse. During signal acquisition the sampling precision of waveform data was set to a sampling rate of 1 kHz, with 12 bits AD conversion precision. Three segments were recorded and saved per subject, each segment included 2100 sampling points, which corresponds to a length of 2.1 seconds. During the 3 min data collection phase, every PPG segment of a particular subject scored a Skewness SQI value; values greater than Zero were saved, and if a value was less than Zero the app prompted the user to recollect the PPG signal. This step was developed to reduce including PPG segments with high noise and motion artifacts.

The BP collection device (Omron HEM-7201) requires at a minimum a 30 second waveform to detect the systolic and diastolic period. The BP reading represents the blood pressure value for the 3 minute data recording for each subject, as shown in Figure 1. During the data collection process, we aimed to collect the BP and PPG data immediately after each other respectively. Three PPG segments were saved during the data collection period in addition to the BP recording. Every participant was asked to breath as they normally would on day-to-day basis for practical applications. Note that we did not investigate the baroreflex response to stress. The dataset includes BP and PPG information from subjects that were diagnosed with normotension, prehypertension, and stage I/stage II hypertension, which can be helpful and valuable for researchers.

Patients Characteristics:

The dataset was collected from 219 adult subjects and currently contains 657 PPG waveform segments. The dataset covers individuals aged 21–86 years, and males account for 48% of participants. The dataset also covers several different CVDs, including hypertension, cerebral infarction, and insufficient brain blood supply and other related diseases such as diabetes.

Data Record:

The dataset has been fully uploaded to the network, and users can download them through the Figshare repository with the title PPG-BP Database and reference (Data Citation 1). The dataset comprises 1 table file and 219 waveform data folders, which include three 2.1-secondlength infrared PPG signal text files

and physiological information recording files. Among these, the PPG signal data is the 2.1-second-length 12 bits AD raw value. The ID_1, ID_2, and ID_3 text files represent three separate segments of waveform data Table 1 (available online only). The "PPG-BP database.xlsx" table file contains aggregated subjects of physiological information and disease information. Information records include ID, sex, age, height, weight, systolic pressure, diastolic pressure, heart rate, and disease records. Before the participant record is archived, it was required to conduct data integrity screening, data availability screening, and a waveform signal quality evaluation (to remove inconsistent, abnormal, and high noise data) in order to form a high-quality dataset. The detailed process of inclusion and exclusion, is described as follows:

- Data integrity screening: This process includes the screening of missing and abnormal values for: basic physiological information, disease information, blood pressure, heart rate, and 3 segments waveform data. If one or more items are missing or if there was an abnormal value, the participant record was removed.
- Data availability screening: This dataset is designed to focus on the clinical information for CVDs and other closely related diseases such as diabetes. Data from the CVD patients who were diagnosed with non-CVD diseases (except diabetes) were excluded during the screening process to ensure that the dataset only contains data from participants who were diagnosed with the disease of interest.
- Waveform signal quality evaluation: All 3 segments for each participant went through a signal quality evaluation, and a robust signal quality index (SQI) method was applied in order to achieve this step. If the SQIs of the 3 segments in one subject were lower than the mean SQI calculated from the segments of all subjects, the subject data was removed.

Technical validation:

The process of data collection experiment consists of five stages. The stage I and stage II conduct some preparations of the customized hardware and software, training of operators and recruitment of participants. Stage III is the phase of data collection in hospitals, including the acquisition of basic physiological information of participants, hospital electronic medical records, PPG signals and blood pressure data. Stage IV is the data archiving part, including de-identification, format conversion, data matching, data inclusion and exclusion for all the collected data. Stage V is the public release of the PPGBP dataset; researchers can download the dataset and validate their algorithms. At present, Perfusion Indices (PSQI) are regarded as the gold standard of PPG Signal Quality Indices (SQI). Various other signal quality evaluation methods have been proposed and studied in order to identify more simple and accurate evaluation methods for signal quality assessment. Elgendi¹³ compared eight different signal quality indices: PSQI, Skewness (S_{SQI}), Kurtosis (K_{SQI}), Entropy (E_{SQI}), Signal-tonoise ratio (N_{SQI}), Zero-crossing (Z_{SQI}), Matching of multiple systolic wave detection algorithms (M_{SQI}), and Relative power (R_{SQI}). For varying lengths of PPG waveform recordings (i.e., from 2 s to 30 s), the SSQI method demonstrated better performance when compared to other methods ((P_{SQI}) , (K_{SQI}), (E_{SQI}), (N_{SQI}), (M_{SQI}), (Z_{SQI}), and (R_{SQI})). Moreover, PPG waveform classification is possible with 2 s length recording (excellent vs. unfit) using the (S_{SQI}) index. These results motivated collecting PPG signals with 2 s length. Skewness is used to measure the probability distribution of symmetric signals, which can distinguish the periodic, symmetrical, stationary signals and sudden jumps, periodic signals, and irregular signals. The specific definition is as follows:

$$S_{SQI} = \frac{1}{N} \sum_{i=1}^N (x_i - \frac{\mu_x}{\sigma})^3 \quad (8.1)$$

where, N is the sample number of PPG signal, μ_x and σ are empirical estimates of the mean and standard deviation of x_i , respectively.

In the process of data collection, the data is evaluated using the PPG signal quality before it was saved, and the evaluation method adopted the SSQI index. Each segment of PPG signal was evaluated against the classification threshold of

excellent, acceptable, or unfit PPG waveform in order to determine whether it should be saved. During the evaluation of signal quality for each participant, the (S_{SQI}) for the three segments were compared. Among the three the segments, the segment with the highest (S_{SQI}) was deemed as "high quality", the segment with the lowest (S_{SQI}) was deemed as "low quality" and the remaining segment was deemed as "medium quality". Note, we are providing the PPG segments and their corresponding (S_{SQI}) values to make it easier for investigators to select the segment with highest quality. Additionally, with the availability of the three (S_{SQI}) values, researchers will be able to analyze each segment, if needed, for validation, etc.

Appendix B: Design in Xilinx System Generator

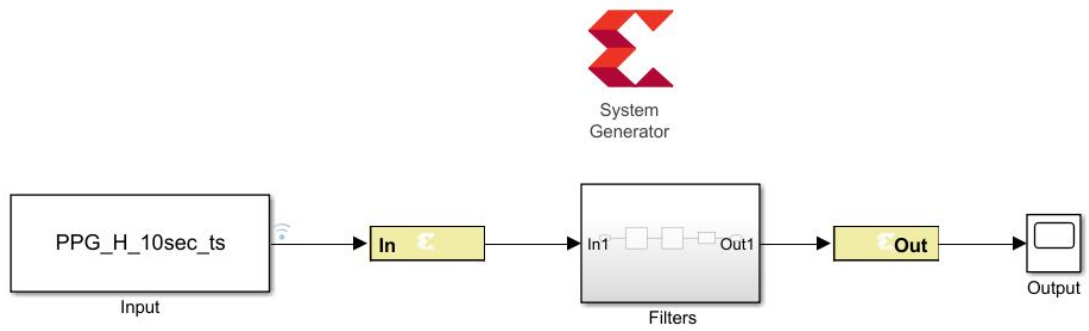


Figure B1. Preprocessor

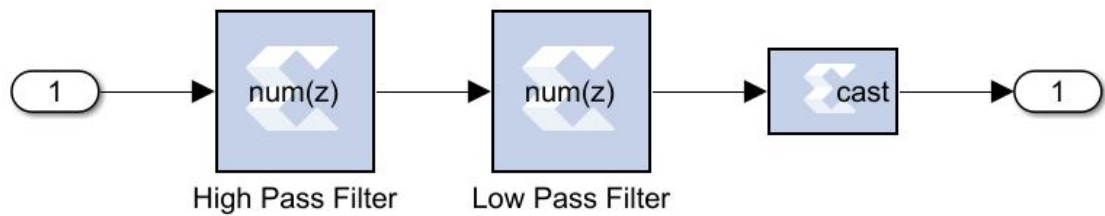


Figure B2. Filters Subsystem

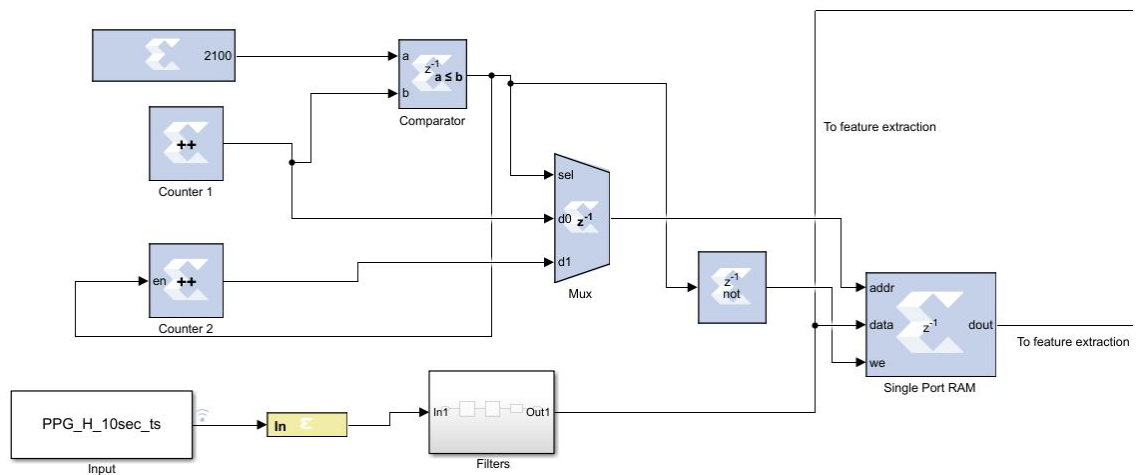


Figure B3. Memory and control system

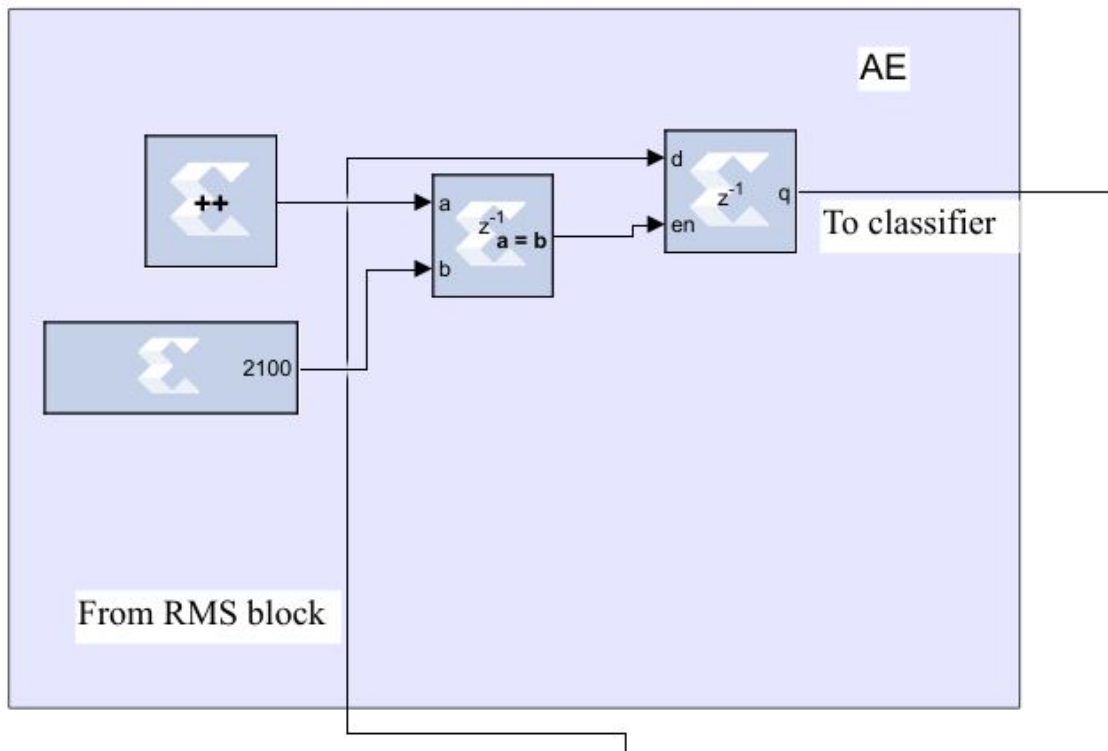


Figure B6. AE extraction

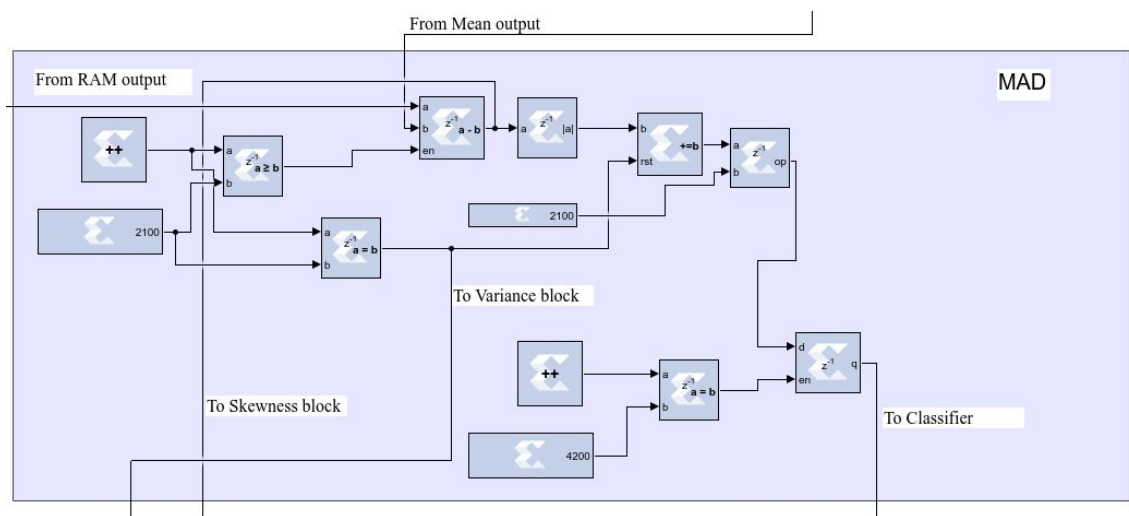


Figure B7. MAD extractionr

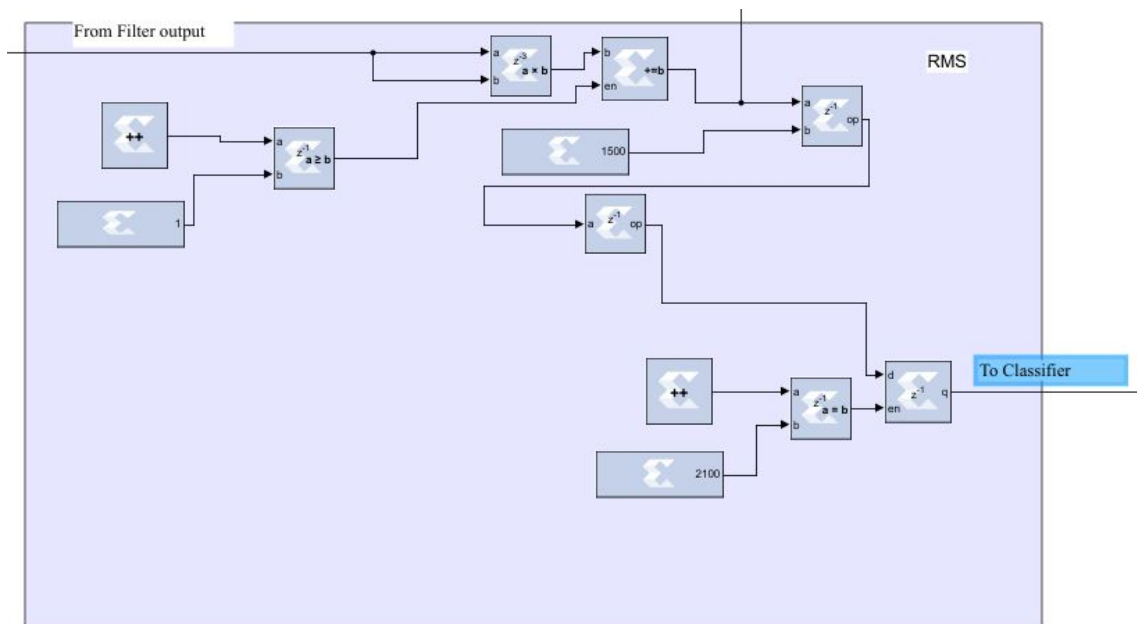


Figure B8. RMS extraction

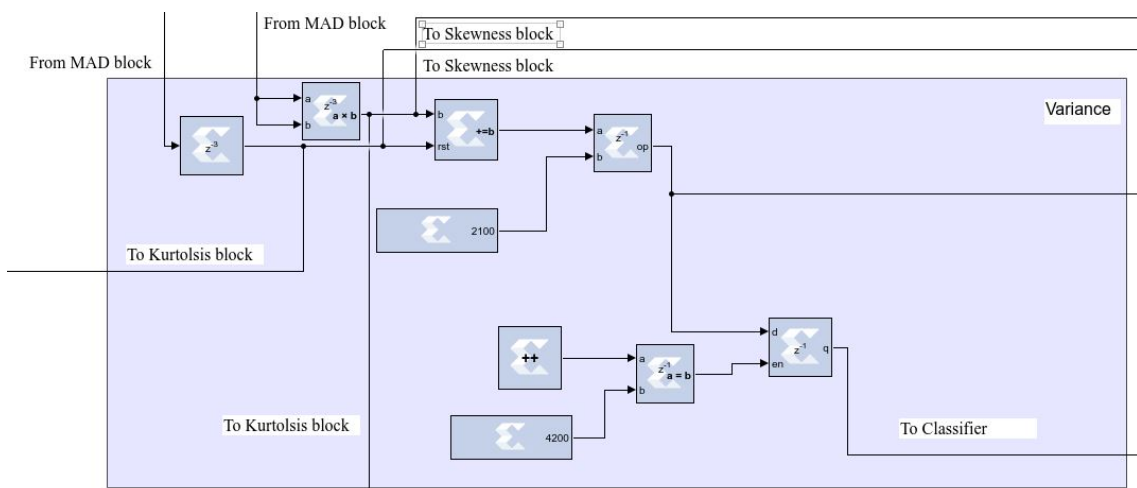


Figure B9. Variance

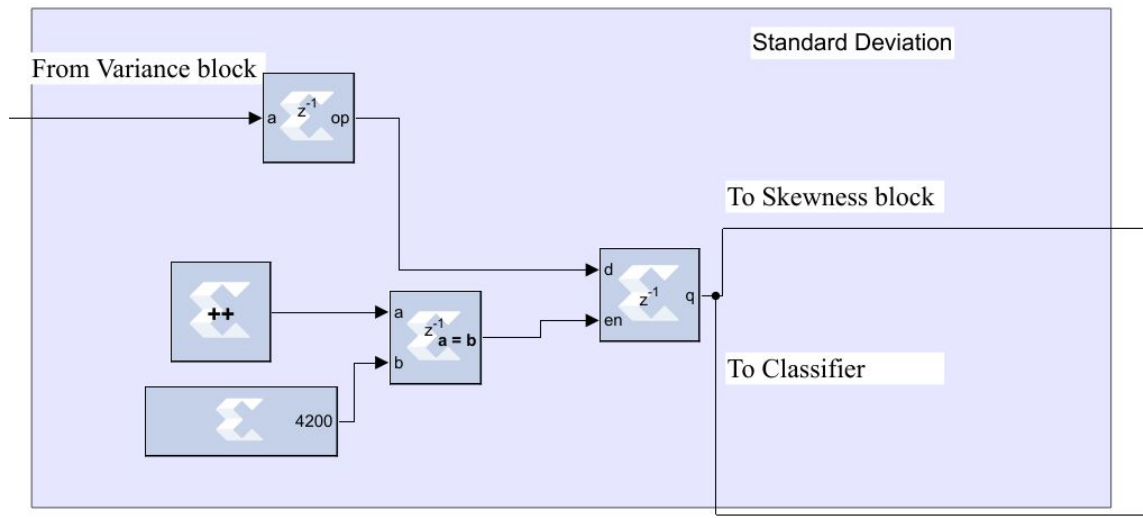


Figure B10. Standard deviation extraction

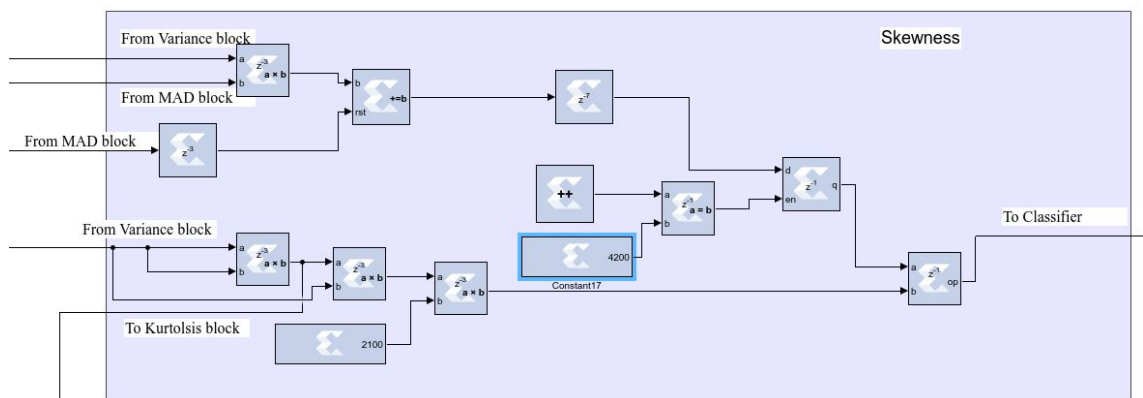


Figure B11. Skewness

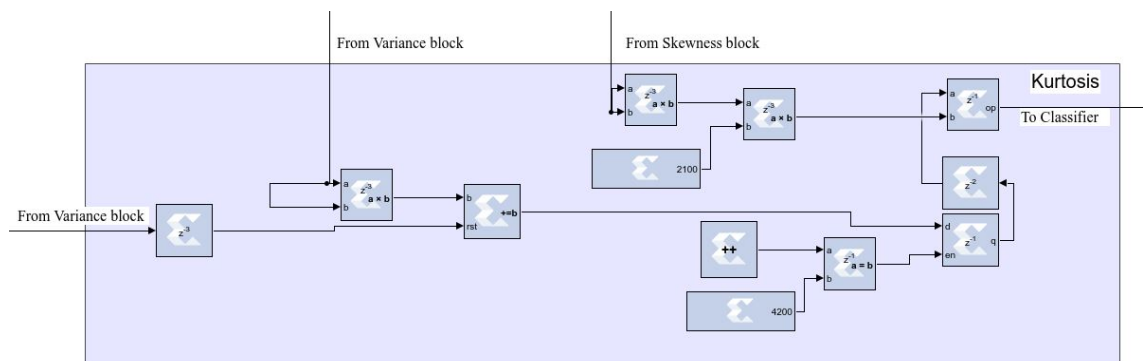


Figure B12. Kurtosis extraction

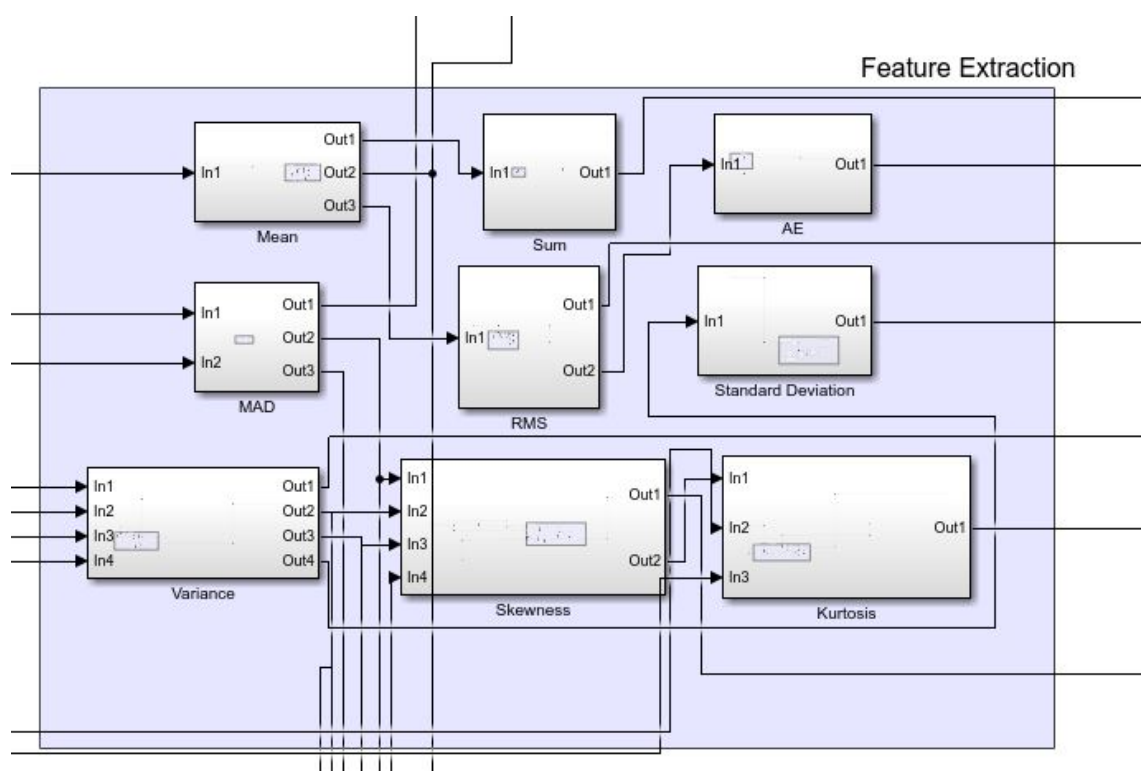


Figure B13. Feature extraction subsystems

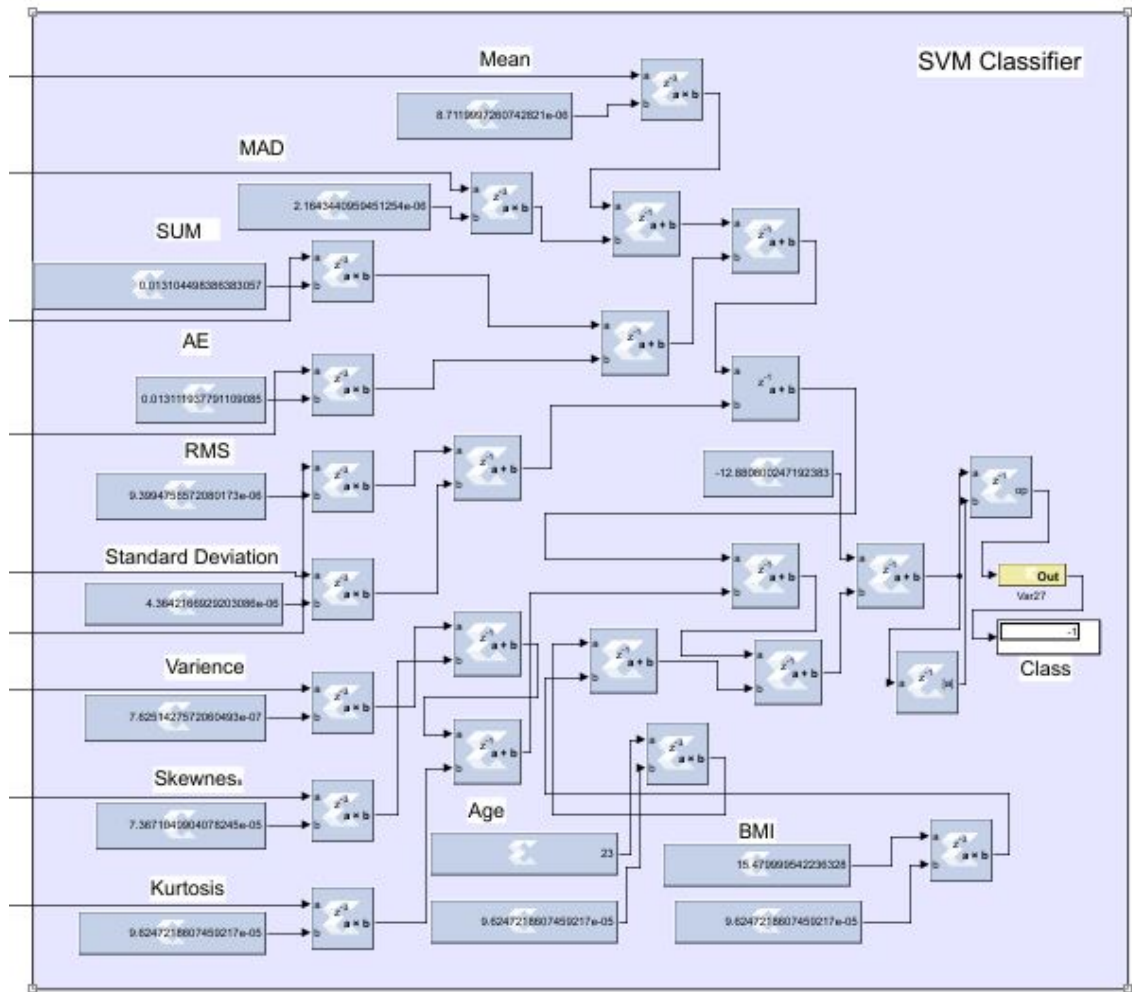


Figure B14. SVM classifier for binary classification

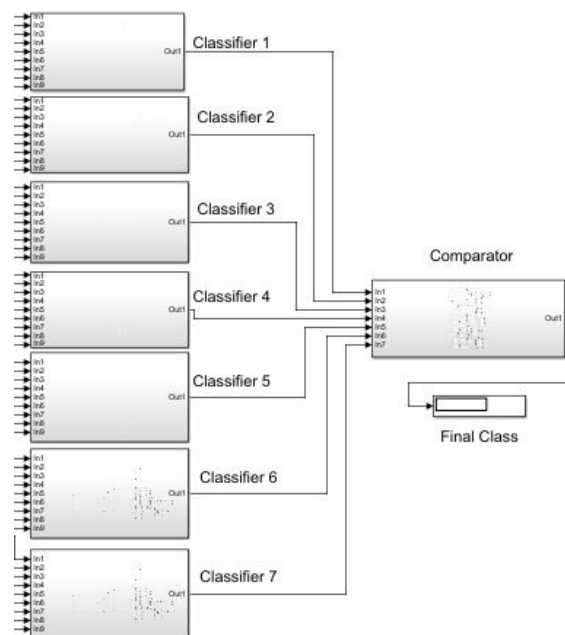


Figure B15. Multiclass Classifier with 7 SVM classifiers

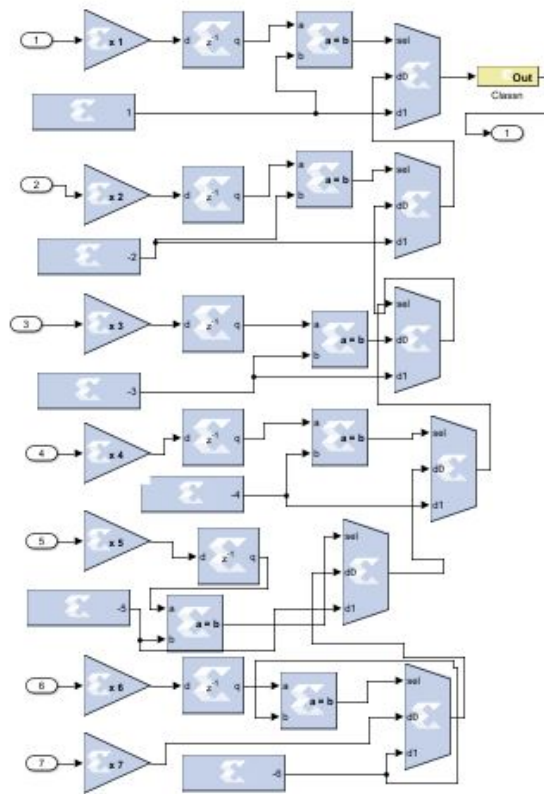


Figure B16. Comparator subsystem

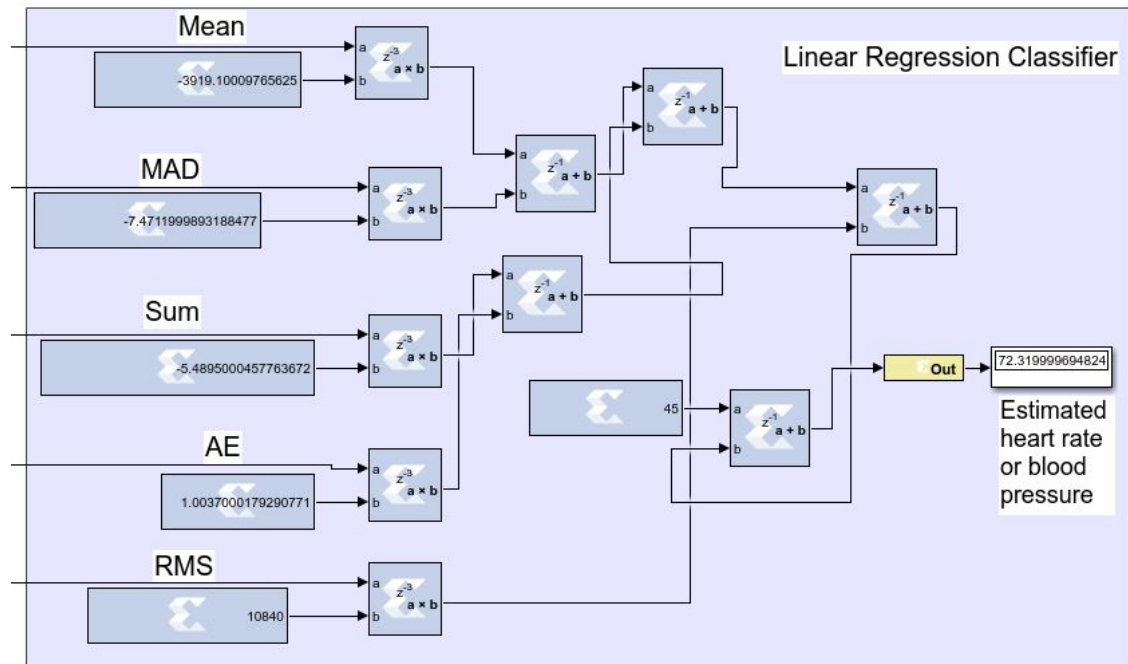


Figure B17. Linear regression classifier for heart rate and blood pressure estimation